TRIBHUVAN UNIVERSITY

INSTITUTE OF ENGINEERING

PULCHOWK CAMPUS

THESIS NO: *M-398-MSREE*-2021-2025

Dynamic Thermal Rating for Congestion Management in Regions with Renewable Energy Generation: A Case Study in Dana-Kushma-New Butwal 220 kV Transmission Line

by

Khil Nath Aryal

A THESIS

SUBMITTED TO THE DEPARTMENT OF MECHANICAL AND AEROSPACE ENGINEERING IN PARTIAL FULFILLMENT OF THE REQUIREMENTS FOR THE DEGREE OF MASTERS OF SCIENCE IN RENEWABLE ENERGY ENGINEERING

DEPARTMENT OF MECHANICAL AND AEROSPACE ENGINEERING

LALITPUR, NEPAL

APRIL 2025

COPYRIGHT

TRIBHUVAN UNIVERSITY

INSTITUTE OF ENGINEERING

PULCHOWK CAMPUS

DEPARTMENT OF MECHANICAL AND AEROSPACE ENGINEERING

LETTER OF ACCEPTANCE

The undersigned certify that they have read, and recommended to the Institute of Engineering for acceptance, a thesis entitled "Dynamic Thermal Rating for Congestion Management in Regions with Renewable Energy Generation: A Case Study in Dana-Kushma-New Butwal 220 kV Transmission Line" submitted by Khil Nath Aryal in partial fulfillment of the requiremnets for the degree of Master of Science in Renewable Energy Engineering.

.....

Supervisor, Sanjaya Neupane

Assistant Professor

Department of Mechanical and Aerospace Engineering

Pulchowk Campus, IOE, TU

.....

Supervisor, Shahabuddin Khan

Assistant Professor

Department of Electrical Engineering

Pulchowk Campus, IOE, TU

.....

External Examiner, Er. Subrat Aryal

Deputy Manager

Nepal Electricity Authority

Tribhuvan University
Institute of Engineering
Pulchowk Campus

.....

Committee Chairperson, Sudip Bhattarai, PhD

Assistant Professor, Head of Department

Department of Mechanical and Aerospace Engineering

Pulchowk Campus, IOE, TU

ABSTRACT

Transmission grid congestion in Nepal is caused by unplanned penetration of distributed renewable energy generators, electric vehicles, and cooking loads, leading to increased congestion management costs, while the conventional static thermal rating method underutilizes transmission grid capacity; Dynamic Line Rating (DLR), by assessing real-time meteorological conditions, offers higher line capacity and helps manage congestion using existing infrastructure. Many studies on dynamic line rating use probabilistic approaches. Still, they struggle with weather uncertainties, spatial features of transmission lines, and high computational costs. In contrast, no studies have addressed dynamic rating for transmission lines in Nepal's grid with renewable energy penetration, highlighting the need for techno-economic analysis of capacity expansion for major transmission lines. This study aims to develop a DLR application scheme for managing transmission grid congestion caused by renewable energy sources. A DLR forecasting model will be designed to predict real-time thermal ratings, with the results used for congestion management of specific transmission lines. The proposed model is tested on the Dana-Kushma-New Butwal 220 kV transmission line of the Integrated Nepalese Power System (INPS) that includes wind and solar power generation. Results show shows that DLR consistently exceeds static ratings, providing extra capacity. This is especially beneficial during winter, when lower ambient temperatures in the Terai region enhance thermal capacity, allowing for better handling of heating loads. DLR forecasting for 2020 indicates a 20-30% increase in line capacity compared to static ratings, allowing the evacuation of an additional 743 GWh of renewable energy annually with minimal added costs.

ACKNOWLEDGMENT

Throughout the writing of this thesis report, I have received a great deal of support and assistance. I would like to express my deepest gratitude to my supervisors, Assistant Professor Sanjaya Neupane, Department of Mechanical and Aerospace Engineering, Pulchowk Campus, Institute of Engineering and Assistant Professor Shahabuddin Khan, Department of Electrical Engineering, Institute of Engineering, Pulchowk Campus, Institute of Engineering for their exceptional guidance, support, and encouragement throughout the course of this research. Their expertise, insightful feedback, and continuous motivation have been invaluable in shaping the direction and quality of this study.

I would also like to extend my gratitude to Associate Professor Dr. Hari Bahadur Darlami, MSc Program Coordinator for Renewable Energy Engineering (MSREE), Pulchowk Campus, Institute of Engineering and Assistant Professor Dr. Sudip Bhattarai, Head of the Department, Department of Mechanical and Aerospace Engineering, Pulchowk Campus, Institute of Engineering for providing me with the opportunity to pursue this study.

In addition, I would like to acknowledge faculties from the Master's Degree in Renewable Energy Engineering program at the Pulchowk Campus, Institute of Engineering for their guidance and suggestions.

I would also like to acknowledge my colleagues who have helped me with their valuable suggestions and have been helpful in various phases of this research.

TABLE OF CONTENTS

LIST OF FIGURES

LIST OF TABLES

ABBREVIATIONS AND ACRONYMS

ACSR	Aluminum Conductor Steel Reinforced
AEG	Annual Energy Generation
CAPM	Capital Asset Pricing Model
CIGRE	International Council on Large Electric Systems
DTR	Dynamic Thermal Rating
EV	Electric Vehicle
GoN	Government of Nepal
HEP	Hydro-electric Plant
IEEE	Institute of Electrical and Electronics Engineers
INPS	Integrated Nepalese Power System
kV	Kilo Volt
NEA	Nepal Electricity Authority
PDF	Probability Density Function
RE	Renewable Energy
RH	Relative Humidity
RoR	Run of River
SS	Substation
STR	Static Thermal Rating
TL	Transmission Line
VD	Voltage Drop
WACC	Weighted Average Cost of Capital

CHAPTER 1 INTRODUCTION

1.1 Background

Transmission line congestion is a phenomenon, which restricts the transfer capacity of the transmission system with available generation capacity and demanded load [1]. The main objective of congestion management is to implement re-dispatching effectively [2] so that congestion caused by overloading of the electrical equipment will be resolved. Transmission line congestion generally occurs when multiple scheduled/forced outage exists in the power system [1] leading unavailability of transmission lines to meet load and generation. Similarly, modern power systems are continuously developing penetration of electrical vehicles (EV), distributed energy resources (DER), and many more renewable energy resources [3] increasing the cost of congestion management for utilities.

The interconnection between generation and load is achieved through transmission line conductors. Overhead transmission lines are facing new challenges of under-utilization of line assets which consequently affects planning, operation, and control actions. As per the transmission line loadability curve also known as the St. Clair Curve, transmission line capability is limited by thermal constraints in addition to voltage drops and stability limits [14]. Thermal transmission capacity is affected by the temperature effect on sag clearances along the line spans caused by weather fluctuations which are time and space dependent time and space-dependent [4]. The thermal capacity of a transmission line conductor is the maximum current that the conductor can flow without being damaged by heating loss [5]. The current carrying capacity is different for different conductors and is affected by various local meteorological conditions. Traditionally, transmission capability is being determined for unfavorable weather conditions i.e. very high ambient temperature and low wind speed [6]. This conservative approach results in the under-utilization of the transmission line as the worst weather conditions appear for a very short period during its life span [7]. For the grids with higher penetration of wind energy generators, generation needs to be curtailed due to insufficient line capacity [8].

The Dynamic Line Rating (DLR) technology of computing dynamic rating of transmission lines by real-time monitoring of environmental parameters maximizes

the ampacity of the conductor and hence increases utilization of existing assets [14]. The use of real-time meteorological data in line capacity computation improves the performance and operating efficiency of transmission networks. DLR is determined by evaluating the heat balance equation of the conductor [9] considering heat loss such as convection cooling, radiation cooling, and precipitation cooling as well as heat gains such as solar heat gain and electrical loss in the conductor. That heat exchange is strongly influenced by wind speed, air temperature, and solar radiation [7], parameters that can vary considerably in the space of one day or even one hour. With the increasing penetration of renewable wind energy resources, transmission systems need to be operated more flexibly with increased capability leading to network reinforcement [10]. Constructing new lines in a restructured competitive electricity market is not an economically feasible way for congestion management for transmission utilities due to the scarcity of space and land.

Transmission line congestion as well as an increment of margin under contingencies can be achieved using the DLR approach [11]. DLR implementation enhances line capability, enhances system reliability, helps in congestion management, supports wind power integration [4] and improves the tolerability of the system during the event of N-1 contingencies [12]. Dynamic rating techniques also prevent premature aging due to increased conductor temperature when the conditions are worse than the nominal conditions [13]. Dealing with errors exists in weather data measurement and unpredictable changes in weather conditions maximum thermal rating with greater reliability can be achieved [12].

1.2 Problem Statement

There is increasing penetration of renewable energy resources such as wind generators and solar PV generators located far away from load centers increasing congestion in transmission grids. The need for flexibility in transmission system operation is increasing day by day due to renewable integration, the aging of transmission facilities, and load growth. Congestion management with generation rescheduling introduces large operational costs for transmission system operators (TSOs). As the construction of new lines is not feasible for the utilities under a competitive restructured electricity market because of cost, time, space, and land constraints, congestion management using a dynamic line rating approach can be one

possible solution. Congestion management using a dynamic line rating approach helps transmission system operators in congestion management by utilization of real-time ampacity forecasting. Appropriate DLR forecasting with the integration of the day-ahead market provides more economic benefits for transmission utilities.

Transmission Congestion issues in Nepalese Grid:

Day by day the penetration of renewable energy generators on the Nepalese transmission network is increasing dramatically. Unplanned random penetration of renewal energy generators in transmission networks leads to increased transmission congestion and hence larger congestion management costs for Nepalese utilities. As the existing transmission grids are being overloaded, Nepalese transmission utility is also striving to increase line capability for the efficient utilization of existing overhead transmission lines. Nepal Electricity Authority (NEA) is facing load curtailment problems mainly in major populated cities during winter peaks.

There is a major transmission and distributed energy generation outage problem caused by the short-time overloading of some critical transmission lines of INPS. Some of our transmission lines are not capable of handling congestion in the case of contingencies as it is already being operated in overloaded conditions. Using old and conservative techniques of static rating for increased DER penetration leads the utility here to construct a new transmission line as soon as existing assets are not optimally utilized. Implementing DLR for congestion management in INPS provides an additional current-carrying capacity for transmission lines and thus can mitigate system congestion and reduce generation re-dispatching in cases when congestion is caused by the transmission thermal limit. DLR implementation can help to reduce congestion costs and therefore load-shedding risk. Implementing DLR is especially important to relieve congestion on the transmission lines that are constrained due to the integration of renewable energy resources.

1.3 Objective

1.3.1 Main Objective

The main objective of this research is to develop a Dynamic Line Rating forecasting model and its application for transmission line congestion management of Integrated Nepalese Power System (INPS).

1.3.2 Specific Objectives

To achieve the the main objective, the followings are the specific objectives:

i. To develop a DTR forecasting model, which will then be used to evaluate dynamic line ratings based on all available weather data

ii. To create a congestion management model for transmission lines using forecasted DLR.

iii. To test the developed model on the Dana-Kushma-New Butwal 220 kV line of INPS, which includes renewable energy generation, in order to demonstrate the model's effectiveness.

1.4 Scopes of Study

This study covers the dynamic line thermal rating forecasting of overhead transmission line conductors based on real-time meteorological data and its application in transmission line congestion management. The major weather factors that can affect transmission line rating will be selected based on different past research articles. Dynamic line thermal rating is determined by using methodologies provided by IEEE and CIGRE standards. Numerical testing of the proposed model will be analyzed on some transmission lines of INPS. Solar PV generators are taken as renewal energy penetrator on Nepalese transmission grids.

1.5 Limitations of Study

The following are the limitations of this study:

i. There is more benefit of the proposed model for wind generators dominated transmission lines. Maximum optimization may not be possible for other renewable-dominated transmission systems like INPS.

ii. The uncertainties of the renewal energy generators may not be considered in this study.

iii. The accuracy of the line rating forecasting model depends upon historical data available and the accuracy of weather forecasting agencies.

iv. Introducing congestion management with DLR technologies for intraday power trade introduces challenges for TSOs.

1.6 Rationale/Case Study

Different 66 kV, 132 kV, and 220 kV transmission lines of Integrated Nepalese Power System (INPS) with higher transmission congestion can be the study case for this methodology. Transmission lines at the voltage level of 220 kV are being constructed in a different region of INPS. According to the NEA annual report [14], there are four existing 220 kV transmission lines with a total length of 332.6 circuit km. These lines connect some of the larger hydropower and grid substations to load centers in the southern part and cities of Nepal. ACSR BISON, DRAKE, and MOOSE are the most commonly used conductors in 220 kV transmission lines. Also, a total of 509 circuit km of 220 kV transmission lines are in different phases of construction. To simulate the proposed methodology, a Dana-Kushma-New Butwal 220 kV transmission line which connects the northern wind generation region with the southern region with high solar PV generation feasibility, is taken under consideration.

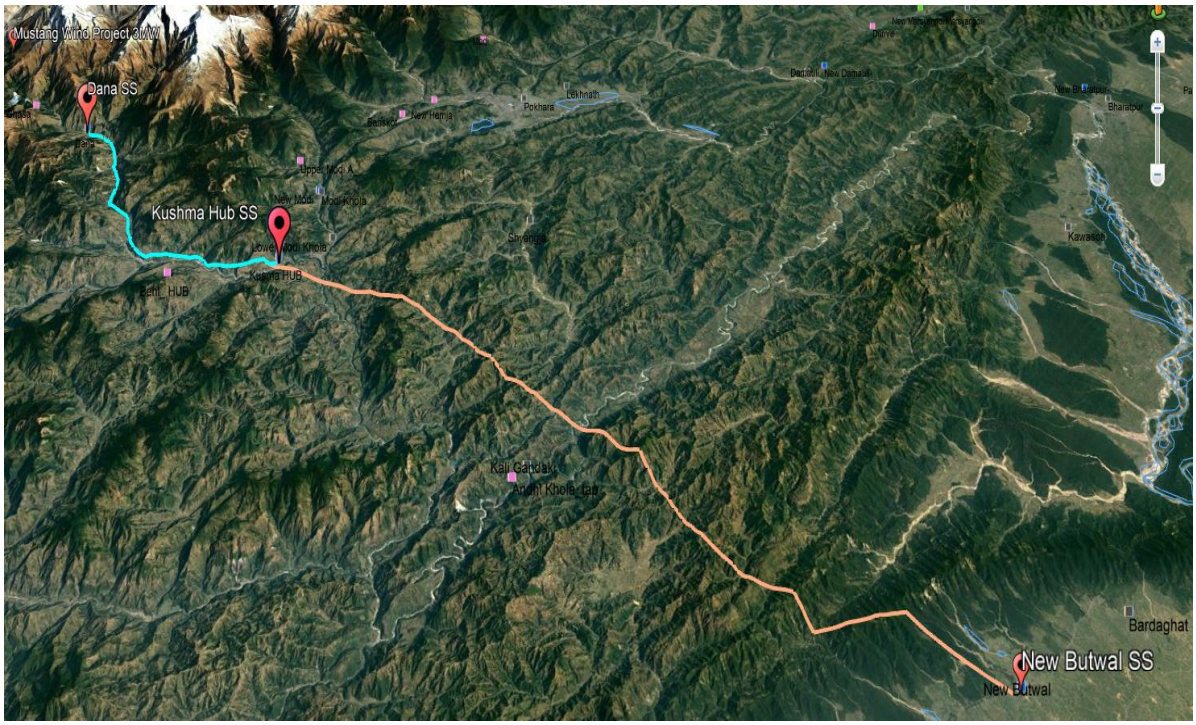

Figure 1- 1 Snip showing proposed line (Dana-Kushma-New Butwal 220 kV) for Numerical Testing

This transmission line with wind and solar PV generation feasibility and the possibility of connection at its ending substation in the near future is studied for the evaluation of the efficiency of the proposed model. Also, this transmission line has the probability of future renewable energy-based generation installation and is divided

into two regions namely the wind region which is the Dana-Kushma segment of the transmission line consisting of larger wind generation potential, and the solar region which is Kushma-Butwal segment with large solar potential.

1.7 Dana-Kushma-New Butwal 220 kV TL

A 220-KV transmission line of INPS from Dana Substation Myagdi (28.54°, 83.65°, 1418 m) to New Butwal Substation (27.57°, 83.69°, 142 m), Rupandehi, via intermediate Kushma Substation (28.24°, 83.65°, 930 m), Parbat, Nepal is investigated. The total line length is about 128 km connecting three substations. This transmission line is divided into two major sections which are discussed in the following subsections.

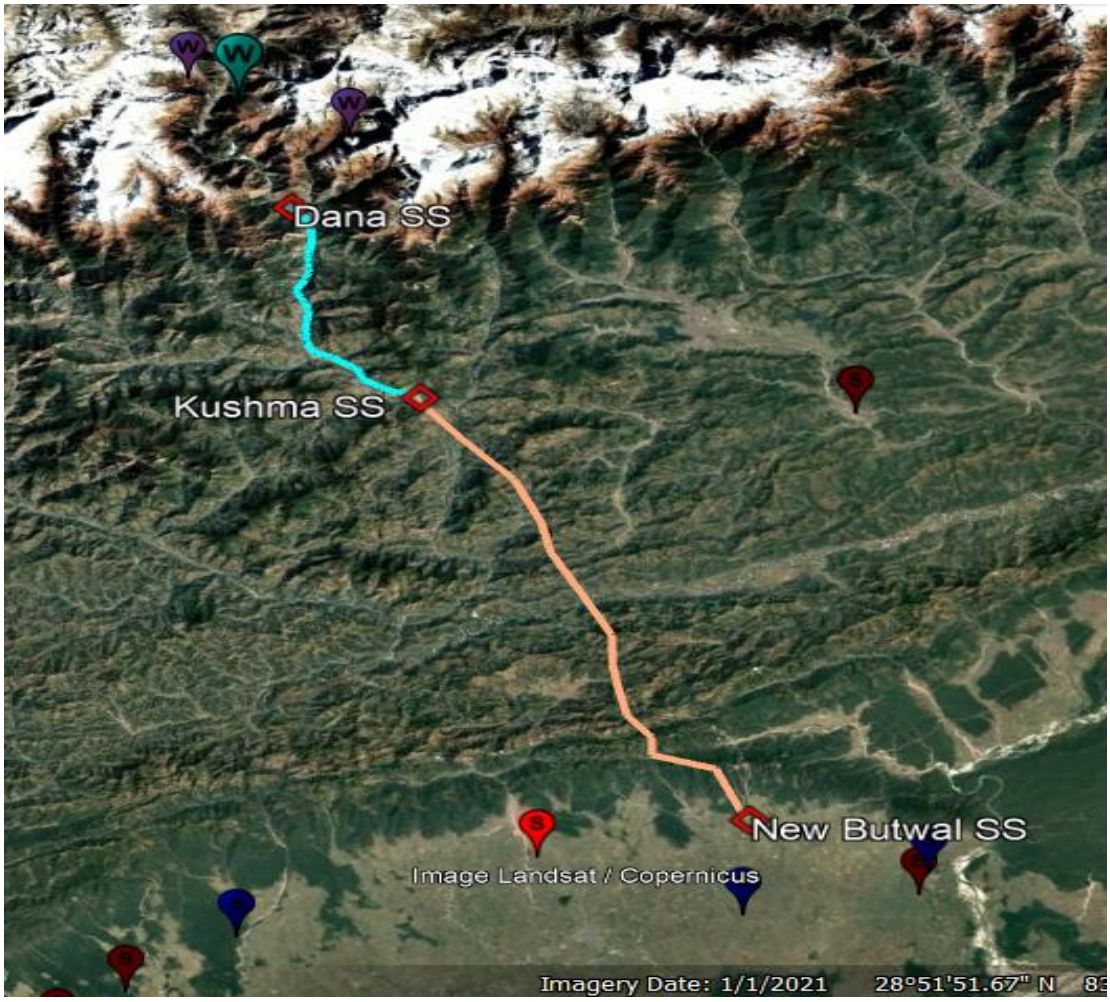

Figure 1- 2 Snip showing wind and solar energy generating stations near Dana-Kushma-New Butwal 220 kV TL

1.7.1 Dana-Kushma 220 kV TL Section

The 40 km long Dana-Kushma 220 kV transmission line consists of twin MOOSE conductors and the associated 220/132/33kV, 100MVA substation at Dana, Myagdi, and another 220/132kV, 100MVA substation at Kushma, Parbat have been commissioned and are now operating in INPS [15]. This section of the transmission line traverses near the windy zone terrains of the Myagdi and Mustang districts of Nepal having the feasibility of wind energy generation. **Error! Reference source not found.** presents the detailed characteristics of the 220 kV Dana-Kushma TL section.

Table 1- 1 Line Detail of 220 kV Dana-Kushma Transmission Line Section

SN	Details	Symbol	Value	Unit
1	Starting SS	Dana SS		
2	Ending SS	Kushma SS		
3	Characteristics	Covers uphill areas of Nepal rich in future wind energy generation.		
4	Voltage Level	V	220	kV
5	Line Length	L	40	km
6	Power Transmitted	P_T	800	MW
7	Conductor Used	ACSR MOOSE		
8	Area of a cross-section of conductor	A	500	mm^2
9	Number of Circuits	Nc	2	Nos.
10	Number of Conductors in Bundling	Nb	2	Nos.
14	Conductor Outside Diameter	D0	31.77	mm
15	Emissivity	ε	0.8	Number
16	Solar absorptivity	α	0.8	Number
17	Conductor Resistance	RTs	0.0547	Ohm/km
18	Static Thermal Rating	STR	980	Amps

1.7.2 Kushma-New Butwal 220 kV TL Section

This section of the transmission line consists of an 88 km long double circuit 220kV twin bundle HTLS DRAKE conductor that originates from the Kushma substation of Parbat District and terminates at the New Butwal substation Rupandehi district, Nepal [15]. As this section of the transmission line passes through diverse terrains including the Terai region of Palpa, Rupandehi, and Nawalparasi district, there will be high penetration of solar generators in its ending substations resulting in high congestion on line.

Table 1- 2 Line Detail of 220 kV Kushma-New Butwal Transmission Line Section

SN	Details	Symbol	Value	Unit
1	Starting SS	Kushma SS		
2	Ending SS	New Butwal SS		
3	Characteristics	Covers terai areas of Nepal rich in future solar energy generation.		
4	Voltage Level	V	220	kV
5	Line Length	L	88	km
6	Power Transmitted	P_T	800	MW
7	Conductor Used	HTLS DRAKE		
8	Area of a cross-section of the conductor	A	519.7	mm^2
9	Number of Circuits	Nc	2	Nos.
10	Number of Conductors in Bundling	Nb	2	Nos.
14	Conductor Outside Diameter	D0	28.11	mm
15	Emissivity	ε	0.8	Number
16	Solar absorptivity	α	0.8	Number
17	Conductor Resistance	RTs	0.0717	Ohm/m
18	Static Thermal Rating	STR	1480	Amps

CHAPTER 2 LITERATURE REVIEW

Different studies have been carried out on congestion management and dynamic thermal rating. Subsection 2.1 reviews the different DLR studies carried out related to congestion management and dynamic line rating applications till now. Subsection 2.2 presents the research gap between past studies and considerations of this research to address such research gaps.

2.1 Previous Studies

A large number of studies have been done based on DLR optimization of transmission lines and its application in transmission congestion management. Nabav et al. [3] addresses the issue of congestion management in electricity markets using the nodal pricing mechanism. Nodal pricing is an approach that determines the price of electricity at each node (or location) in the power grid, which helps in efficiently dispatching power. However, congestion in the transmission network can lead to inefficiencies and price distortions. The authors propose using a genetic algorithm (GA) to optimize the allocation of generation and transmission resources to alleviate congestion while maintaining system reliability and minimizing costs. The GA approach is used to determine the optimal generation dispatch and transmission switching strategy, considering the dynamic nature of power systems.

The proposed method is tested on a simulated power system, and the results show that the genetic algorithm can effectively manage congestion by finding optimal solutions that balance load, generation, and transmission constraints. The GA-based approach demonstrates its ability to adapt to complex, nonlinear optimization problems, providing better economic dispatch and improved grid stability compared to traditional methods. This method not only addresses congestion but also offers a flexible and scalable solution for congestion management in larger, more complex power grids. The authors conclude that genetic algorithms are a promising tool for improving the efficiency of congestion management in electricity markets while ensuring the stability of the power system.

The analysis of the potential of dynamic line rating on congestion management for a large power system network is analyzed in Schneider et al. [2]. It explores the use of dynamic line ratings (DLR) as an innovative approach to managing congestion in large-scale power systems. DLR refers to the real-time assessment of the thermal

limits of transmission lines, which can vary depending on environmental factors such as temperature, wind speed, and solar radiation. The authors examine how DLR can be leveraged to increase the utilization of existing transmission lines, thus alleviating congestion without the need for costly infrastructure upgrades. By integrating DLR into power system operation, congestion management can become more flexible and responsive to changing conditions, improving the overall efficiency and reliability of the grid.

The paper presents a theoretical analysis to quantify the potential benefits of DLR in managing congestion within large power networks. Using case studies and simulations, the authors demonstrate that DLR can significantly enhance the capacity of transmission lines during peak load periods, reducing the need for curtailment and providing better economic outcomes. The results show that DLR can contribute to more efficient use of transmission assets, improve the dispatch of power, and decrease operational costs. The authors conclude that while the full implementation of DLR in practice requires overcoming challenges related to data acquisition and system integration, its potential for improving congestion management in power systems is substantial, especially in regions with constrained transmission capacity.

Kosec et al. [6] investigates the use of dynamic thermal ratings (DTR) for assessing the real-time thermal limits of power transmission lines. The authors focus on how environmental factors, particularly rainy conditions, influence the thermal behavior of power lines and, consequently, their capacity for power transmission. A comprehensive model is developed to simulate the dynamic rating of transmission lines, which adjusts based on changing weather conditions, such as ambient temperature, wind speed, and precipitation. This model allows for more accurate predictions of the maximum current a line can carry without exceeding its thermal limit, compared to traditional static ratings that do not account for weather variations.

The paper presents both theoretical models and experimental measurements to validate the dynamic thermal rating approach in rainy conditions. The authors conduct field measurements to evaluate the accuracy of the DTR model and its ability to adjust for the cooling effects of rain, which can reduce the risk of overheating and allow for higher power transmission. The results show that accounting for real-time environmental factors leads to a more efficient and reliable operation of the power

grid, particularly during adverse weather conditions. The authors conclude that incorporating dynamic thermal ratings into the management of power lines can enhance grid flexibility, optimize the use of existing infrastructure, and improve overall system performance, particularly in regions where weather conditions frequently vary.

Bhattarai et al. [16] explores the potential of using weather-based dynamic line rating (DLR) to improve the utilization of transmission line ampacity, which is the maximum amount of current a power line can safely carry. Bhattarai argues that traditional static ratings, which are based on conservative assumptions and do not consider real-time environmental conditions, significantly underutilize the capacity of transmission lines. By incorporating weather data such as temperature, wind speed, and humidity into the calculation of line ratings, the author proposes a more accurate and adaptive approach that can increase the amount of power transmitted through existing infrastructure, thus improving efficiency and reducing the need for costly upgrades or expansions of the grid.

The paper presents a detailed analysis of how weather-based DLR can optimize the use of transmission lines by adjusting ampacity based on real-time weather conditions. Through simulations and case studies, Bhattarai demonstrates that the weather-based DLR method can significantly enhance the performance of the grid by increasing the available capacity during favorable weather conditions and reducing the risk of overheating under extreme conditions. The results show that using this approach can lead to better utilization of transmission assets, improving grid stability and reliability while minimizing operational costs. The author concludes that integrating weather-based DLR into power system operations provides a promising solution for managing transmission line capacity more effectively, particularly in areas where weather conditions vary frequently.

Alvarez et al. [11] focuses on improving the accuracy of dynamic line rating (DLR) for transmission lines by utilizing both direct and indirect measurements. The authors propose a state estimation method that aims to predict the thermal status of power lines in real-time, considering both the electrical parameters (such as current and voltage) and environmental factors (such as temperature and wind speed). The approach combines direct measurements of line temperature with indirect estimates

derived from electrical measurements and weather data, enabling a more precise calculation of the line's thermal steady state.

Through their methodology, the authors demonstrate that this hybrid approach to state estimation can significantly enhance the performance of DLR systems, especially in capturing the dynamic thermal conditions of transmission lines. By integrating direct temperature measurements with indirect ones, the approach offers a more reliable and cost-effective solution to monitor and estimate the real-time thermal behavior of transmission lines. The results show that this method provides a more accurate assessment of line ampacity, thus improving the capacity utilization of power lines while ensuring safe operating conditions. The authors conclude that the proposed state estimation technique can be a valuable tool for optimizing the operation of transmission grids, particularly in real-time applications where accurate and continuous monitoring of transmission line conditions is crucial.

Andersson et al. [10] investigates the integration of dynamic line ratings (DLR) into power system corrective control strategies. The authors focus on the challenges posed by real-time changes in transmission line capacities due to varying environmental conditions, and how DLR can be used to enhance the robustness of corrective control measures. These measures are crucial for maintaining grid stability and reliability, particularly during periods of congestion or unexpected system disturbances. The paper presents a framework for incorporating DLR into control strategies that can respond effectively to sudden changes in line capacity, ensuring optimal operation while preventing system overloads or failures.

In their approach, Andersson and Bucher explore the application of robust optimization techniques to develop corrective control actions that can quickly adapt to real-time line rating changes. The authors propose methods to adjust the power flow in the grid, manage line loadings, and prevent line overheating, thereby improving system performance and reducing the likelihood of violations of thermal limits. Through simulations and case studies, the paper demonstrates that the inclusion of DLR in the corrective control process improves the flexibility and responsiveness of power systems under dynamic conditions. The results highlight that DLR-based control measures can lead to more efficient and stable grid operation, particularly

during periods of high demand or adverse weather, enhancing the overall reliability and economic performance of the power system.

Fan et al. [17] presents a method for forecasting the real-time thermal ratings (RTR) of overhead power lines using probabilistic models. The authors introduce a novel approach based on Conditionally Heteroscedastic Auto-Regressive (CHAR) models to predict the thermal behavior of transmission lines. These models account for the inherent variability and uncertainty in environmental factors such as temperature, wind speed, and humidity, which influence the thermal rating of overhead lines. By incorporating probabilistic forecasting, the authors aim to provide more reliable and accurate real-time thermal ratings, allowing for better management of transmission line capacities.

Through the use of CHAR models, the paper demonstrates how the dynamic and uncertain nature of environmental conditions can be incorporated into real-time forecasting of line temperatures. The authors show that this approach provides a probabilistic forecast that reflects the uncertainty of line ratings, enhancing the decision-making process in grid management. The results indicate that using these probabilistic models can improve the accuracy of RTR predictions, leading to better utilization of transmission lines and reducing the risk of overheating. The authors conclude that this method is a valuable tool for optimizing the operation of power grids, allowing grid operators to make more informed decisions about load management and congestion alleviation, while improving the reliability and efficiency of the system.

Tech et al. [8] provides a comprehensive review of the potential benefits and challenges associated with integrating dynamic thermal rating (DLR) systems into the management of electrical networks. The author discusses how DLR systems offer a more accurate and real-time assessment of the thermal limits of transmission lines compared to traditional static ratings, which are based on fixed, conservative assumptions. By accounting for varying environmental conditions such as temperature, wind speed, and humidity, DLR systems can improve the utilization of existing transmission infrastructure, increase the transmission capacity of overhead lines, and contribute to more efficient power flow management in electrical networks.

The paper also examines the various methodologies and technologies used in DLR systems, including sensor-based measurements, forecasting models, and real-time data integration, which enable grid operators to optimize power system operations. Tech highlights the potential of DLR to enhance the reliability and flexibility of electrical networks, particularly in areas with high renewable energy penetration or in regions prone to congestion. While the paper acknowledges the challenges of implementing DLR, such as the need for accurate weather data, system integration, and real-time monitoring, it concludes that the widespread adoption of DLR systems could significantly improve grid performance. The author emphasizes that DLR can lead to more reliable and resilient electrical networks, reduce operational costs, and improve the overall efficiency of transmission systems.

Metwaly et al. [18] explores the integration of a fuzzy logic-based dynamic thermal rating (DLR) system with a System Integrity Protection Scheme (SIPS) to improve the security and reliability of transmission lines. The authors propose using fuzzy logic to manage the uncertainties associated with environmental factors affecting the thermal limits of transmission lines. This fuzzy-based approach enables real-time adjustments to the thermal ratings by considering various uncertain and imprecise data inputs, such as weather conditions, line loading, and system behavior. By combining this with a SIPS, which protects the power system from potential instability or overloads, the authors aim to enhance the overall security of transmission line operations.

The paper presents a model where the fuzzy DLR system continuously adjusts the thermal rating of lines based on real-time data and, when necessary, activates protective measures through SIPS to prevent line failures or overheating. The authors demonstrate, through simulations, that this integrated approach improves transmission line security by ensuring that lines are operated within their safe thermal limits, even under fluctuating load and weather conditions. The results show that the proposed system enhances grid resilience, reduces the risk of transmission line outages, and optimizes the use of available capacity, leading to more efficient and reliable operation of the power network. The authors conclude that the fuzzy DLR system, when paired with a SIPS, offers a promising solution for ensuring the security of transmission lines, particularly in regions with high system variability or congestion.

Dawson et al. [13] examines the potential benefits and challenges of applying dynamic thermal line rating (DLR) to long transmission lines. The authors focus on how DLR, which adjusts the thermal rating of power lines in real-time based on environmental conditions, can improve the utilization and efficiency of long-distance transmission systems. Long transmission lines typically face limitations in capacity due to static thermal ratings, which do not account for varying weather conditions such as temperature, wind speed, and humidity. By integrating DLR, the authors propose that the capacity of these lines can be better optimized, leading to more reliable and cost-effective power delivery over long distances.

Through their analysis, Dawson and Knight explore both the technical feasibility and economic implications of implementing DLR on long lines. They present simulations and case studies showing that DLR can significantly enhance the transmission capacity of these lines during favorable weather conditions, thus reducing the need for additional infrastructure investments or system upgrades. However, the authors also highlight the challenges of implementing DLR, such as the need for accurate and continuous weather data, the integration of monitoring systems, and the potential risks associated with real-time control. Despite these challenges, the paper concludes that DLR offers substantial benefits for long transmission lines, improving grid efficiency and capacity utilization while ensuring the safe operation of the power system.

Cheng et al. [19] presents a novel approach for real-time dynamic line rating (DLR) of transmission lines. The authors combine a live simulation model with a Tabu search optimization algorithm to determine the real-time thermal rating of transmission lines based on continuously updated environmental data, such as temperature, wind speed, and humidity. The live simulation model dynamically simulates the line's temperature and loading conditions, while the Tabu search algorithm optimizes the transmission line's capacity, taking into account real-time system conditions and network constraints. This method enhances the accuracy and adaptability of DLR, making it more effective for managing power transmission in real-time.

Through their approach, the authors demonstrate how the combination of live simulation and Tabu search can improve the operational efficiency of transmission lines. The paper shows that this method allows for optimal use of available

transmission capacity by adjusting the line ratings according to fluctuating environmental and system conditions. The results from the simulations highlight that the proposed technique provides significant benefits in terms of grid reliability, efficiency, and congestion alleviation. The authors conclude that the integration of live simulation and Tabu search in real-time DLR can help maximize the utilization of existing transmission infrastructure, reduce operational costs, and enhance the overall performance of the power grid.

Similarly, Madadi et al. [20] presents a probabilistic approach for forecasting real-time dynamic line ratings (DLR) of transmission lines. The authors propose using a Dynamic Stochastic General Equilibrium (DSGE) model combined with stochastic volatility to account for the uncertainties and dynamic behaviors in the factors affecting line ratings, such as weather conditions and power system variables. This approach enables the forecasting of transmission line ratings in a probabilistic framework, capturing the inherent variability and uncertainty of both environmental factors and system conditions. By incorporating stochastic volatility, the method enhances the accuracy of forecasting by reflecting the fluctuating nature of environmental and operational parameters that influence line temperatures.

Through their proposed method, the authors demonstrate how incorporating stochastic models can provide more reliable and accurate predictions for real-time DLR. The probabilistic forecasting approach not only improves the understanding of line behavior under varying conditions but also aids in the decision-making process for grid operators, helping them optimize power flow and minimize the risk of transmission line overloads. The results from simulations show that this method can significantly enhance the efficiency of transmission lines by providing more precise real-time ratings, thus improving the utilization of existing infrastructure and contributing to more stable and reliable grid operations. The authors conclude that probabilistic DLR forecasting using DSGE with stochastic volatility offers a promising tool for advanced grid management, particularly in addressing the challenges posed by dynamic and uncertain operating environments.

2.2 Research Gap

Many studies are carried out for the evaluation of dynamic line rating via probabilistic approaches. Many relevant weather factors are involved as seen from the weather

model and impose difficulties in weather forecasting due to inherent uncertainties. Also, not any studies carry the spatial features of transmission line due to different geographical conditions along the line. Probabilistic approaches such as Monte Carlo Sampling provide similar results but need higher iteration levels for complex long transmission networks resulting in high computational costs. Weather uncertainties and spatial topology of TL will be captured using a regression model. A fast iterative truncated normal probability distribution of line thermal capacity is proposed for calculation with lower cost.

Similarly, in the case of INPS, there is no such study carried out considering the dynamic nature of transmission line conductors incorporating weather uncertainties and geographical conditions. The congestion management with a dynamic rating concept is not studied for the case of transmission lines penetrated with a large number of small renewal generators. Many of the transmission lines in INPS are being used in overloaded conditions during evening peaks of daily load. Also, some other transmission lines connecting major cities' loads are being overloaded during seasonal peaks. A study for the capacity expansion of major transmission lines present in the Nepalese grid will be beneficial for transmission utilities from a techno-economic prospective.

CHAPTER 3 RESEARCH METHODOLOGY

After reviewing various studies related to line dynamics and weather forecasting models/algorithms, it is evident that much of the research has focused on evaluating dynamic line ratings for transmission lines while minimizing uncertainties and computational costs. Despite numerous studies, challenges such as reducing computational costs, capturing the spatial features of transmission lines, and minimizing weather uncertainties remain unresolved. This research aims to address these gaps. Figure 3- 1 below represents the generalized flowchart of the proposed methodology. In the first step, the details of transmission line topology, the electro-mechanical characteristics of the overhead conductor used for the transmission, and the geographical location along the transmission line for weather data collection are determined. The second step of the methodology is to collect weather data such as wind speed and incidence angle, ambient temperature, solar radiation, etc. for the different sections of the transmission line. In the third step, the dynamic rating of the individual span of the transmission line is estimated using IEEE standards. The span for which the dynamic rating is minimal is termed a critical span and the rating of the whole transmission line is governed by the thermal rating of that critical span. The additional capability released compared to primitive techniques of static thermal rating is the available congestion limit for renewal energy generators and therefore the power generated from renewal energy resources can be evacuated by using this additional line capacity.

3.1 Transmission Line Data Collection

In the proposed methodology, detailed information about the transmission line is crucial, as it forms the foundation for accurately modeling and validating the DTR system. The transmission line selected serves as the reference network, meaning that all modeling, analysis, and testing will be based on its real-world parameters and conditions. Firstly, the topology of the transmission line is a critical factor. Topology refers to the physical and geographical arrangement of the line, including its layout, elevation, orientation, and proximity to environmental factors like mountains, rivers, or urban infrastructure. The topology directly influences the meteorological parameters that the line is exposed to, such as wind patterns, ambient temperature, humidity, and precipitation. For instance, a line segment passing over a river or valley

may experience different wind speeds compared to one running through an open plain or an urban area. These variations significantly affect the DTR, as the conductor's ability to dissipate heat and carry current safely is influenced by surrounding environmental conditions. Thus, understanding the topology helps in determining localized weather effects, which is vital for accurate DTR calculation.

To ensure precision, the geographical coordinates (latitude and longitude) of different line segments are collected. This segmentation allows the model to consider location-specific weather variations. For instance, if a transmission line spans a large geographical area, segments in higher altitudes might experience cooler temperatures and stronger winds, enhancing the conductor’s cooling effect. Conversely, segments in lower or urban areas may be exposed to higher ambient temperatures and lower wind speeds, potentially reducing the line’s thermal capacity. Therefore, weather data specific to each location including temperature, wind speed, humidity, and precipitation is gathered for accurate analysis. This data can be sourced from historical weather databases or real-time meteorological monitoring systems.

In addition to geographical and meteorological data, the electro-mechanical characteristics of the overhead bare conductor used in the transmission line are also collected. These characteristics include the conductor’s material composition (such as aluminum, steel, or composite materials), diameter, weight, thermal conductivity, emissivity, heat capacity, and resistance. Each of these properties affects how the conductor heats up and dissipates heat. For example, a conductor with higher thermal conductivity can dissipate heat faster, thus allowing higher current flows. Similarly, the conductor's tensile strength and sag characteristics are essential for determining its mechanical stability and safe operating limits under varying thermal loads.

By combining the topological data, localized meteorological parameters, and conductor characteristics, the model can accurately simulate real-world conditions affecting the DTR of the transmission line. This detailed data collection ensures that the model reflects the actual operational environment, leading to reliable and precise thermal rating predictions. This, in turn, supports the safe and efficient optimization of the transmission line's capacity, particularly for integrating additional renewable energy into the grid.

3.2 Generalized Flowchart

The flowchart titled Figure 3- 1 outlines a systematic approach for enhancing the capability of a 220 kV transmission line using Dynamic DTR and weather data analysis. The process begins with a literature review, where existing studies and methodologies related to DTR, transmission line optimization, and congestion management are thoroughly examined. This step establishes a foundational understanding and identifies existing practices, trends, and limitations. Following this, the researcher engages in identifying the research gap, critically analyzing the literature to pinpoint areas that lack sufficient exploration or solutions. This ensures that the study is directed toward addressing significant challenges in the field. Once the research gaps are identified, the next phase is the formulation of clear objectives, focusing on optimizing the TL's thermal capacity and improving the integration of renewable energy into the power grid.

Subsequently, the methodology emphasizes variable identification, classifying the variables into independent and dependent categories. The independent variables consist of key weather parameters such as temperature, wind velocity, relative humidity (RH), and precipitation, all of which significantly impact the transmission line's performance. The dependent variable is the line thermal rating, representing the maximum safe current-carrying capacity of the TL under varying environmental conditions. Understanding the interaction between these variables is critical for developing an accurate DTR model. Following this, comprehensive data collection is conducted, focusing on gathering detailed information about the TL's topology, materials, and meteorological data relevant to the independent variables. This ensures that the model is grounded in accurate and realistic conditions.

The core of the methodology involves the development of an IEEE-based DTR calculation model integrated with a congestion release model. This dual approach allows for accurate estimation of the TL's real-time thermal capacity while also addressing potential congestion issues in the power system. The developed model is then subjected to testing on an actual 220 kV transmission line to validate its effectiveness under real-world conditions. A critical decision point follows, where the model's results are analyzed for verification. If the results are verified, it confirms that the model accurately predicts thermal capacity and efficiently manages congestion,

leading to the output of additional capability released for RE integration. This means the transmission line can accommodate higher renewable energy penetration without risking thermal overload or operational inefficiencies. However, if the results are not verified, the process loops back for refinement, possibly involving recalibration of the model, additional data collection, or re-evaluation of the methodology.

The final outcome of this methodological framework is a validated, reliable model that enhances the transmission line's capacity while supporting the integration of renewable energy. This systematic approach ensures accuracy, efficiency, and practicality, contributing to the optimization of power systems and promoting sustainable energy distribution. By incorporating iterative feedback loops and meticulous data analysis, the methodology ensures continuous improvement, aligning with modern energy system requirements and facilitating the transition toward a more resilient and efficient grid.

3.3 Simulating Proposed Model

The MATLAB model is developed for the simulation of the transmission line dynamic rating calculation and its capability release for the injection of additional power generated through renewal energy generators. This section represents the MATLAB simulation model to evaluate additional transmission line capability released via the existing transmission line.

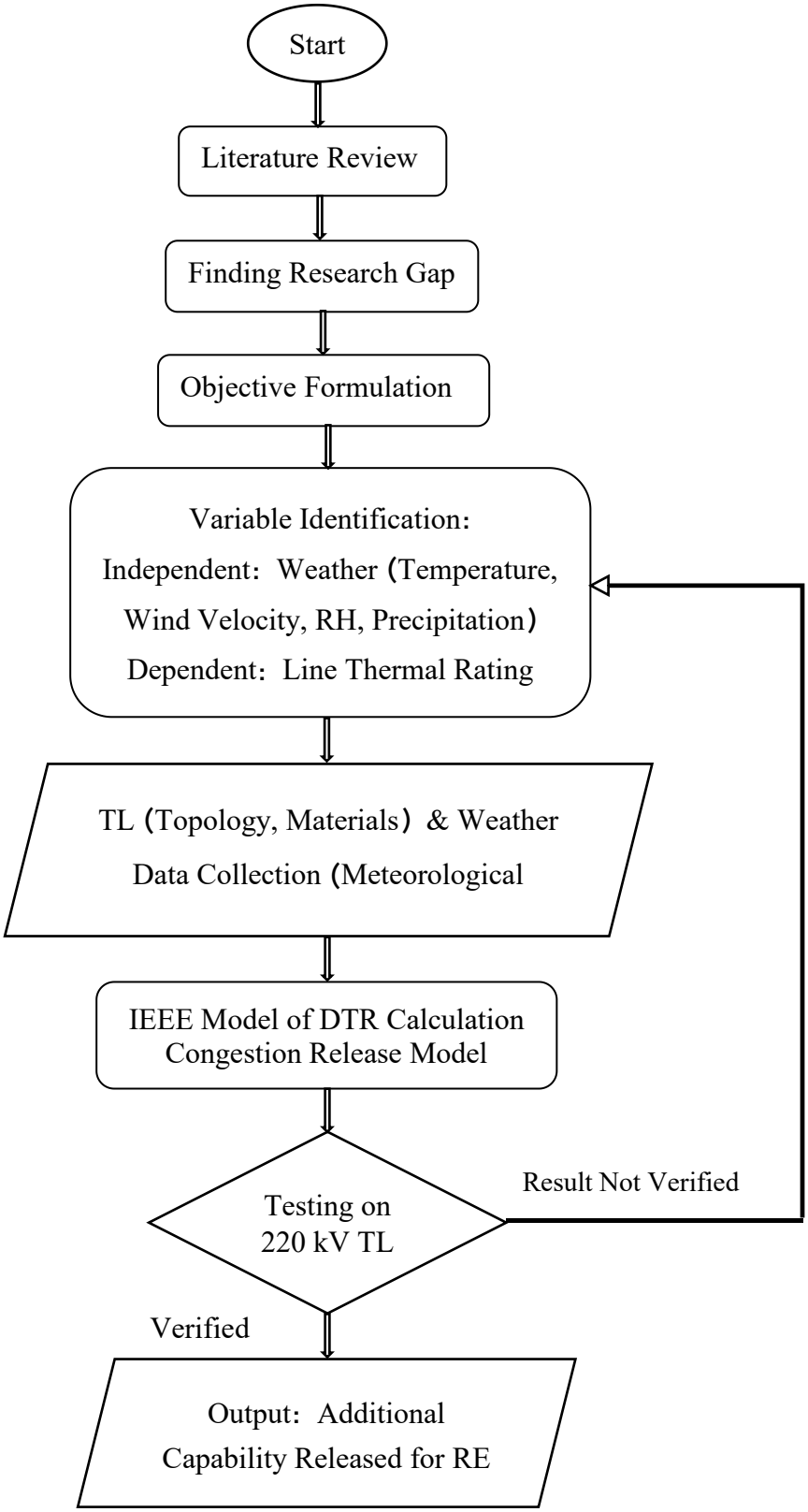

Figure 3- 1 Generalized Flowchart for the methodology

3.3.1 Simulation Model for DTR Evaluation:

After collecting the weather parameters using the different weather forecasting agencies and calculating their impact on transmission line thermal rating as discussed earlier in subsection 3.4, the dynamic thermal rating of critical transmission line spans is evaluated using DLR modeling as presented in subsection 3.5. The overall block diagram for the MATLAB DTR simulation block is presented below.

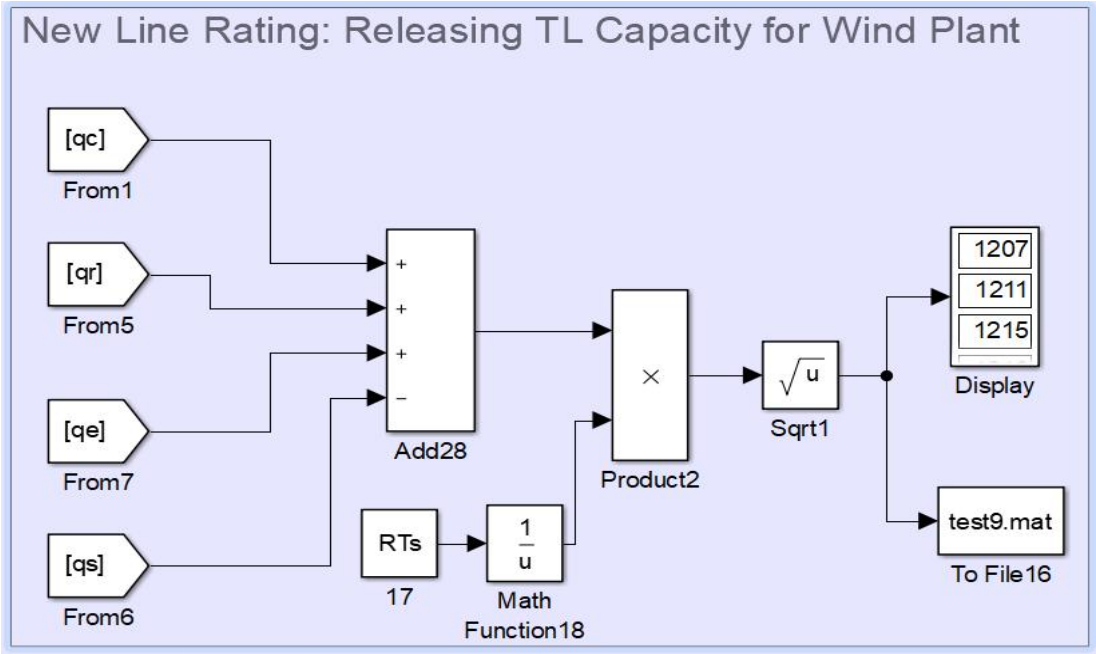

Figure 3- 2 MATLAB simulation model for new line rating estimation

The inputs used for this model are as presented in the IEEE approach for DTR evaluation [9] where convection cooling loss is the heat loss through the transmission line conductor due to convection cooling. Using the heat balance expression presented in different literatures, it can be noted that convection cooling loss is a function of conductor temperature Tc, ambient temperature Ta, wind velocity V, and wind incidence angle ϕ. Here, weather data obtained from the weather agencies are used to calculate the data required to evaluate convection cooling loss. Precipitation cooling is the heat loss through the transmission line conductor due to precipitation cooling. It is noted that precipitation cooling loss depends on the rainfall rate Pr, humidity present in air RH, and ambient pressure Pa. Literature [21] , [6] provides the numerical modeling to achieve heat loss due to precipitation cooling in overhead transmission line conductors. Radiation cooling loss is the heat loss through a transmission line conductor due to radiation heat transfer via a heated conductor surface. It is noted that

radiation cooling loss is a function of conductor temperature Tc, and ambient temperature Ta. Literature [9] provides numerical modeling to achieve heat loss due to radiation cooling in overhear transmission line conductors. Heat gain from solar density is the heat gain of the transmission line conductor due to radiation heat transfer via solar energy on the conductor surface. Solar radiation heat gain Qs is determined by solar heat density Qse which is represented by a polynomial function with the independent variable of the date of the calendar. Literature [9] provides numerical modeling to achieve heat gain due to solar radiation on an overhead transmission line conductor. With these heat loss and gain data, the thermal rating of the transmission line can be evaluated by modeling equation (1) of subsection 3.5.1.

3.4 Impact Analysis of Weather Factors

In this section, weather factors are modeled to evaluate the required dynamic thermal capacity evaluations. The impacts of different weather parameters on transmission line span thermal capacity are studied. As the topology of the transmission line is different for long-length transmission, the thermal capacity of the conductor varies with varying weather conditions. There is a large number of weather factors affecting the thermal rating. The impact of weather factors on transmission line thermal capability will be carried out in different past studies. While analyzing one weather factor, the rest are fixed at basis values commonly used in STR as provided in [9].

For the identification of the weather factors with higher impact levels, the difference between the maximum and minimum line thermal capacity to minimum line thermal capacity by the varying value of weather factor is estimated and given by,

$$Impact\ Level = \frac{Max.\ Capacity - Min.\ Capacity}{Min.\ Capacity} * 100\% \ldots\ldots\ldots\ldots (4)$$

3.5 DLR Modeling

The dynamic thermal rating of an overhead bare conductor is estimated using standards like IEEE and CIGRE standards for the calculation of the ampacity of an overhead bare conductor. Subsection 3.5.1 presents the IEEE model of line span thermal capability calculation. Subsection 3.5.2 discusses about calculation of dynamic rating for the whole transmission line segment considering the minimal span thermal capability of individual span.

3.5.1 IEEE Approach of DLR Modeling of Individual Span

From the heat balance equation, it is known that span thermal capacity is a nonlinear function of multiple weather factor variables and therefore it is difficult to hundred percent accurate dynamic rating of a transmission line. By using topological weather data collected across different sections of transmission line, the dynamic thermal rating as per IEEE standard [9] is given as:

$$I_k = \sqrt{\frac{Q_r\left(T_{c\,max}, T_{a,k}\right) + Q_c\left(T_{c\,max}, T_{a,k}, V_k, \phi_k\right) + Q_e(P_{r,k}) - Q_s(Q_{se})}{R(T_{c\,max})}} \quad \ldots\ldots\ldots\ldots(1)$$

Where,

Qs: is heat gain rate from the sun, W/m

Qr: is radiated heat loss rate per unit length, W/m

Qc: is convection heat loss rate per unit length, W/m

R: is the resistance of the conductor, Ω

Tc, max: is maximum conductor temperature, ^{o}C

Ta: is ambiant temperature, ^{o}C

Vk: is wind velocity at kth section, m\s

Φk: is wind incidence angle at kth section, degree

Pr: is precipitation rate, mm\hr

3.5.2 DLR Evaluation of the Whole Transmission Line

The length of the long transmission line under study has to be divided into several critical segments where there can occur worst weather conditions. Dividing TL into multiple span locations, the thermal capacity of each segment is evaluated and the rating of the whole transmission line is given by the most critical span thermal capacity. The minimum value of thermal capacity among all critical spans is the dynamic thermal rating of that transmission line.

If Ik is the span thermal capacity of a particular span k and T is the thermal rating of the transmission line, then we can write

$$T = \min (I_k) \ldots\ldots\ldots\ldots (2)$$

This least thermal capability among all of the spans gives the minimum thermal rating of the whole transmission line under consideration.

4.1.1 Impact on 500 mm^2 ACSR MOOSE

Evaluation of weather impact level in span thermal capacity is achieved using MATLAB coding and Excel. Here, while evaluating the impact of one factor, others are taken at the same value as taken for the calculation of Static Line Thermal Rating (STR). The figure below shows the effect of different weather factors discussed in subsection 3.4 on the line thermal rating of ACSR MOOSE.

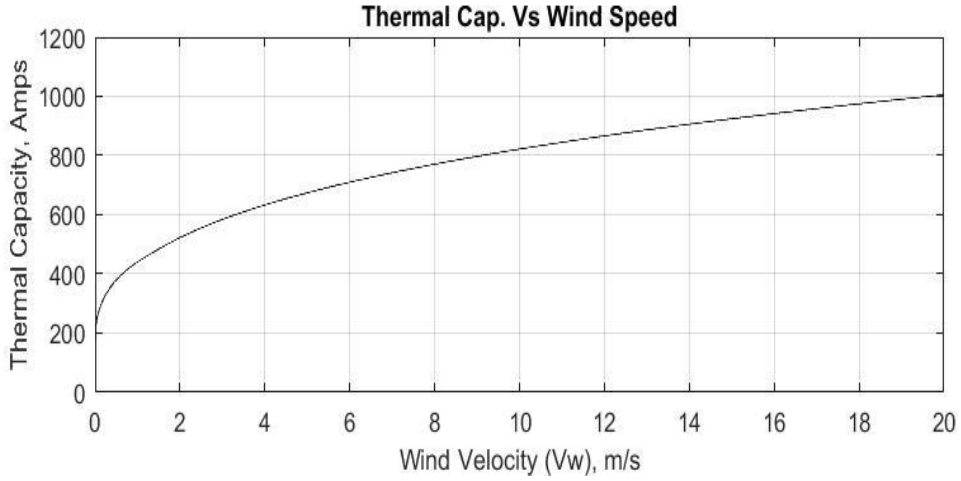

Figure 4- 1 Impact of wind velocity in span thermal capacity of ACSR MOOSE

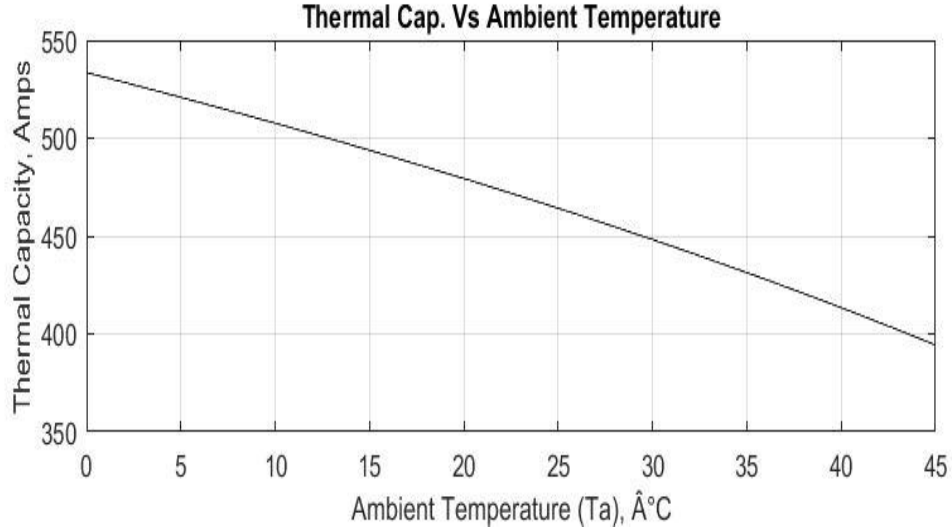

Figure 4- 2 Impact of ambient temperature in span thermal capacity of ACSR MOOSE

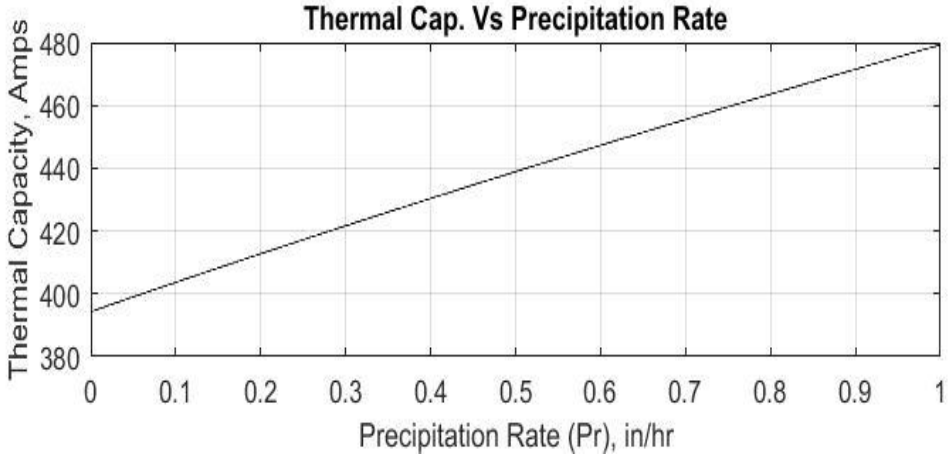

Figure 4- 3 Impact of precipitation in span thermal capacity of ACSR MOOSE

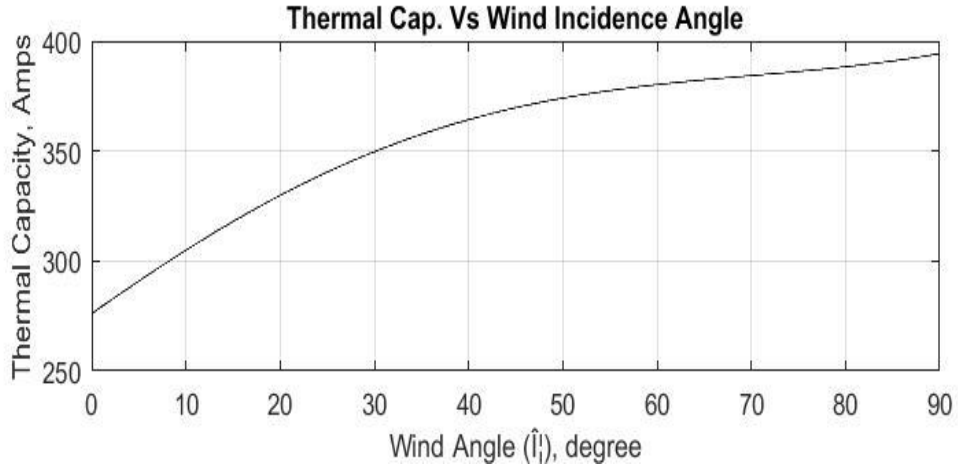

Figure 4- 4 Impact of wind incidence angle in span thermal capacity of ACSR MOOSE

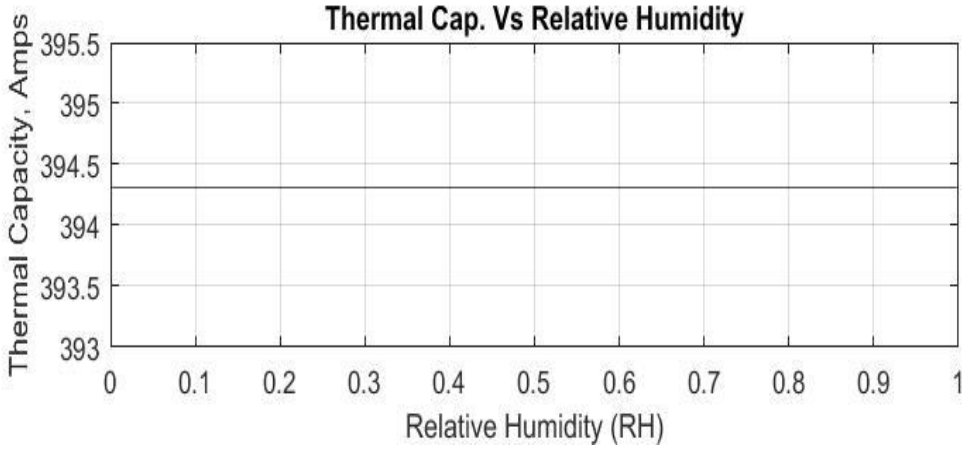

Figure 4- 5 Impact of relative humidity in span thermal capacity of ACSR MOOSE

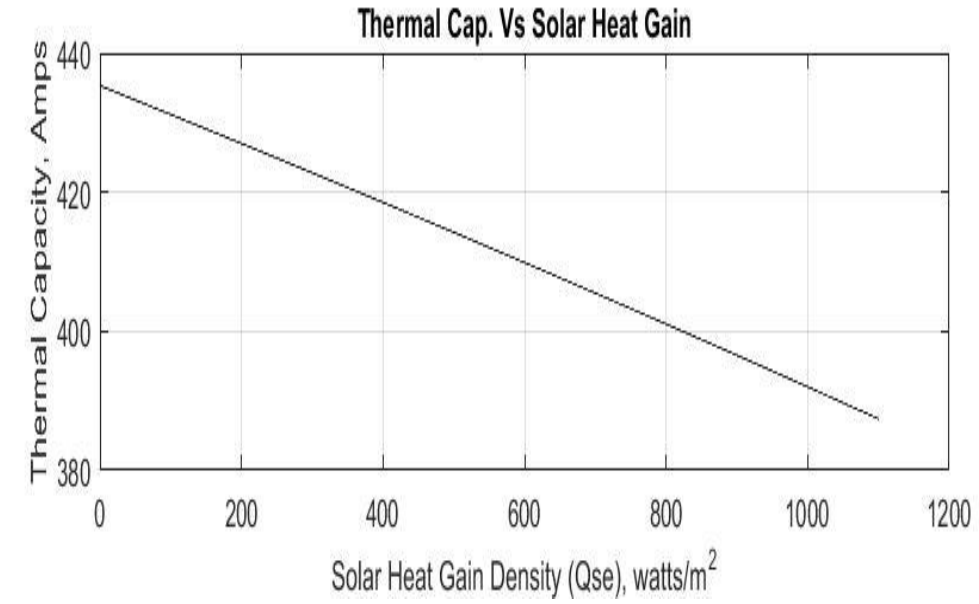

Figure 4- 6 Impact of solar heating gain density in span thermal capacity of ACSR MOOSE

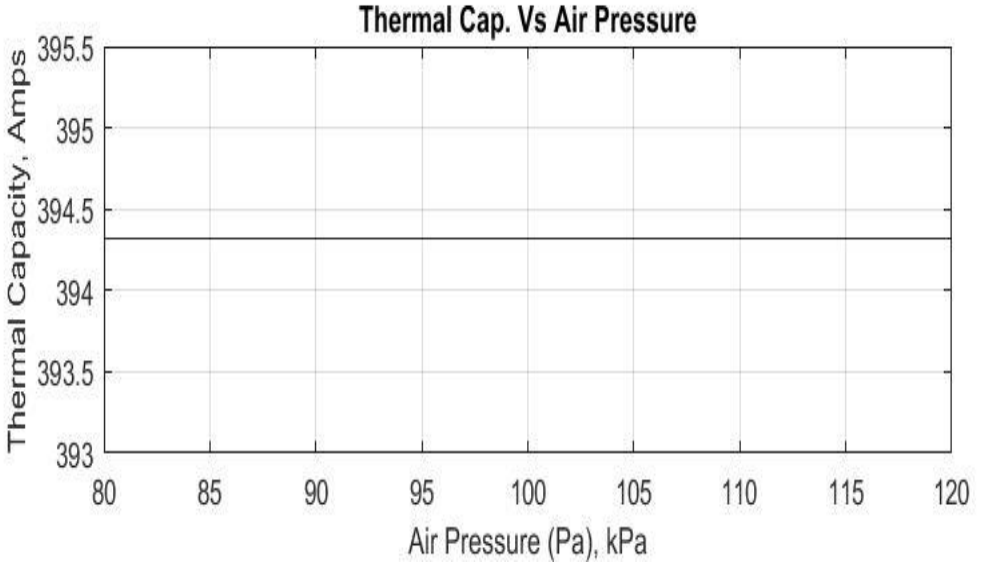

Figure 4- 7 Impact of atmospheric pressure in span thermal capacity of ACSR MOOSE

Performing impact analysis on ACSR MOOSE conductor, it is proved that there is the greatest variation of span thermal capability of the transmission line concerning wind velocity. Here impact level of remaining weather factors is evaluated for different wind velocities. This percentage impact level for different wind velocities is presented in Table 4- 1 below:

Table 4- 1 Percentage impact level of weather factor on ACSR MOOSE

Factors	Limits	Wind Velocity, V (m/s)				
		0.6	2	4	8	12
Ta	0-45 °C	35.30	34.45	33.98	33.66	33.52
φ	0-90°	42.83	49.71	52.92	55.28	56.33
Qse	0-1100 w/m2	12.36	7.10	4.86	3.29	2.61
Pr	0-1 in/h	21.55	13.23	10.18	9.18	9.53
RH	0-100%	0.00	0.00	0.00	0.00	0.00
Pa	80-120 kPa	0.00	0.00	0.00	0.00	0.00

From this discussion, it is clear that wind speed, ambient temperature, wind incidence angle, solar heat density, and rainfall rate have the greatest impact on the line current carrying capabilities of the transmission line. There are negligible effects of relative humidity and ambient pressure and related uncertainties to those factors can be neglected. Those most influential weather factors should be considered while modeling the regression method of forecasting and non-influential can be fixed at the basis value as taken in the case of STR. The effect of wind incidence angle is greater terrain information has a greater role in critical span selections.

4.2 Numerical Testing of Proposed Model

Different 66 kV, 132 kV, and 220 kV transmission lines of Integrated Nepalese Power System (INPS) with higher transmission congestion can be the study case for this methodology. Transmission lines at the voltage level of 220 kV are being constructed in a different region of INPS. According to the NEA annual report [14], there are four existing 220 kV transmission lines with a total length of 332.6 circuit km. These lines

connect some of the larger hydropower and grid substations to load centers in the southern part and cities of Nepal. ACSR BISON, DRAKE, and MOOSE are the most commonly used conductors in 220 kV transmission lines. Also, a total of 509 circuit km of 220 kV transmission lines are in different phases of construction. To simulate the proposed methodology, a Dana-Kushma-New Butwal 220 kV transmission line which connects the northern wind generation region with the southern region with high solar PV generation feasibility, is taken under consideration.

Figure 4- 8 Snip showing proposed line (Dana-Kushma-New Butwal 220 kV) for Numerical Testing

This transmission line with wind and solar PV generation feasibility and the possibility of connection at its ending substation in the near future is studied for the evaluation of the efficiency of the proposed model. Also, this transmission line has the probability of future renewable energy-based generation installation and is divided into two regions namely the wind region which is the Dana-Kushma segment of the transmission line consisting of larger wind generation potential, and the solar region which is Kushma-Butwal segment with large solar potential.

4.3 Testing result of Dana-Kushma-New Butwal 220 kV TL

4.3.1 Weather Data Collection

As the weather sensors are not available along a line segment, historical data from organizations such as the National Renewable Energy Laboratory (NREL) [22] , NASA Power Data Access [23] , and the Department of Meteorology, Nepal [24] is

used. For this numerical testing example past meteorological data from 2016 to 2019 are used for generating the regression equation, and data from the year 2020 is used for future weather prediction.

Table 4- 2 Weather Station Detail of 220 kV Dana-Kushma-New Butwal TL

SN	Station Name	Latitude	Longitude	Elevation
1	WS1	28.53	83.65	1422
2	WS2	28.39	85.59	1135
3	WS3	28.24	83.64	930
4	WS4	28.04	83.68	944
5	WS5	27.88	83.67	893
6	WS6	27.76	83.63	1141
7	WS7	27.58	83.68	146

These weather station locations are assumed hypothetically so as to cover the weather parameters around the transmission line under consideration.

Figure 4- 9 Snip Showing Weather Locations for Dana-Kushma-New Butwal 220 kV TL Section

The wind measured for the different times of day of the year 2020 AD along the Dana-Kushma 220 kV section of the transmission line is analyzed and plotted in the histogram as represented in Figure 4- 10. The historical weather data shows that there is a wind speed of 1-1.5 m/s about 60% of the time in a whole year. About 95% of the time in the year 2020, there exists wind with a speed of about 1 m/s and above.

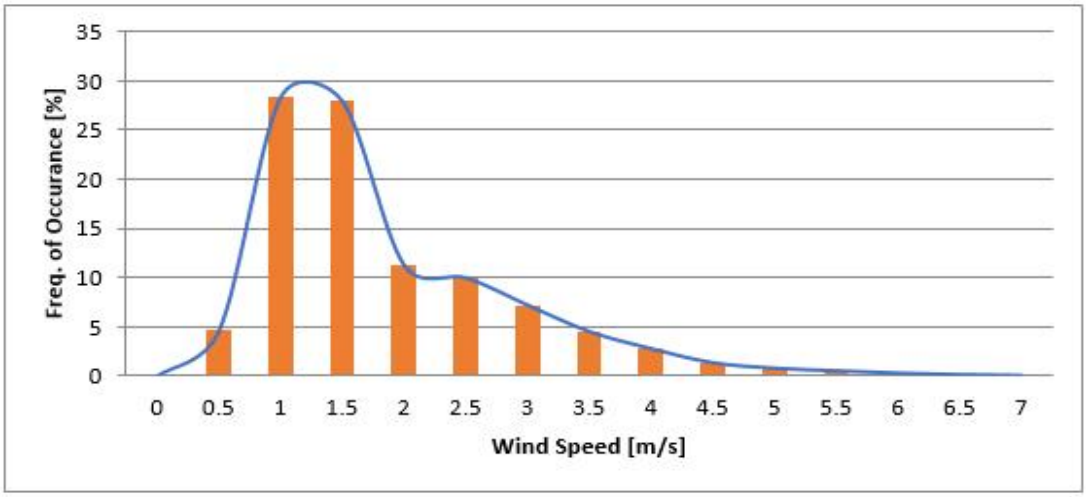

Figure 4- 10 Histogram Plot for Occurance of Wind in Dana-Kushma 220 kV TL Section for the Year 2020 AD

Similarly, Figure 4- 11, represents the histogram plot of the wind measured for the different times of day of the year 2020 AD along the Kushma-New Butwal 220 kV section of the transmission line. The historical weather data shows that there is a wind speed of 1 m/s about 35% of the time in a whole year. About 90% of the time in the year 2020, there exists wind with a speed of about 1 m/s and above. This wind speed data illustrates that there will be the highest chances of increased actual line thermal rating as compared to static thermal rating even in the Terai region of the transmission line where the solar radiation is very high as compared to uphill hilly areas.

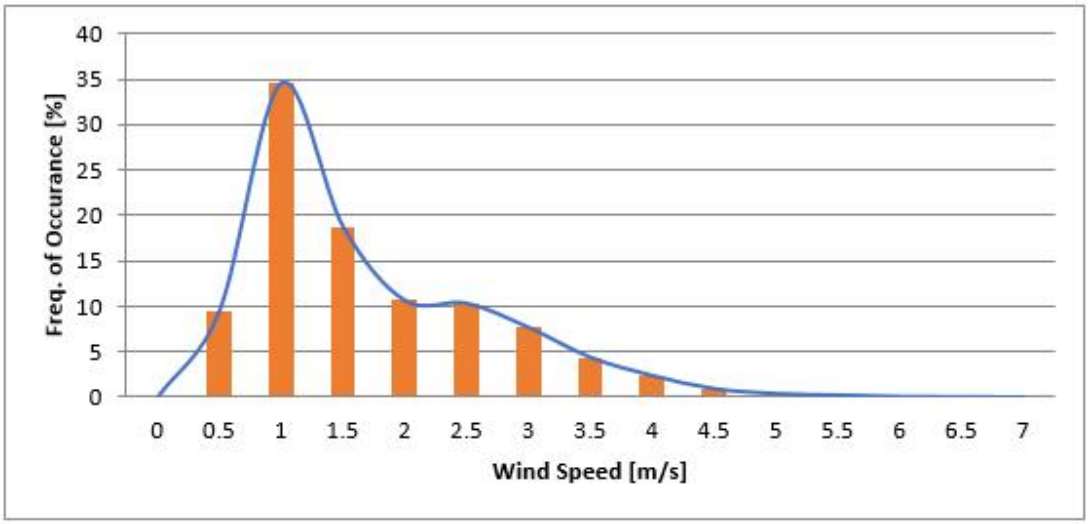

Figure 4- 11 Histogram Plot for Occurance of wind in Solar Region of Kushma-New Butwal 220 kV TL Section for the Year 2020 AD

After collecting different weather data along the Data-Kushma-New Butwal 220 kV transmission line sections, wind speed, the most influential weather factor to line thermal rating (as discussed in earlier subsection 3.4) is analyzed and plotted separately. The magnitude and frequency of wind occurrence in the whole transmission line section are plotted in the histogram plot Figure 4- 12. From these comparative graphs, it can be concluded that there will be a higher thermal rating than the traditional STR of this transmission line despite having climate and geographical variations.

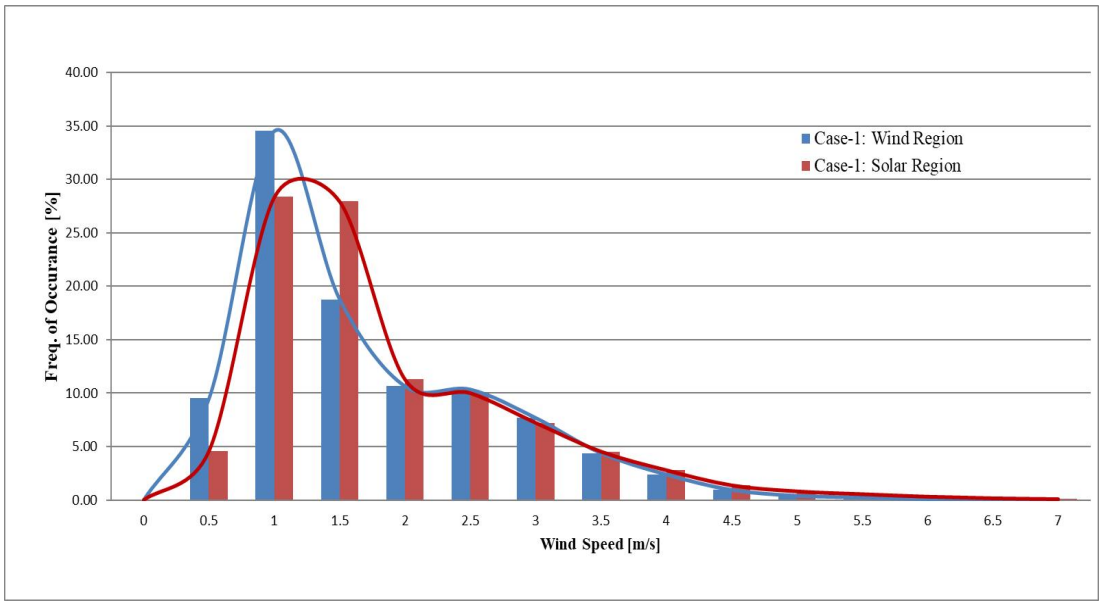

Figure 4- 12 Histogram Plot for Occurance of Wind on Dana-Kushma-New Butwal 220 kV TL Section for the Year 2020 AD

4.3.2 Estimating DTR "Releasing Congestion for Wind Plant"

With the weather data measured from the three nearby weather at the critical span of different transmission line sections, we can calculate different heat loss and gained parameters which will be used as an input for our DTR model. The dynamic thermal rating for a particular day can be estimated using weather data for that particular day. The actual dynamic line rating is calculated by using the exact weather conditions of the day by using the IEEE approach for DTR calculation as discussed in earlier subsection 3.5.1. After evaluating the dynamic thermal rating of the transmission line using actual weather data, a comparative analysis of DTR with traditional STR is performed. Figure 4- 13 represents the annual minimum, maximum, and average DTR to STR ratio for the year 2020 AD. From the annual maximum ratio curve, there will

be up to 70% higher dynamic line rating as compared to static rating. Similarly, the annual minimal ratio curve represents about a 25% decrease in line rating as compared to static rating, which occurs during the worst weather conditions. On average, there will always be a 20% higher capability available for additional congestion flow when dynamic thermal rating is applied as compared to the conventional static rating technique.

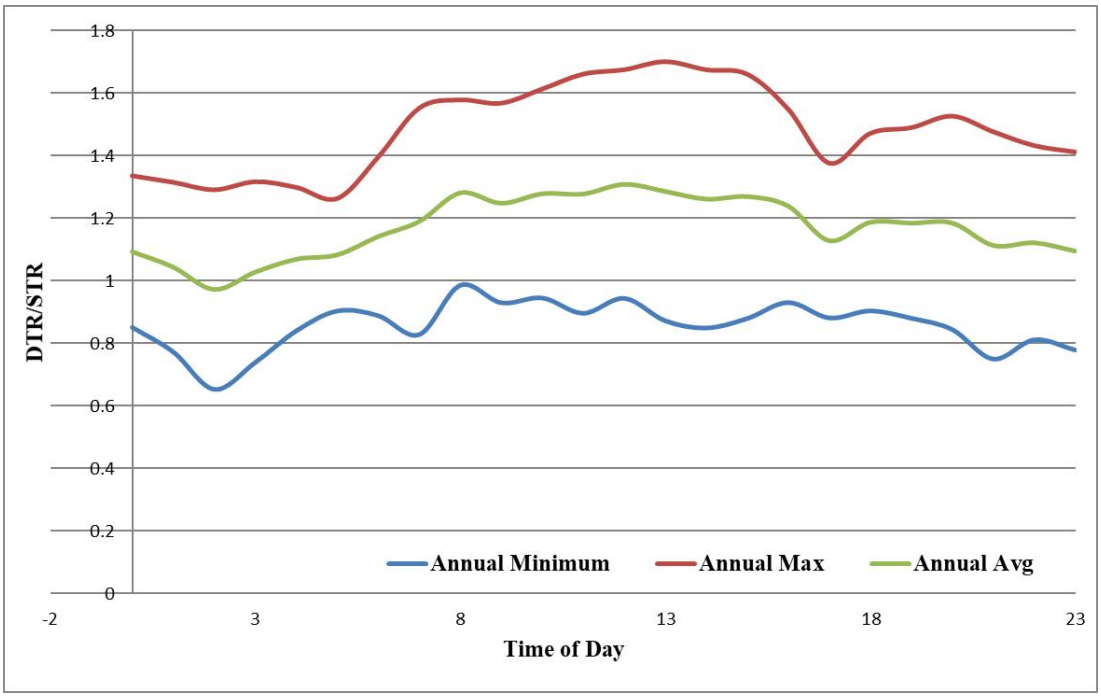

Figure 4- 13 Plot for DTR/STR vs. Time of Day for Dana-Kushma-New Butwal 220 kV TL for the Year 2020 AD

The plot in Figure 4- 14 represents the DTR/STR ratio for different months of the year 2020 AD. As discussed in the earlier section, the wind speed parameter is the most influential factor in line dynamic line rating and thus there are wide variations in DTR/STR ratios for different months. Comparatively, winter months have a larger DTR/STR ratio than summer hot months as the second most influential factor for dynamic thermal rating is ambient temperature and some sections of the transmission line under this study traverses through the Terai region having very high ambient temperature during the summer hot days.

The figures below from Figure 4- 15 to Figure 4- 20 represent the dynamic thermal rating forecasting for different sections of the Dana Kushma-New Butwal 220 kV Transmission line on different dates in the year 2020. One span within all sections has

been considered a critical span for the study of DTR. The static line rating for the transmission line is about 980 amperes which are shown in the graph above using a straight line. The nature of DTR estimated using actual weather data is evaluated and plotted by using an area plot indicated by green color. The results above show that the evaluated DTR usually lie below the STR.

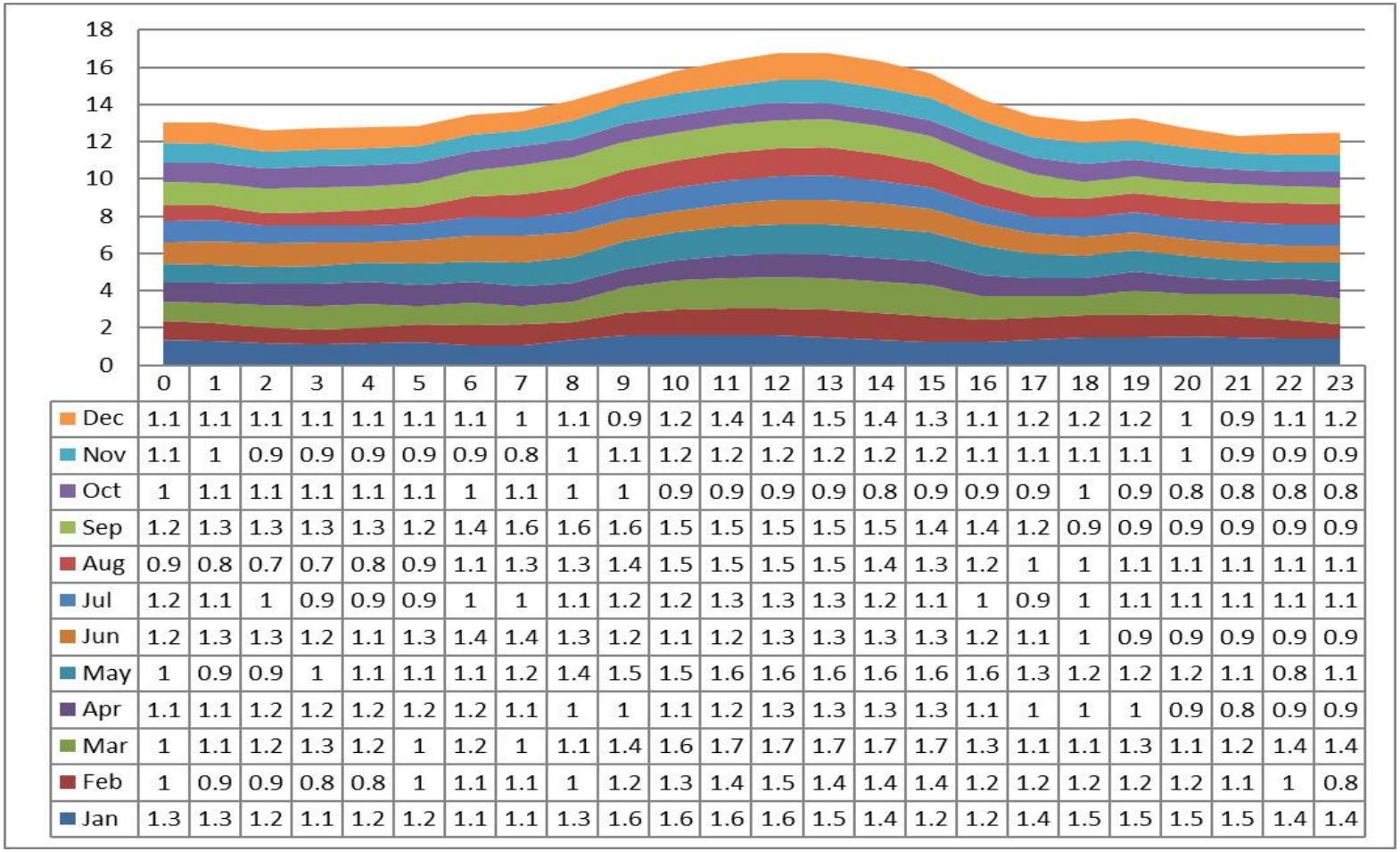

	0	1	2	3	4	5	6	7	8	9	10	11	12	13	14	15	16	17	18	19	20	21	22	23
Dec	1.1	1.1	1.1	1.1	1.1	1.1	1.1	1	1.1	0.9	1.2	1.4	1.4	1.5	1.4	1.3	1.1	1.2	1.2	1.2	1	0.9	1.1	1.2
Nov	1.1	1	0.9	0.9	0.9	0.9	0.9	0.8	1	1.1	1.2	1.2	1.2	1.2	1.2	1.2	1.1	1.1	1.1	1.1	1	0.9	0.9	0.9
Oct	1	1.1	1.1	1.1	1.1	1.1	1	1.1	1	1	0.9	0.9	0.9	0.9	0.8	0.9	0.9	0.9	1	0.9	0.8	0.8	0.8	0.8
Sep	1.2	1.3	1.3	1.3	1.3	1.2	1.4	1.6	1.6	1.6	1.5	1.5	1.5	1.5	1.5	1.4	1.4	1.2	0.9	0.9	0.9	0.9	0.9	0.9
Aug	0.9	0.8	0.7	0.7	0.8	0.9	1.1	1.3	1.3	1.4	1.5	1.5	1.5	1.5	1.4	1.3	1.2	1	1	1.1	1.1	1.1	1.1	1.1
Jul	1.2	1.1	1	0.9	0.9	0.9	1	1	1.1	1.2	1.2	1.3	1.3	1.3	1.2	1.1	1	0.9	1	1.1	1.1	1.1	1.1	1.1
Jun	1.2	1.3	1.3	1.2	1.1	1.3	1.4	1.4	1.3	1.2	1.1	1.2	1.3	1.3	1.3	1.3	1.2	1.1	1	0.9	0.9	0.9	0.9	0.9
May	1	0.9	0.9	1	1.1	1.1	1.1	1.2	1.4	1.5	1.5	1.6	1.6	1.6	1.6	1.6	1.6	1.3	1.2	1.2	1.2	1.1	0.8	1.1
Apr	1.1	1.1	1.2	1.2	1.2	1.2	1.2	1.1	1	1	1.1	1.2	1.3	1.3	1.3	1.3	1.1	1	1	1	0.9	0.8	0.9	0.9
Mar	1	1.1	1.2	1.3	1.2	1	1.2	1	1.1	1.4	1.6	1.7	1.7	1.7	1.7	1.7	1.3	1.1	1.1	1.3	1.1	1.2	1.4	1.4
Feb	1	0.9	0.9	0.8	0.8	1	1.1	1.1	1	1.2	1.3	1.4	1.5	1.4	1.4	1.4	1.2	1.2	1.2	1.2	1.2	1.1	1	0.8
Jan	1.3	1.3	1.2	1.1	1.2	1.2	1.1	1.1	1.3	1.6	1.6	1.6	1.6	1.5	1.4	1.2	1.2	1.4	1.5	1.5	1.5	1.5	1.4	1.4

Figure 4- 14 Plot for DTR/STR vs. Time of Day for Dana-Kushma-New Butwal 220 kV TL for the Year 2020 AD

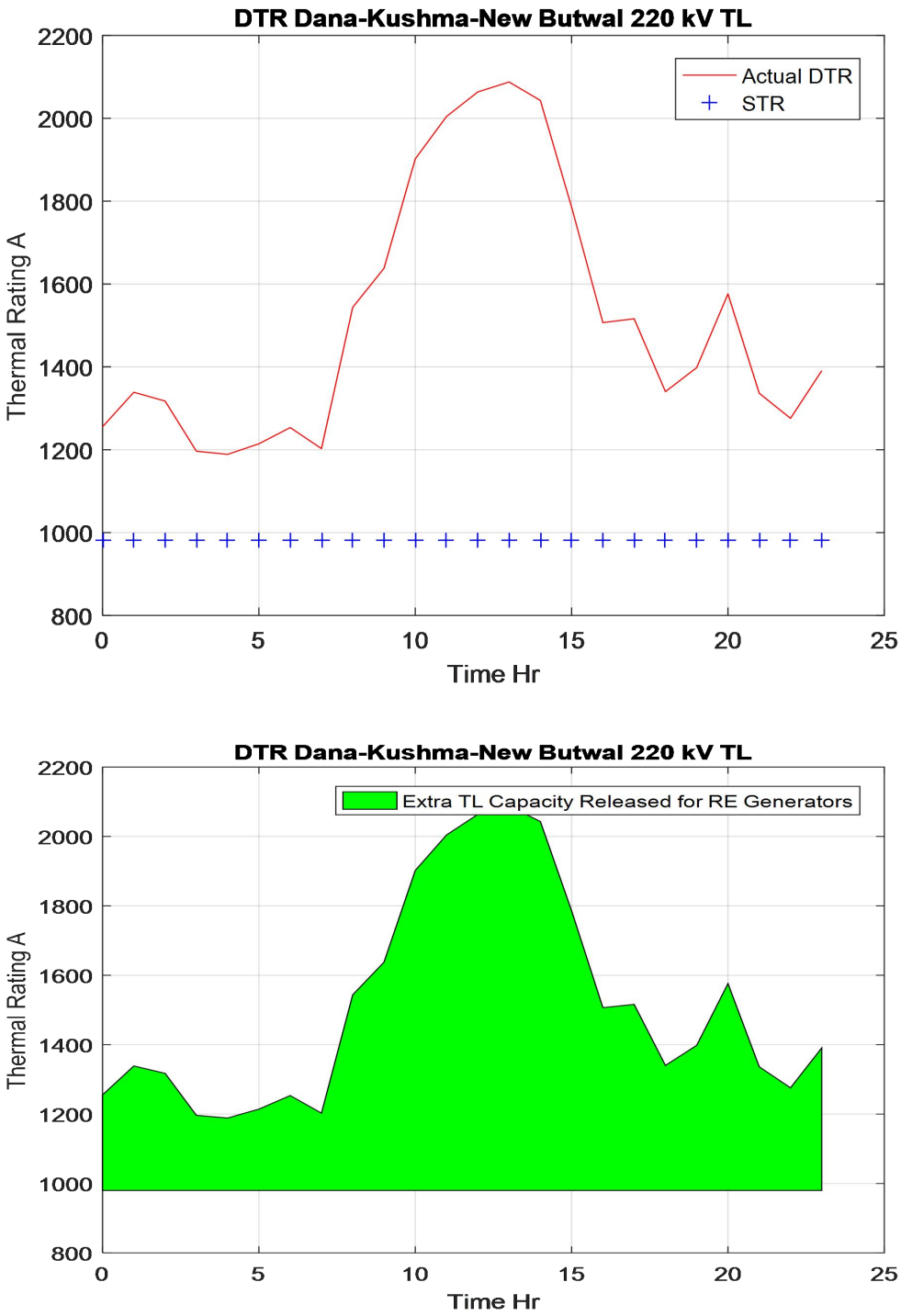

Figure 4- 15 Additional Capacity Available by Using DTR Technique for Dana-Kushma-New Butwal 220 kV TL on 25th November 2020

Figure 4- 15 represents the comparison of the minimal dynamic thermal rating and static rating of the Dana-Kushma-New Butwal 220 kV Transmission Line for the time of day on 25th November 2020. The DTR of the transmission line is varying as per the weather conditions at that particular day. As we discussed in an earlier section,

wind velocity has the greatest effect on thermal rating. Even in the day time at that particular day the dynamic thermal rating is highest as there is rapid increase in wind velocity of 0.6 m/s at 7:00 AM to 2.3 m/s at 13:00 PM and then 0.8 m/s at 16:00 AM. It is observed that the dynamic rating of the conductor varies from about 1200 Amps to 2100 Amps releasing additional TL capability as indicated by the shaded region.

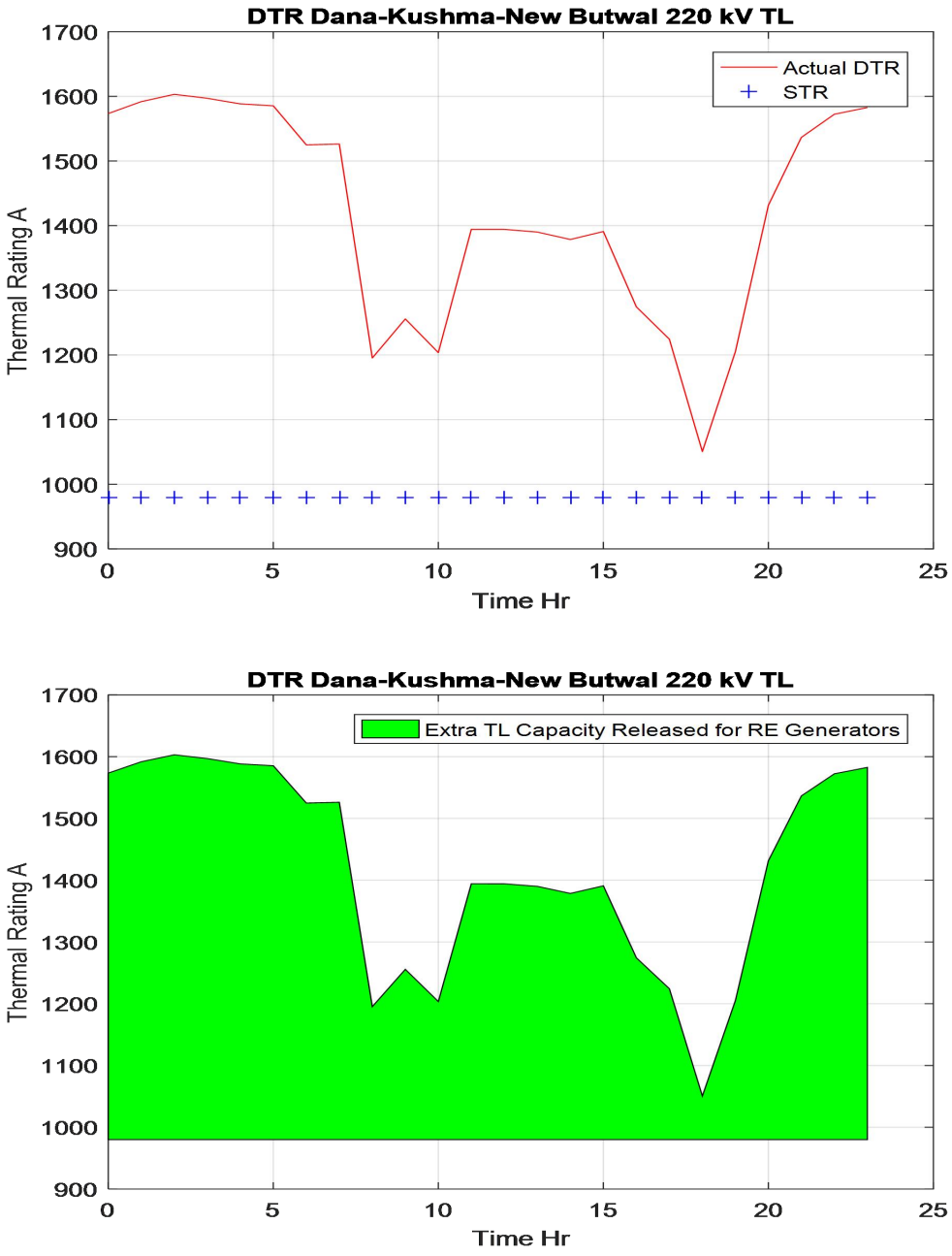

Figure 4- 16 Additional Capacity Available by Using DTR Technique for Dana-Kushma-New Butwal 220 kV TL on 15th October 2020

Figure 4- 16 represents the comparison of the minimal dynamic thermal rating and static rating of the Dana-Kushma-New Butwal 220 kV Transmission Line for the time of day on 15th October 2020. The DTR of the transmission line is varying as per the weather conditions at that particular day. It is observed that the dynamic rating of the conductor varies from about 1050 Amps to 1600 Amps releasing additional TL capability as indicated by the shaded region.

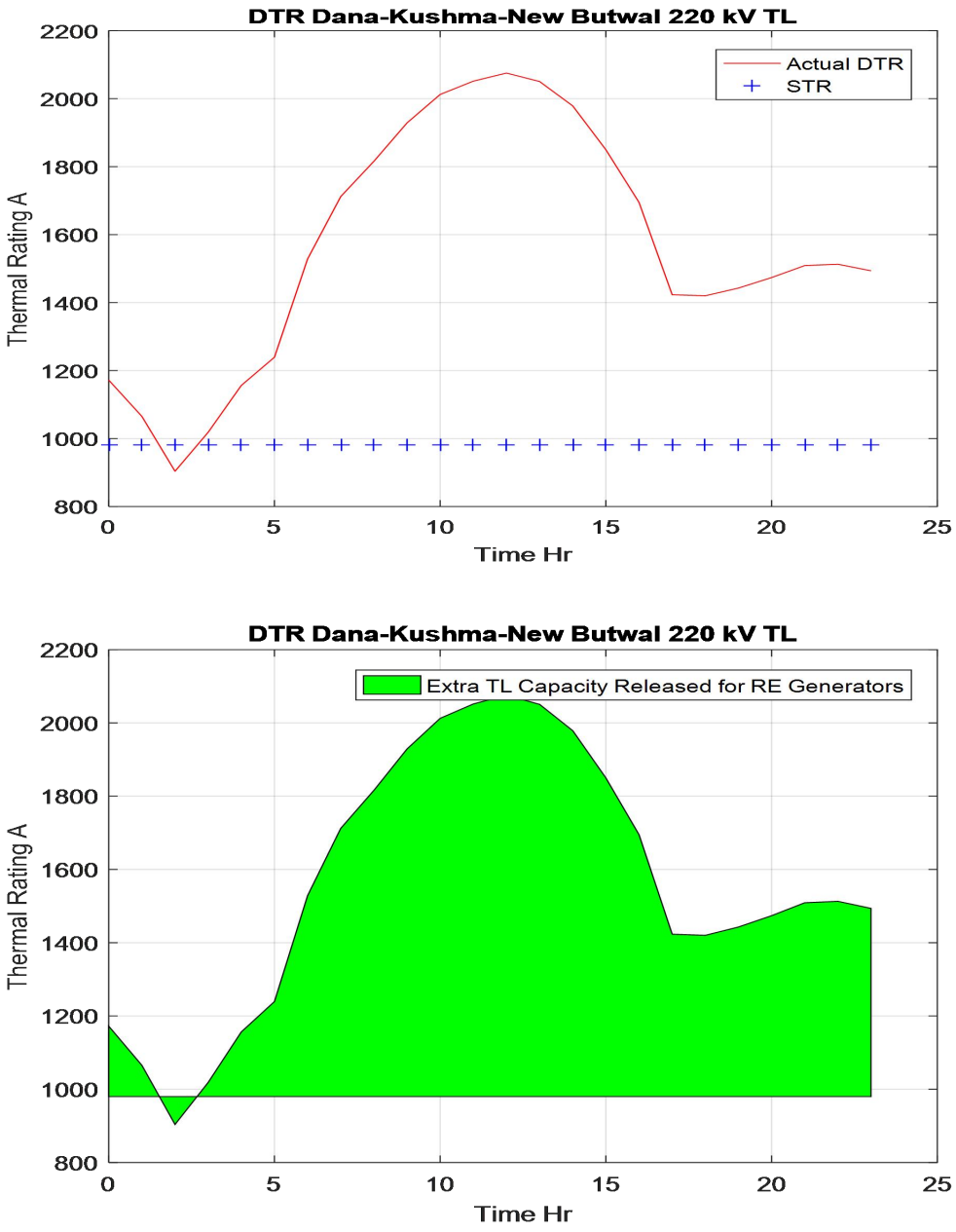

Figure 4- 17 Additional Capacity Available by Using DTR Technique for Dana-Kushma-New Butwal 220 kV TL on 10th August 2020

Figure 4- 17 represents the comparison of the minimal dynamic thermal rating and static rating of the Dana-Kushma-New Butwal 220 kV Transmission Line for the time of day on 10th August 2020. The DTR of the transmission line is varying as per the weather conditions at that particular day. It is observed that the dynamic rating of the conductor varies from about 920 Amps to 2050 Amps releasing additional TL capability as indicated by the shaded region.

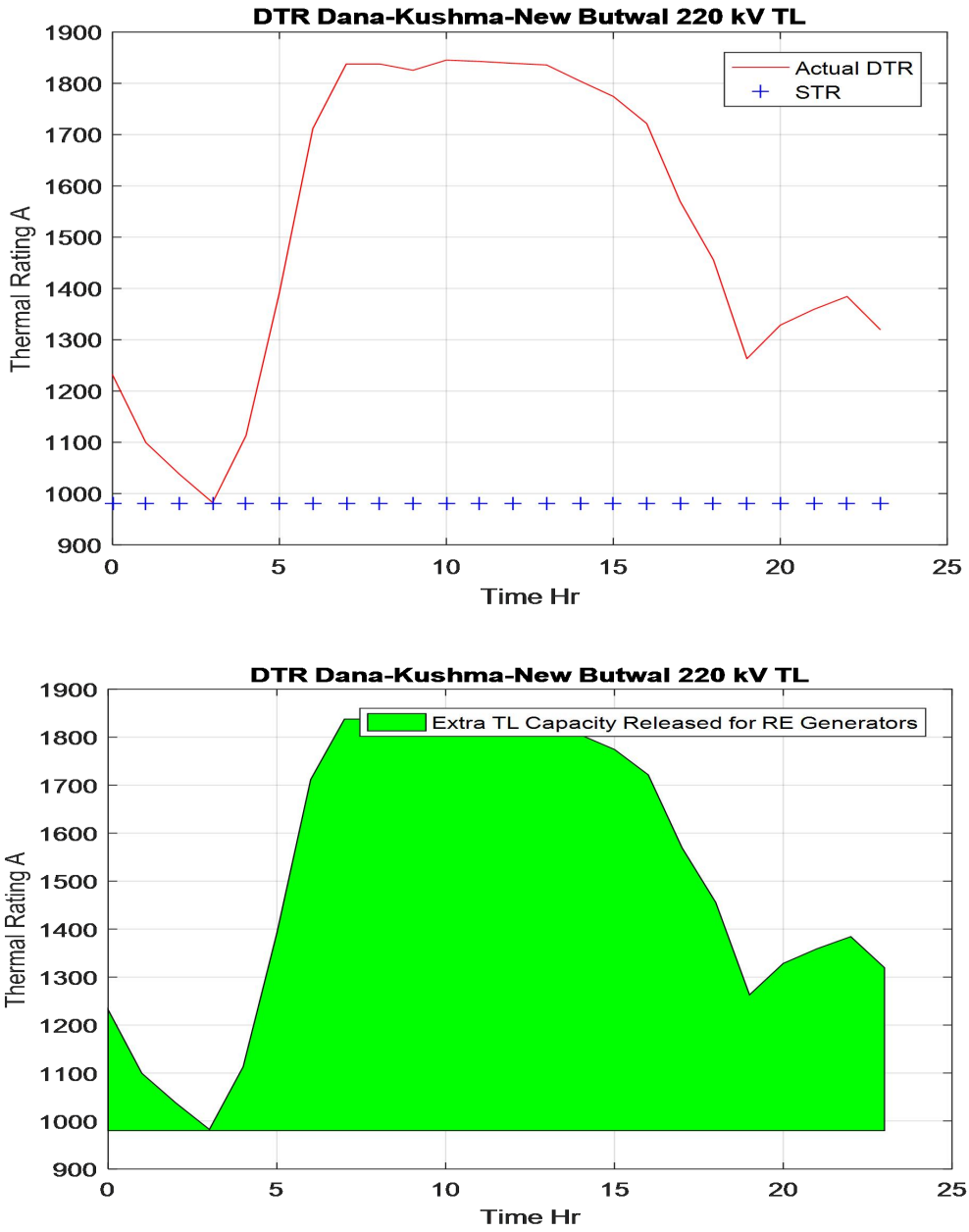

Figure 4- 18 Additional Capacity Available by Using DTR Technique for Dana-Kushma-New Butwal 220 kV TL on 12th June, 2020

Figure 4- 18 represents the comparison of the minimal dynamic thermal rating and static rating of the Dana-Kushma-New Butwal 220 kV Transmission Line for the time of day on 12th June 2020. The DTR of the transmission line is varying as per the weather conditions at that particular day. It is observed that the dynamic rating of the conductor varies from about 1000 Amps to 1850 Amps releasing additional TL capability as indicated by the shaded region.

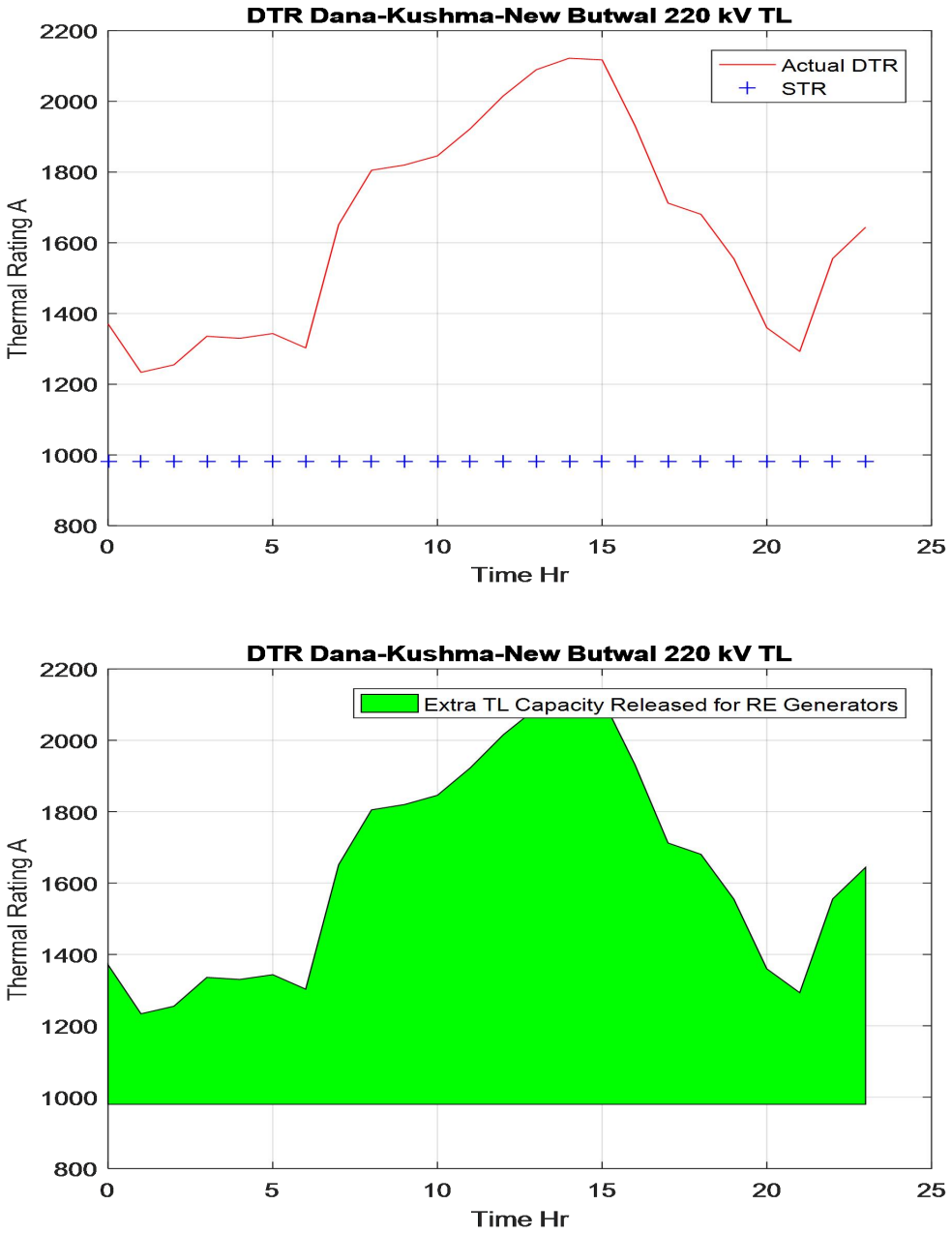

Figure 4- 19 Additional Capacity Available by Using DTR Technique for Dana-Kushma-New Butwal 220 kV TL on 22nd March 2020

Figure 4- 19 represents the comparison of the minimal dynamic thermal rating and static rating of the Dana-Kushma-New Butwal 220 kV Transmission Line for the time of day on 22nd March 2020. The DTR of the transmission line is varying as per the weather conditions at that particular day. It is observed that the dynamic rating of the conductor varies from about 1250 Amps to 2100 Amps releasing additional TL capability as indicated by the shaded region.

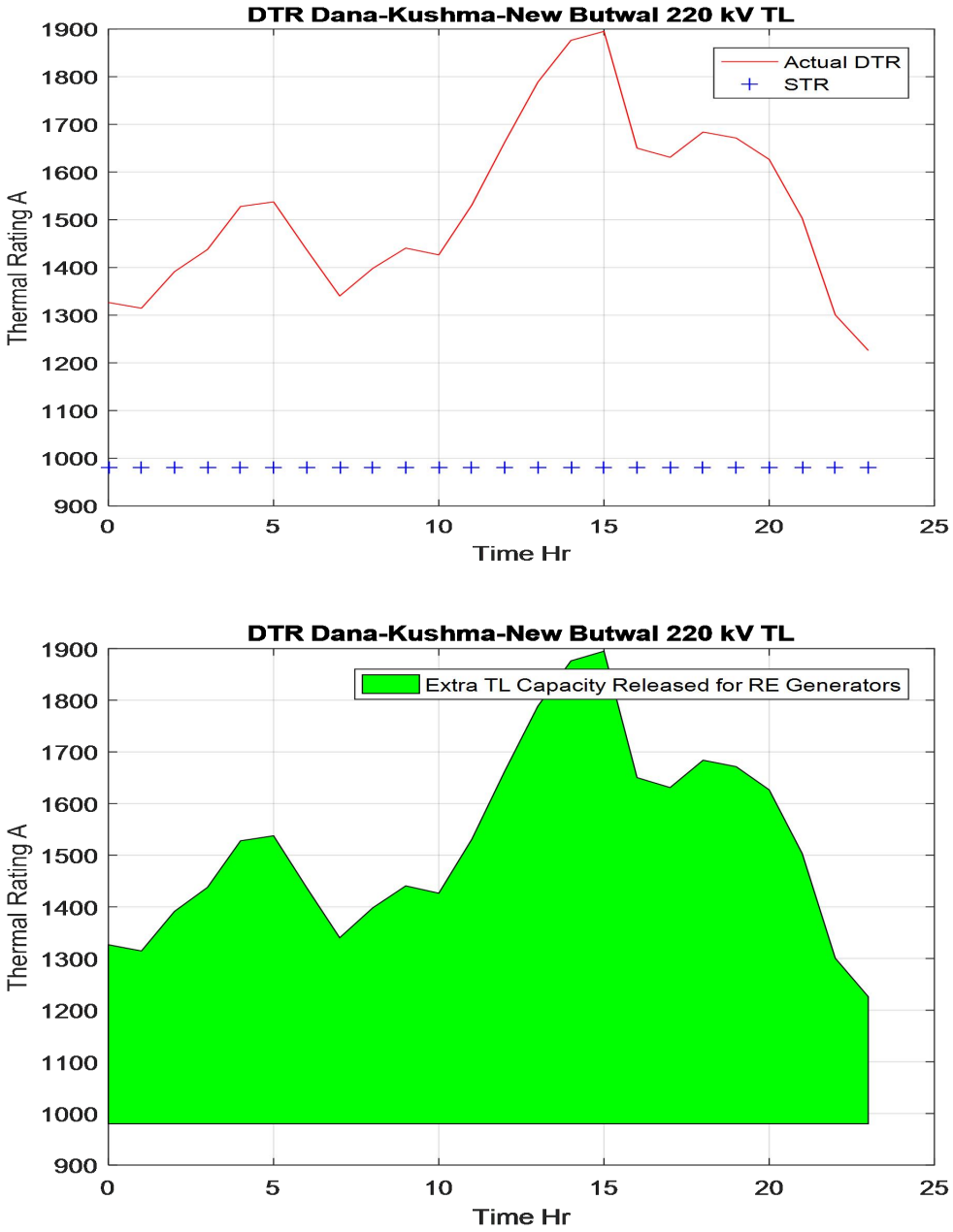

Figure 4- 20 Additional Capacity Available by Using DTR Technique for Dana-Kushma-New Butwal 220 kV TL on 28th February 2020

Figure 4-20 represents the comparison of the minimal dynamic thermal rating and static rating of the Dana-Kushma-New Butwal 220 kV Transmission Line for the time of day on 28th February 2020. The DTR of the transmission line is varying as per the weather conditions at that particular day. It is observed that the dynamic rating of the conductor varies from about 1200 Amps to 1900 Amps releasing additional TL capability as indicated by the shaded region.

By estimating the actual line thermal rating of the transmission line, the accurate amount of additional transmission line capacity as compared to the static rating can estimated. With this estimation, the transmission line congestion injected into the transmission line from different renewal energy sources can handled. For example, the area plot of Figure 4-15 represents the additional transmission line capability released for the Dana-Kushma-New Butwal 220 kV transmission line on 25th November 2020. Here we can observe that there will be a minimal increment of about 300 A current carrying capacity during morning time while a maximum increment of about 1000 Amps during windy daytime. Implementing this additional capacity in generation scheduling, the transmission system operators (TSOs) can reduce the transmission line congestion by evacuating power generated from renewal energy resources like wind turbines and solar PV generators through the same transmission line. This technique shifts the transmission congestion of one particular transmission line to other where additional capability is available and thus reduces the additional cost imposed to TSOs due to transmission congestion issues.

The congestion introduced by the continuous penetration of renewal energy generators, electrical vehicles, distributed energy resources, and electrical cooking loads can be managed by scheduling generators and loads as per the availability of the transmission line capability. Dynamic line rating provides increased congestion handling capability and additional flexibility of operation to handle such congestions. Therefore, congestion management with DLR application has techno-economic benefits for transmission system operators and utilities. Some of the transmission lines of the Integrated Nepalese Power System (INPS) are already facing congestion management problems due to unplanned penetration of renewables and distributed energy resources. The DLR of the whole transmission segment can approximately be considered as the thermal capacity of any individual span. The application of the

proposed model in transmission line segments of INPS having a large number of wind generators will be much more beneficial as compared to transmission lines with higher solar penetration. However, the thermal capability will be always more than the static rating for all types of transmission lines. The proposed model works properly for all 220 kV Dana-Kushma-New Butwak Transmission Line of INPS. Analysis of this transmission line that connects load centers in the southern part of Nepal i.e. Terai region to the generating stations at the northern uphill region of Nepal covering different geographical and climatic locations it can be concluded that the DTR/STR ratio is higher than unity for most of the time releasing the extra transmission line capability. In addition, there is a significant enhancement of line thermal capability of transmission lines in the Terai region during winter cold days as the ambient temperature falls by a larger amount. This increased line capacity can be utilized to cater to the increased heating loads in different cities of the Terai region during those winter cold days. DTR estimation of different month days of the year 2020 by using forecasted weather data shows that there will be about an average of 20% increment in transmission line capability as compared to STR. Therefore, using the existing transmission line infrastructure and very small additional cost, we can annually evacuate an additional amount of about 556 GWh energy generated by renewal energy generators within the premises of Dana-Kushma-New Butwal substations.

CHAPTER 5 FINANCIAL ANALYSIS

DTR is a solution designed to enhance transmission capacity, improve operational flexibility, and provide tools for managing congestion. Alternative solutions include rerating, reconductoring, and rebuilding the line. A detailed analysis of benefits and costs for different alternatives is performed for the comparison. The cost used in this study is taken from the competitive bidding cost of various transmission line and substation projects in Nepal. The breakdown of benefit and cost analysis for implementing DTR along with other alternatives on Dana-Kushma-New Butwal 220 kV transmission line are as represented in the following subsections.

5.1 System Component Cost Breakdown

5.1.1 System Cost Breakdown for Ending Substation Construction

The ending substation of the transmission line should be upgraded for an average thermal rating increment of about 20-30% with DTR implementation. The existing substation at Dana SS, Kushma SS, and New Butwal SS has a capacity of 100 MVA and a voltage rating of 132/220 kV. After implementing DTR at Dana-Kushma-New Butwal 220 kV TL, consider an additional 25 MVA, 132/220 kV capacity. The approximate substation cost breakdown is presented in Table 5- 1.

Table 5- 1 System cost breakdown for 132/220 kV end substation

Item No.	Description	Qty	Unit	Equipment Cost (kUSD)	
				Unit Rate	Total Amount
1	ELECTRICAL WORKS AT DANA SUBSTATION				
1.1	Power Transformer (132/220 kV)				
	132/220 kV, Single Phase, OFWF/OFWF Power Transfromer complete with On load Tap Changer (OLTC) and RTCC facility with Tank Mounted LA at LV side and Bushing CT on both sides, complete with all accessories. ascified	1	Set	410	410

Item No.	Description	Qty	Unit	Equipment Cost (kUSD)	
				Unit Rate	Total Amount
1.2	Trasformer bay Module (220 kV)				
	Transformer bay module, SF6 gas insulated comprising of one set of 245 kV, 1250 A, single phase, SF6 Circuit Breaker, complete with all accessories as per specification, two set of 245 kV, 1250 A, single phase Disconnecting Switch with Grounding Switch complete with all accessories as per specification, one set of 245 kV, 30 VA, 5 core Current Transformer complete with all accessories as per specification, one set of 245 kV, 50 VA, 220/√3 /110/√3 kV, Class 0.5/3P Capacitor Voltage Transformer complete with all accessories as per specification and one set of 120` kV, 10 kA Lightening Arrestor including Discharge Counter complete with all accessories.	1	Sets	450	450
1.3	Busbar Module (220 kV)				
	Busbar module, SF6 gas insulates comprising of copper bus bar	1	Sets	100	100
1.4	Bus Coupler Module (220 kV)				

Item No.	Description	Qty	Unit	Equipment Cost (kUSD)	
				Unit Rate	Total Amount
	Bus coupler module, SF6 gas insulates comprising of one set of 245 kV, 1250 A, single phase, SF6 Circuit Breaker, complete with all accessories as per specification, two set of 245 kV, 1250 A, single phase Disconnecting Switch with Grounding Switch complete with all accessories as per specification and two set of 245 kV, 30 VA, 5 core Current Transformer complete with all accessories.	1	Sets	440	440
1.5	Line Bay Module (220 kV)				
	Line module, SF6 gas insulates comprising of one set of 245 kV, 1250 A, single phase, SF6 Circuit Breaker, complete with all accessories as per specification, two set of 245 kV, 1250 A, single phase Disconnecting Switch with Grounding Switch complete with all accessories, one set of 245 kV, 30 VA, 5 core Current Transformer complete with all accessories as per specification, one set of 245 kV, 50 VA, 220/√3 /110/√3 kV, Class 0.5/3P Capacitor Voltage Transformer complete with all accessories as per specification and one set of 120 kV, 10 kA Lightening Arrestor including Discharge Counter complete with all accessories.	2	Sets	575	1150
2	ELECTRICAL WORKS AT EVACUATION SUBSTATION (BUTWAL)				

Item No.	Description	Qty	Unit	Equipment Cost (kUSD)	
				Unit Rate	Total Amount
2.1	Line Bay Module (220 kV)				
	Line module, SF6 gas insulates comprising of one set of 245 kV, 1250 A, single phase, SF6 Circuit Breaker, complete with all accessories as per specification, two set of 245 kV, 1250 A, single phase Disconnecting Switch with Grounding Switch complete with all accessories, one set of 245 kV, 30 VA, 5 core Current Transformer complete with all accessories as per specification, one set of 245 kV, 50 VA, 220/√3 /110/√3 kV, Class 0.5/3P Capacitor Voltage Transformer complete with all accessories as per specification and one set of 120 kV, 10 kA Lightening Arrestor including Discharge Counter complete with all accessories.	2	Sets	572.5	1145
2.2	Busbar Module (220 kV)				
	Busbar module, SF6 gas insulates comprising of copper bus bar	1	Sets	100	100
TOTAL					**3,795.0**

From Table 5-1 it is known that for a construction of a new 25 MVA, 132/220 kV end substation after DTR implementation, about 3795.00 kUSD investment is required for the upgradation of existing substation to cope up with increased power flow.

5.1.2 System Cost Breakdown for Transmission Line Construction

Transmission line costs are stated based on current market price. The estimated costs in US Dollars per km represents total line costs including all materials, construction works, survey, design, right of way compensation and engineering. Taxes and duties have been excluded in the calculation of project cost.

Table 5- 2 System cost breakdown for 220 kV transmission line construction

Conductor	**132 kV**		**220 kV**		**400 kV**	
	SC	**DC**	**SC**	**DC**	**SC**	**DC**
Bear	120	190.4	-	-	-	-
Duck	220	260	-	-	-	-
Cardinal	240	290	-	-	-	-
Bison	-	-	190	278	-	-
Moose	-	-	202	294	-	-
2xBison	-	-	-	-	-	298
2xMoose	-	-	-	-	-	341

Table 5- 2 presents a detailed cost comparison, in thousands of US dollars (kUSD), for the construction of transmission lines at 132kV, 220kV, and 400kV, focusing on the impact of conductor type and circuit configuration (single circuit - SC, or double circuit - DC) on overall system costs. Starting with 132kV lines, the table reveals a clear cost progression: "Bear" conductors are the most economical at 120 kUSD, followed by "Duck" at 220 kUSD, and "Cardinal" at 240 kUSD. The shift from SC to DC configurations significantly increases costs across these conductor types, with "Bear" rising from 120 kUSD to 190.4 kUSD, "Duck" from 220 kUSD to 260 kUSD, and "Cardinal" from 240 kUSD to 290 kUSD. Moving to 220kV lines, the table contrasts "Bison" and "Moose" conductors, showing "Bison" as the less expensive option with a cost of 190 kUSD in SC configuration, compared to "Moose" at 202 kUSD. Again, doubling the circuit to DC results in a substantial cost increase, with

"Bison" rising to 278 kUSD and "Moose" to 294 kUSD. Finally, the 400kV section exclusively features bundled conductors, "2xBison" and "2xMoose," reflecting their typical use in high-voltage transmission. "2xBison" costs 298 kUSD in the DC configuration, while "2xMoose" is notably more expensive at 341 kUSD. Overall, the table demonstrates a consistent trend: higher voltage levels and double circuit configurations lead to significantly increased construction costs, highlighting the economic considerations involved in transmission line design and planning. The cost values are presented in thousands of US dollars (kUSD), providing a clear understanding of the financial scale involved.

We have, line length for Dana-Kushma-New Butwal TL = 128 km

Per km cost for double circuit 220 kV line with ACSR MOOSE = 294 kUSD

Therefore, total TL construction cost = 294*128 = 37632 kUSD

5.1.3 System Cost Breakdown for DTR Implementation

The details of cost requirement for DTR implementation with its accessories with reference to study [25] is presented in Table 5-3 below. This table presents the equipment costs, in thousands of US dollars (kUSD), for the DTR instrumentation required for a project, likely located in Bidur, Bagmati Province, Nepal as indicated by the context. The DTR Instrumentation Cost is broken down into two sub-items. Sub-item 2.1 details the DTR sensor, software, and communication equipment, with one set priced at 480 kUSD. Sub-item 2.2 lists Wireless weather stations that measure temperature, wind speed, and precipitation. Seven sets are required, each costing 2.5 kUSD, totaling 17.5 kUSD. The combined total cost for the DTR instrumentation is 497.5 kUSD. This table provides a clear breakdown of the expenses associated with implementing DTR technology, highlighting the major cost components and their respective contributions to the total investment. The total DTR implementation cost for the Dana-Kushma-New Butwal transmission line is about 497.5 kUSD.

Table 5-3 System cost breakdown for DTR implementation

Item No.	Description	Qty	Unit	Equipment Cost (kUSD)	
				Unit Rate	Total Amount
2	DTR INSTRUMENTATION COST [25]				

2.1	DTR sensor, software and communication equipment	1	Sets	480	480
2.2	Wireless weather station (Temperature, Wind Speed, Precipitation)	7	Sets	2.5	17.5
TOTAL					497.5

5.2 Benefit-Cost Analysis with DTR

The annual benefits from additional energy flow through the Dana-Kushma transmission line with the implementation of DTR are presented in Table 5-4.

Table 5-4 DTR Benefit Analysis of 220 kV Dana-Kushma TL with DTR on 2020

Capacity Expansion with DTR Installation in Dana-Kushma-New Butwal 220 kV TL				
S.N	Day	% Increment in Thermal Capacity	MWh Increment	Monthly MWh Increment
1	January 2020	27.22%	2195.40	65862.10
2	February 2020	22.11%	1783.77	49945.56
3	March 2020	27.51%	2218.86	68784.66
4	April 2020	27.22%	2195.37	65861.08
5	May 2020	25.49%	2056.41	63748.71
6	June 2020	24.86%	2005.62	60168.51
7	July 2020	23.60%	1903.56	59010.36
8	August 2020	19.30%	1556.91	46707.30
9	September 2020	30.07%	2425.59	75193.29
10	October 2020	26.30%	2121.29	63638.79
11	November 2020	22.33%	1801.15	55835.65
12	December 2020	28.56%	2303.29	69098.70
		Total Annual Energy Increment, MWh		743854.71

Table 5-4 details the capacity expansion achieved through the installation of Dynamic Thermal Rating (DTR) technology on the Dana-Kushma-New Butwal 220 kV Transmission Line (TL) in 2020. It presents a month-by-month breakdown, starting with January and ending with December. The second column, simply lists the corresponding month. The third column, shows the average percentage increase in the line's thermal capacity due to the DTR installation. This increment varies throughout

the year, ranging from a low of 19.30% in August to a high of 30.07% in September, indicating fluctuations in weather conditions which directly impact the DTR. The fourth column quantifies the daily increase in energy transmission capacity in megawatt-hours (MWh). Finally, the fifth column, calculates the total monthly increase in energy transmission capacity, also in MWh. The table concludes with the Total Annual Energy Increment, which is 743,854.71 MWh, representing the overall gain in transmission capacity for the year resulting from the DTR installation. This data demonstrates the significant impact of DTR technology in enhancing the capacity of existing transmission lines, enabling the integration of more power, likely from renewable sources. This analysis shows that there can be a total average annual increase of about 743 GWh energy flow in the Dana-Kushma-New Butwal Transmission line using existing assets. This generates approximately about 40535.91 kUSD revenue per year for the utility (NEA).

Also, with increase in average of 25% of line flow i.e. 0.25*800 = 200 MW power from same existing transmission line, the annual revenue generated by utility is:

Annual revenue from energy sell = KW*8760*Plant Factor* Rs/KWh

= 200*1000*8760*0.6*Rs 5

= NPR 5,25,60,00,000 /-

= 40,430.7 kUSD

The annual revenue collected from additional power flow of 200 MW is about 40,430.7 kUSD. This is the large amount for developing utility like NEA.

5.3 Summary of Benefit-Cost Analysis for Two Different Alternatives

Table 5- 5 Comparative BC analysis of 220 kV Dana-Kushma-New Butwal TL

S.N.	Particular	Option-1: New Line Construction (kUSD)	Option-2: DTR Implementation (kUSD)
1	End substation construction cost	3795 /-	3795 /-
2	Transmission line construction cost	37632 /-	-
3	DTR implementation cost	-	497.5 /-
4	Total cost (1+2+3)	41,427/-	4,292.5/-
5	Annual energy sales revenue	40,430.7/-	40,430.7/-
6	Total Benefits (5-4)	-	36,138.2/-
7	Additional Benefits from DTR	36138.2/-	

The Table 5-5 presents a detailed cost-benefit analysis comparing two strategic options for enhancing power system capacity: Option-1: New Line Construction and Option-2: Dynamic Thermal Rating (DTR) Implementation, with all values expressed in thousands of US dollars (kUSD). Both options require an identical end substation construction cost of 3,795 kUSD, as upgrading or constructing substations is essential in either approach. However, the cost diverges significantly when it comes to the transmission infrastructure. Option-1 incurs a transmission line construction cost of 37,632 kUSD, representing the substantial investment needed for building new physical infrastructure. In contrast, Option-2 avoids this cost by leveraging the existing infrastructure and instead incurs a DTR implementation cost of 497.5 kUSD, which includes installing the necessary technology to optimize the thermal capacity of the existing line. Consequently, the total cost (sum of substation, transmission line, and DTR implementation costs) for Option-1 amounts to 41,427 kUSD, while Option-2 requires significantly less investment, totaling 4,292.5 kUSD. Despite the difference in costs, both options yield the same annual energy sales revenue of 40,430.7 kUSD, indicating that either approach can facilitate similar energy sales capacity. However, when considering total benefits, calculated by subtracting the total costs from annual revenue, Option-1 results in no benefits, while Option-2 delivers higher benefits of 36,138.2 kUSD, due to its lower initial costs. The final row highlights the additional benefits from DTR, quantified at 36,138.2 kUSD, which signifies the financial advantage of selecting DTR implementation over new line construction.

Overall, the analysis clearly demonstrates that DTR implementation is the more cost-effective and financially advantageous option. It minimizes initial investment costs while delivering higher net benefits without compromising energy sales revenue. This approach not only optimizes existing infrastructure but also offers a quicker and less capital-intensive solution for enhancing transmission capacity, making it an economically superior alternative to constructing new transmission lines. From the detail cost-benefit analysis for two different alternative, it is concluded that transmitting power with existing transmission line with DTR scheme is about three times cheaper that constructing new transmission line.

5.4 WACC Calculation

Weighted Average Cost of Capital (WACC) is the average rate of return a company is expected to pay to its investors (both equity holders and debt holders) to finance its assets. It represents the company's overall cost of capital, weighted by the proportion of debt and equity in its capital structure. WACC is a crucial financial metric used to evaluate investment opportunities and assess whether a company is generating sufficient returns to satisfy its cost of capital. WACC plays a critical role in investment decision-making, capital budgeting, and valuation, particularly in discounting future cash flows for net present value (NPV) analysis. It reflects the minimum return that a company must earn on its investments to maintain its value and satisfy its investors. The Importance of WACC are as follows:

i. Investment Evaluation: It serves as the discount rate in capital budgeting decisions (e.g., NPV and IRR analysis). When evaluating potential projects or investments, a company should expect a return greater than its WACC to generate value for shareholders.

ii. Risk Assessment: WACC incorporates both debt and equity costs, allowing it to reflect the risk of a company's capital structure.

iii. Optimal Capital Structure: By calculating WACC, companies can assess whether their mix of debt and equity financing is optimal for minimizing the cost of capital and maximizing shareholder value.

To calculate the WACC for the application of DTR technologies in congestion management of Dana-Kushma-New Butwal 220 kV Transmission Line, let assume

NEA and GoN is investing in this project and the parameters for WACC calculations are based on the assumptions considering Nepalese market trend.

i. **Calculation of the Cost of Debt (Rd)**

Assumptions:

a. The annual interest rate paid on the loan of GoN is 8%

b. The corporate tax rate in Nepal is 25% (As per the tax code in Nepal for corporate income)

The pre-tax cost of debt is the annual interest rate paid on the GoN loan which is assumed as 8%.

i.e. Cost of Debt (Rd) = Annual Interest Rate

= 8%

Since interest expenses are tax-deductible, the adjusted cost of debt after tax shield is given by:

$$\text{Or, After} - \text{tax Cost of Debt} = R_d + (1 - T)$$

Where T is the corporate tax rate in Nepal = 25%.

Therefore,

$$\text{After} - \text{tax Cost of Debt} = 8\% + (1 - 0.25)$$

$$\text{or, After} - \text{tax Cost of Debt} = 8\% * 0.75$$

$$\text{or, After} - \text{tax Cost of Debt} = 6\%$$

ii. **Calculation of the Cost of Equity (Re)**

Assumptions:

a. The risk-free rate (Rf) is the return on the Nepali government bond, which is around 5%.

b. The market return (Rm) in Nepal is typically estimated as 8%

c. The volatility of the stake as compared to market stock (β) is around 1.

Now using the Capital Asset Pricing Model (CAPM) formula to calculate the cost of equity:

$$R_e = R_f + \beta * (R_m - R_f)$$

$$Or, R_e = 5\% + 1 * (8\% - 5\%)$$

$$Or, Cost\ of\ Equity\ (R_e) = 8\%$$

iii. Determine the Market Value of Equity (E) and Debt (D)

Assumptions:

a. The value of equity NEA bears is 40% of the total project implementation cost.

b. The value of debt provided by GoN in the project is 60% of the total project implementation cost.

The total investment required for the implementation of DTR technology in Dana-Kushma-New Butwal 220 kV transmission line as discussed in sub-section 5.3 is 4,292.5/- kUSD.

Therefore, Market value of NEA's equity (E) = 40% of 4292.5

= 1717 kUSD

Market value of GoN loan (D) = 60% of 4292.5

= 2575.5 kUSD

Total market value of project financing for NEA (V) = E+D

= 1717+2575.5

= 4292.5 kUSD

iv. Calculating WACC

The WACC is given by:

$$WACC = \left(\frac{E}{V} * R_e\right) + \left(\frac{D}{V} * R_d * (1 - T)\right)$$

$$Or, WACC = \left(\frac{1717}{4292.5} * 8\%\right) + \left(\frac{2575.5}{4292.5} * 6\%\right)$$

$$Or, WACC = 0.4 * 8\% + 0.6 * 6\%$$

$$Or, WACC = 3.2\% + 3.6\%$$

$$Therefore, WACC = 6.80\%$$

Therefore, the weighted average cost of capital for the DTR implementation project on Dana-Kushma-New Butwal 220 kV transmission line project is 6.80%.

CHAPTER 6 CONCLUSION AND RECOMMENDATIONS

This study demonstrates the significant potential of Dynamic Line Rating (DLR) to enhance the operational efficiency and economic viability of the Integrated Nepalese Power System (INPS). By estimating the actual line thermal rating of transmission lines, it is possible to accurately determine the additional transmission capacity compared to static ratings, which is essential for managing congestion caused by the increasing penetration of renewable energy sources such as wind and solar power. The case study of the Dana-Kushma-New Butwal 220 kV transmission line illustrates how DLR can provide substantial increments in transmission capacity, especially during times of high wind or lower ambient temperatures. The findings suggest that by implementing DLR, Transmission System Operators (TSOs) can mitigate transmission line congestion by effectively evacuating power from renewable energy sources, thus reducing the need for costly infrastructure upgrades. Furthermore, the application of DLR not only increases the capacity for renewable energy integration but also provides greater flexibility for managing congestion and load distribution, particularly in regions with varying climatic conditions, such as Nepal's Terai region.

The results indicate that application of DLR on Dana-Kushma-New Butwal 200 kV Transmission Line offers an average 20-30% increase in capability compared to static ratings, which translates into the ability to evacuate an additional 743 GWh of energy annually from renewable generation sources. This improvement can be achieved with minimal additional investment, making it a cost-effective solution for addressing the challenges posed by the growing demand for electricity and the integration of distributed energy resources.

In conclusion, the adoption of DLR in the transmission lines of the INPS, particularly in areas with high renewable energy generation, can lead to both economic and operational benefits. The integration of dynamic line rating techniques offers a promising approach for enhancing the capacity and flexibility of the transmission system, helping to balance energy supply and demand more effectively while facilitating the transition to a greener and more sustainable energy future.

REFERENCES

[1] S. Nabav, S. Jadid and M. Masoum, "Congestion management in nodal pricing with genetic algorithm," International Conference on Power Electronic, Drives and Energy Systems, 2006.

[2] M. Schneider, A. Hoffrichter and R. Puffer, "Theoretical potential of dynamic line ratings for congestion management in large-scale power systems," 2019 IEEE Milan PowerTech, 2019.

[3] W. Liu, . Q. Wu, F. Wen and J. Østergaard, "Day-Ahead Congestion Management in Distribution Systems Through Household Demand Response and Distribution Congestion Prices," IEEE TRANSACTIONS ON SMART GRID, 2014.

[4] M. Matus, D. Sáez, M. Favley and C. Suazo-Martínez, "Identification of Critical Spans for Monitoring Systems in Dynamic Thermal Rating," *IEEE Transactions on Power Delivery,* vol. 27, pp. 1002-1009, 2012.

[5] S. Xiaorong and J. Chenhao, "Spatio-temporal weather model-based probabilistic forecasting of dynamic thermal rating for overhead transmission lines," *International Journal of Electrical Power & Energy System,* vol. 134, pp. 1-8, 2022.

[6] G. Kosec, M. Maksić and . V. Djurica, "Dynamic thermal rating of power lines – Model and measurements in rainy conditions," *International Journal of Electrical Power & Energy,* vol. 91, pp. 222-229, 2017.

[7] R. Dupin, A. Michiorri and G. Kariniotakis, "Optimal Dynamic Line Rating Forecasts Selection Based on Ampacity Probabilistic Forecasting and Network Operators Risk Aversion," *IEEE Transactions on Power Systems,* vol. 34, pp. 2836-2845, July 2019.

[8] J. Tech, "Prospects of Using the Dynamic Thermal Rating System for Reliable Electrical Networks: A Review," *IEEE Access,* vol. 6, pp. 26765-26778, 2018.

[9] IEEE Power and Energy Society, "IEEE Standard for Calculating the Current-Temperature Relationship of Bare Overhead Conductors," pp. 1-72, 2013.

[10] G. Andersson and M. A. Bucher, "Robust Corrective Control Measures in Power Systems with Dynamic Line Rating," *IEEE Transactions on Power Systems,* vol. 31, pp. 2034-2043, May 2016.

[11] D. L. Alvarez, E. E. Mombello, F. d. Silva and C. L. Bak, "An approach to dynamic line rating state estimation at thermal steady state using direct and indirect measurements," vol. 163, pp. 599-611, 2018.

[12] H. Shaker, M. Fotuhi-Firuzabad and F. Aminifar, "Fuzzy Dynamic Thermal Rating of Transmission Lines," *IEEE Transactions on Power Delivery,* vol. 27, pp. 1885-1892, October 2012.

[13] L. Dawson and A. M. Knight, "Applicability of Dynamic Thermal Line Rating for Long Lines," *IEEE Transactions on Power Delivery,* vol. 33, pp. 719-727, April 2018.

[14] Nepal Electricity Authority, "A Year in Review Fiscal Year 2020/2021," Kathmandu, 2021.

[15] Nepal Electricity Authority, Transmission Directorate, "A Year Book Fiscal Year 2023/2024," Nepal Electricity Authority, Kathmandu, August 2024.

[16] B. P. Bhattarai, "Improvement of Transmission Line Ampacity Utilization by Weather-Based Dynamic Line Rating," vol. 33, pp. 1853-1863, 2018.

[17] F. Fan, K. Bell and D. Infield, "Probabilistic Real-Time Thermal Rating Forecasting for Overhead Lines by Conditionally Heteroscedastic Auto-Regressive Models," *IEEE Transactions on Power Delivery,* vol. 32, pp. 1881-1890, August 2017.

[18] M. K. Metwaly and J. TEH, "Fuzzy Dynamic Thermal Rating System-Based SIPS for Enhancing Transmission Line Security," *IEEE Access,* vol. 9, pp. 83628-83641, 2021.

[19] Y. Cheng, P. Liu, Z. Zhang and . Y. Dai, "Real-Time Dynamic Line Rating of Transmission Lines Using Live Simulation Model and Tabu Search," *IEEE Transactions on Power Delivery,* vol. 36, pp. 1785-1794, June 2021.

[20] S. Madadi, B. Mohammadi-Ivatloo and S. Tohidi, "Probabilistic Real-Time Dynamic Line Rating Forecasting Based on Dynamic Stochastic General Equilibrium with Stochastic Volatility," *IEEE Transactions on Power Delivery,* vol. 36, pp. 1631-1639, June 2021.

[21] P. Pytlak, P. Musilek and J. Toth, "Modelling precipitation cooling of overhead conductors," *Electric Power Systems Research,* vol. 81, no. 12, pp. 2147-2154, 2011.

[22] National Renewable Energy Laboratory, "nrel.gov," [Online]. Available: https://maps.nrel.gov/nsrdb-viewer/.

[23] NASA, "Power Data Access Viewer," [Online]. Available: https://power.larc.nasa.gov/data-access-viewer/.

[24] Government of Nepal, Ministry of Energy, Water and Irrigation, "Department of Meteorology," [Online]. Available: http://dhm.gov.np/meteorology-forecast/4.

[25] U.S. Department of Energy, "Dynamic line ratings for transmission lines – topical report," 2014.

ANNEX A: MATLAB SIMULINK MODEL

1. Models for calculation of Cooling loss and Heat gain

a. Convection Cooling Loss Calculation Block

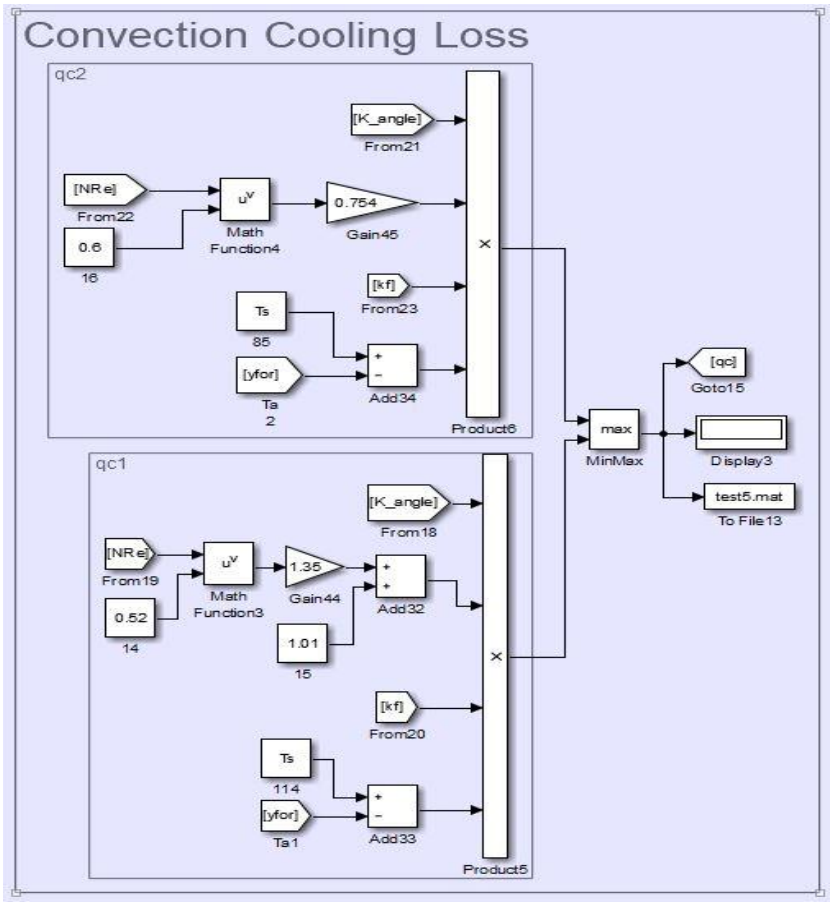

b. Radiation Cooling Loss Calculation Block

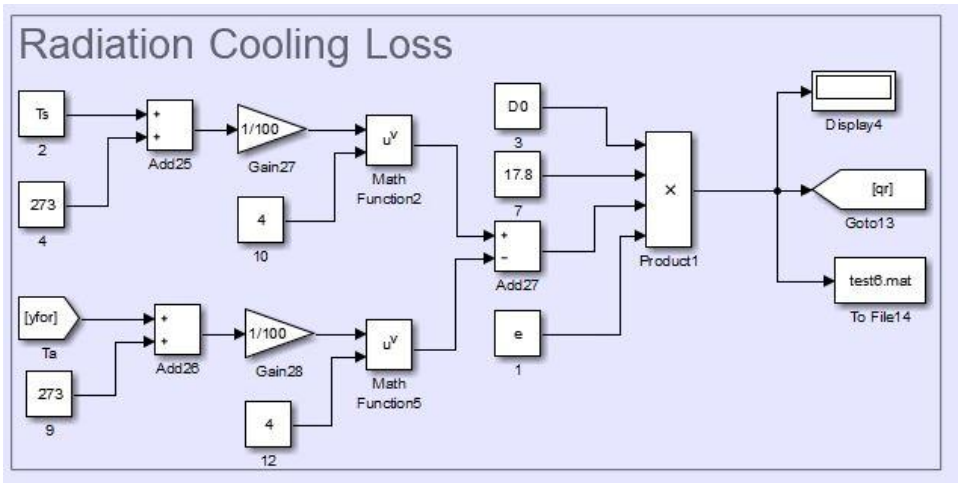

c. Precipitation Cooling Loss Calculation Block

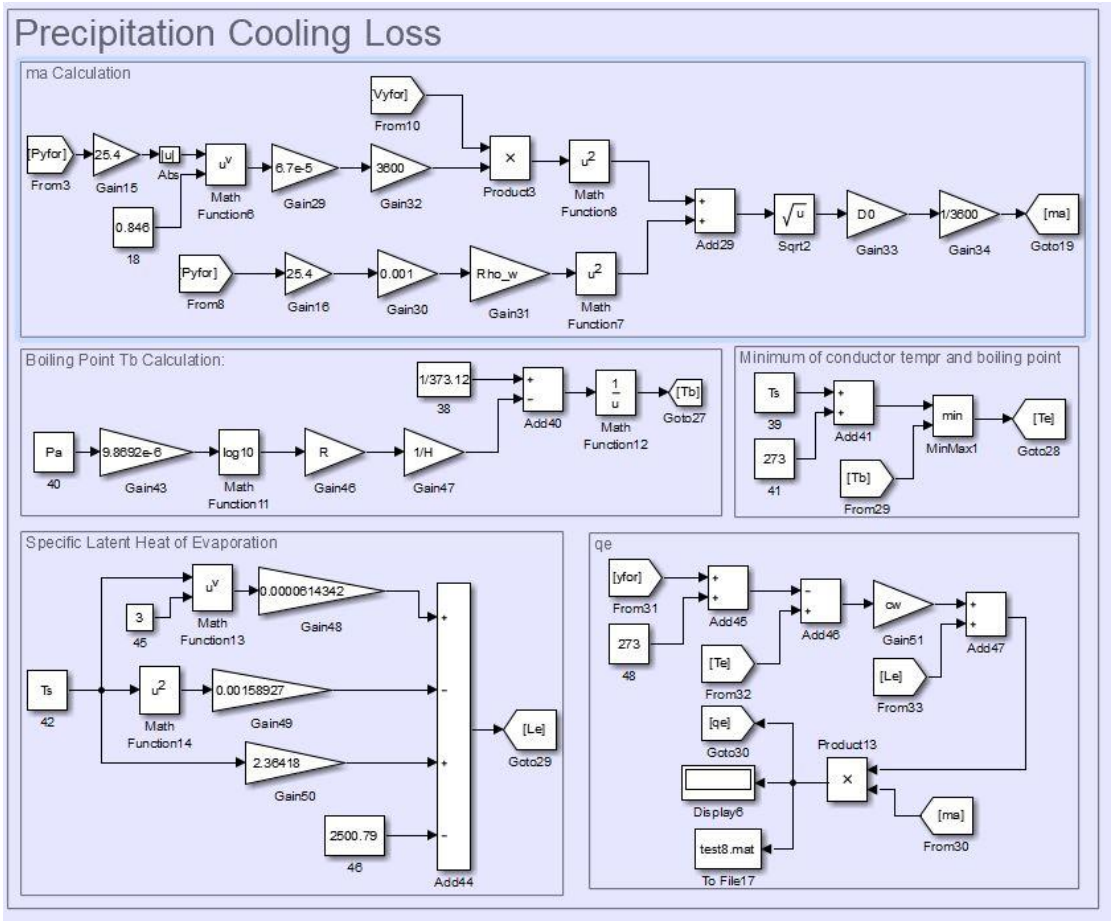

d. DTR Forecasting Calculation Block

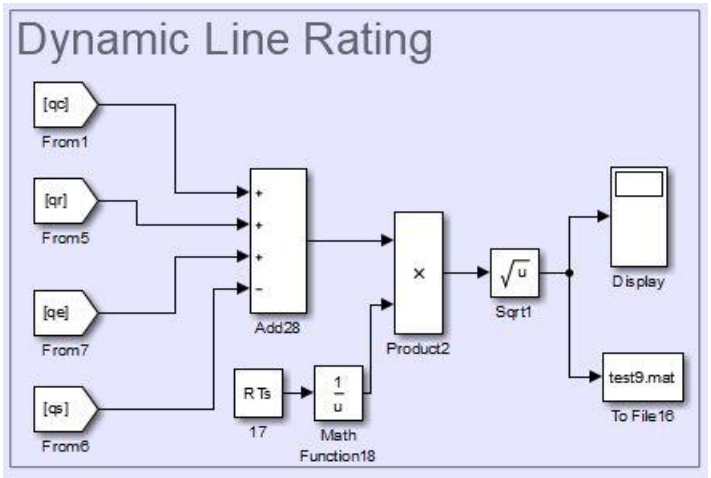

ANNEX B: MATLAB M-FILE CODE FOR PROPOSED MODEL

```
%%      Application of Dynamic Thermal Rating for Congestion Management in Regions with High Renewable
        Energy Generation: A Case Study in Dana-Kushma-New Butwal 220 kV TL     %%
clc
clear all

%% Data inputs for constants of simulink model %%

DTRdata = xlsread('DTR Input 2','Inputs');

Ts = DTRdata(1,1); % Maximum allowable conductor surface temperature
D0 = DTRdata(2,1); % Conductor Outside diameter
He = DTRdata(3,1); % Elevation of conductor above sea level
e = DTRdata(4,1); % Conductor Emissivity
qs = DTRdata(9,1);
Rho_w = DTRdata(10,1); % Density of water
n = DTRdata(11,1); % The number of strands in the outer layer of the conductor
d = DTRdata(12,1); % Strand Diameter
R_H = DTRdata(13,1); % Relative Humidity
k = DTRdata(14,1); % The ratio of the molecular weights of water vapor & dry
air
cp = DTRdata(15,1); % The specific heat of air at constant pressure
Pa = DTRdata(16,1); % Ambient air pressure
R = DTRdata(17,1); % Universal gasconstant
H = DTRdata(18,1); % The enthalpy of vaporization of water,%
cw = DTRdata(19,1); % cw [J kg^-1 K^-1] is the specific heat capacity of liquid
water
RTs = DTRdata(20,1); % Density of water
I_STR = DTRdata(25,1); % Static Thermal Rating of ACSR
I_STR_Existing_Flow = DTRdata(38,1);

%% Input Lat/Long and Altitude Data %%
Lat1= DTRdata(27,1);
Lat2= DTRdata(28,1);
Lat3= DTRdata(29,1);
Lat4= DTRdata(30,1);
Lat5= DTRdata(31,1);
Lat6= DTRdata(32,1);
Lat7= DTRdata(33,1);

Long1= DTRdata(27,2);
Long2= DTRdata(28,2);
Long3= DTRdata(29,2);
Long4= DTRdata(30,2);
Long5= DTRdata(31,2);
Long6= DTRdata(32,2);
Long7= DTRdata(33,2);

Alti1= DTRdata(27,3);
Alti2= DTRdata(28,3);
Alti3= DTRdata(29,3);
Alti4= DTRdata(30,3);
Alti5= DTRdata(31,3);
Alti6= DTRdata(32,3);
Alti7= DTRdata(33,3);

%% Ambient Temperature Data %%
data=xlsread('DTR Input 2','Tempr Coeff');
LY1=data(:,42);
LY2=data(:,43);
```

```
LY3=data(:,44);
LY4=data(:,45);
LY5=data(:,46);
LY6=data(:,47);
LY7=data(:,48);

%% Wind Velocity Data %%
Vdata=xlsread('DTR Input 2','Velocity Coeff');
LVY1=Vdata(:,42);
LVY2=Vdata(:,43);
LVY3=Vdata(:,44);
LVY4=Vdata(:,45);
LVY5=Vdata(:,46);
LVY6=Vdata(:,47);
LVY7=Vdata(:,48);

%% Precipitation Data %%
Pdata=xlsread('DTR Input 2','PPT Coeff');
LPY1=Pdata(:,42);
LPY2=Pdata(:,43);
LPY3=Pdata(:,44);
LPY4=Pdata(:,45);
LPY5=Pdata(:,46);
LPY6=Pdata(:,47);
LPY7=Pdata(:,48);

%% Wind Incidence Angle Data %%
Adata=xlsread('DTR Input 2','Angle Coeff');
LAY1=Adata(:,42);
LAY2=Adata(:,43);
LAY3=Adata(:,44);
LAY4=Adata(:,45);
LAY5=Adata(:,46);
LAY6=Adata(:,47);
LAY7=Adata(:,48);

%% Section-1:Actual DTR calculation %%
Qe_actual = zeros(24,1);    % To store data calculated
Qs_actual = zeros(24,1);
Qc_actual = zeros(24,1);
Qr_actual = zeros(24,1);
Ie_actual = zeros(24,1);

for i=1:1:24
%% Qc: Convection Cooling Calculation %%

Vw = LVY1(i,1); % Actual Velocity given
Ta = LY1(i,1); %% Ambient temperature
phi = LAY1(i,1)*pi()/180; % Wind angle @ radian angle
Pr = LPY1(i,1)*25.4; %% Precipitation rate converted in in/hr

% Calculation Section %

T_film = (Ts+Ta)/2;

Rho_f = (1.293-1.525e-4*He + 6.379e-9*He^2)/(1+0.00367*T_film); % kg/m^3

Mu_f = (1.458e-6*(T_film+273)^1.5)/(T_film+383.4); % kg/m-s or N-s/m^2

kf = 2.424e-2+7.477e-5*T_film-4.407e-9*T_film^2; % Thermal conductivity of air W/m-deg C
```

```
NRe = D0*Rho_f*Vw/Mu_f; % Reynolds Number

K_angle = 1.194-cos(phi)+0.194*cos(2*phi)+0.368*sin(2*phi); % Wind direction
factor

qc1 = K_angle*(1.01+1.35*NRe^0.52)*kf*(Ts-Ta); %watts/m
qc2 = K_angle*0.754*NRe^0.6*kf*(Ts-Ta); % watts/m

qc = max(qc1,qc2);

Qc_actual(i,1) = qc;


%% Qr: Radiation Cooling Calculation %%

qr = 17.8*D0*e*(((Ts+273)/100)^4-((Ta+273)/100)^4); % Watt/m heat loss due to
radiation

Qr_actual(i,1) = qr;

%% Qs: Heat gain from sun Calculation %%
% Modeled as day of the year %
Qs_actual(i,1) = DTRdata(9,1);

%% Qe: Precipitation cooling Calculation %%

% Calculation Section %

w = 6.7e-5*Pr^0.846; % w [kg m?3] is the liquid water content of the
precipitation

maf = sqrt((0.001*Pr*Rho_w)^2+(3600*Vw*w)^2); % The liquid mass flux density maf
[kg m^-1 h^-1] impinging onto the conductor

ma = maf*D0/3600; % ma [kg s^-1 m^-1] is the mass flux rate of water striking the
conductor surface

Pc = n*pi()*d*(0.5+1/n); % Pc [m] is the conductor perimeter

ec = 133.322*10^(8.07131-(1730.63/(Ts+273-39.724))); % ec [Pa] is the saturation
vapour pressure of water at the conductor temperature

ea = 133.322*10^(8.07131-(1730.63/(Ta+273-39.724))); % ea [Pa] is the saturation
vapour pressure of water at air temperature

h = max(qc1,qc2)/(pi()*D0*(Ts-Ta)); % h [Wm^2 K^-1] is the convective heat transfer
coefficient

me = Pc*h*k*(ec-R_H*ea)/(cp*Pa); % The evaporative mass flux me [kg s^-1 m^-1]

if ma<me
    m = ma;      %% where m [kg s^-1 m^-1] is the actual mass flux evaporating from
the conductor surface
else
    m =me;
end

Tb = inv((1/373.12)-((R*log10(Pa*9.8692e-6)/H))); % The boiling point%

Te = min(Ts+273,Tb); % Evaporation temperature%

Tw = Ts+273; %Tw [K] is the water surface temperature%
Tw_temp = Tw-273.15;
```

```
Le = 0.0000614342*Tw_temp^3 - 0.00158927*Tw_temp^2 + 2.36418*Tw_temp -
2500.79; %The specific latent heat of evaporation%

qe = m*(Le+cw*(Te-(Ta+273))); %The precipitation heat loss due to evaporation%

Qe_actual(i,1) = qe;

%% Imax: Dynamic current rating DTR Calculation%%
I_actual_s1(i,1) = sqrt((qr+qc+qe-qs)/RTs);

end

%% Section-2:Actual DTR calculation%%
Qe_actual = zeros(24,1);    % To store data calculated
Qs_actual = zeros(24,1);
Qc_actual = zeros(24,1);
Qr_actual = zeros(24,1);
Ie_actual = zeros(24,1);

for i=1:1:24
%% Qc: Convection Cooling Calculation%%

Vw = LVY2(i,1); % Actual Velocity given
Ta = LY2(i,1); %% Ambient temperature
phi = LAY2(i,1)*pi()/180; % Wind angle @ radian angle
Pr = LPY2(i,1)*25.4; %% Precipitation rate converted in in/hr

% Calculation Section %

T_film = (Ts+Ta)/2;

Rho_f = (1.293-1.525e-4*He + 6.379e-9*He^2)/(1+0.00367*T_film); % kg/m^3

Mu_f = (1.458e-6*(T_film+273)^1.5)/(T_film+383.4); % kg/m-s or N-s/m^2

kf = 2.424e-2+7.477e-5*T_film-4.407e-9*T_film^2; % Thermal conductivity of air
W/m-deg C

NRe = D0*Rho_f*Vw/Mu_f; % Reynolds Number

K_angle = 1.194-cos(phi)+0.194*cos(2*phi)+0.368*sin(2*phi);    % Wind direction
factor

qc1 = K_angle*(1.01+1.35*NRe^0.52)*kf*(Ts-Ta); %watts/m
qc2 = K_angle*0.754*NRe^0.6*kf*(Ts-Ta); % watts/m

qc = max(qc1,qc2);

Qc_actual(i,1) = qc;


%% Qr: Radiation Cooling Calculation%%

qr = 17.8*D0*e*(((Ts+273)/100)^4-((Ta+273)/100)^4); % Watt/m heat loss due to
radiation

Qr_actual(i,1) = qr;

%% Qs: Heat gain from sun Calculation%%
% Modeled as day of the year %
Qs_actual(i,1) = DTRdata(9,1);

%% Qe: Precipitation cooling Calculation%%
```

```
%Calculation Section%

w  = 6.7e-5*Pr^0.846;  % w [kg m?3] is the liquid water content of the
precipitation

maf  = sqrt((0.001*Pr*Rho_w)^2+(3600*Vw*w)^2); % The liquid mass flux density maf
[kg m?2 h?1] impinging onto the conductor

ma = maf*D0/3600; % ma [kg s?1 m?1] is the mass flux rate of water striking the
conductor surface

Pc = n*pi()*d*(0.5+1/n); % Pc [m] is the conductor perimeter

ec  = 133.322*10^(8.07131-(1730.63/(Ts+273-39.724))); % ec [Pa] is the saturation
vapour pressure of water at the conductor temperature

ea  = 133.322*10^(8.07131-(1730.63/(Ta+273-39.724))); % ea [Pa] is the saturation
vapour pressure of water at air temperature

h  = max(qc1,qc2)/(pi()*D0*(Ts-Ta)); % h [Wm?2 K?1] is the convective heat transfer
coefficient

me = Pc*h*k*(ec-R_H*ea)/(cp*Pa); % The evaporative mass flux me [kg s?1 m?1]

if ma<me
    m  = ma;       %% where m [kg s?1 m?1] is the actual mass flux evaporating
from the conductor surface
else
    m =me;
end

Tb = inv((1/373.12)-((R*log10(Pa*9.8692e-6)/H)));  %the boiling point%

Te = min(Ts+273,Tb); % evaporation temperature%

Tw = Ts+273; %Tw [K] is the water surface temperature%
Tw_temp = Tw-273.15;
Le   =  0.0000614342*Tw_temp^3   -  0.00158927*Tw_temp^2   +  2.36418*Tw_temp   -
2500.79; %The specific latent heat of evaporation%

qe = m*(Le+cw*(Te-(Ta+273))); %The precipitation heat loss due to evaporation%

Qe_actual(i,1) = qe;

%% Imax: Dynamic current rating DTR Calculation%%
I_actual_s2(i,1) = sqrt((qr+qc+qe-qs)/RTs);

end

%% Section-3:Actual DTR calculation%%
Qe_actual = zeros(24,1);    % To store data calculated
Qs_actual = zeros(24,1);
Qc_actual = zeros(24,1);
Qr_actual = zeros(24,1);
Ie_actual = zeros(24,1);

for i=1:1:24
%% Qc: Convection Cooling Calculation%%
Vw = LVY3(i,1); % Actual Velocity given
Ta = LY3(i,1); %% Ambient temperature
phi = LAY3(i,1)*pi()/180; % Wind angle @ radian angle
Pr = LPY3(i,1)*25.4; %% Precipitation rate converted in in/hr

% Calculation Section %
```

```
T_film = (Ts+Ta)/2;

Rho_f = (1.293-1.525e-4*He + 6.379e-9*He^2)/(1+0.00367*T_film); % kg/m^3

Mu_f = (1.458e-6*(T_film+273)^1.5)/(T_film+383.4); % kg/m-s or N-s/m^2

kf = 2.424e-2+7.477e-5*T_film-4.407e-9*T_film^2; % Thermal conductivity of air W/m-deg C

NRe = D0*Rho_f*Vw/Mu_f; % Reynolds Number

K_angle = 1.194-cos(phi)+0.194*cos(2*phi)+0.368*sin(2*phi); % Wind direction factor

qc1 = K_angle*(1.01+1.35*NRe^0.52)*kf*(Ts-Ta); %watts/m
qc2 = K_angle*0.754*NRe^0.6*kf*(Ts-Ta); % watts/m

qc = max(qc1,qc2);

Qc_actual(i,1) = qc;


%% Qr: Radiation Cooling Calculation%%

qr = 17.8*D0*e*(((Ts+273)/100)^4-((Ta+273)/100)^4); % Watt/m heat loss due to radiation

Qr_actual(i,1) = qr;

%% Qs: Heat gain from sun Calculation%%
% Modeled as day of the year %
Qs_actual(i,1) = DTRdata(9,1);

%% Qe: Precipitation cooling Calculation%%

%Calculation Section%

w = 6.7e-5*Pr^0.846; % w [kg m?3] is the liquid water content of the precipitation

maf = sqrt((0.001*Pr*Rho_w)^2+(3600*Vw*w)^2); % The liquid mass flux density maf [kg m?2 h?1] impinging onto the conductor

ma = maf*D0/3600; % ma [kg s?1 m?1] is the mass flux rate of water striking the conductor surface

Pc = n*pi()*d*(0.5+1/n); % Pc [m] is the conductor perimeter

ec = 133.322*10^(8.07131-(1730.63/(Ts+273-39.724))); % ec [Pa] is the saturation vapour pressure of water at the conductor temperature

ea = 133.322*10^(8.07131-(1730.63/(Ta+273-39.724))); % ea [Pa] is the saturation vapour pressure of water at air temperature

h = max(qc1,qc2)/(pi()*D0*(Ts-Ta)); % h [Wm?2 K?1] is the convective heat transfer coefficient

me = Pc*h*k*(ec-R_H*ea)/(cp*Pa); % The evaporative mass flux me [kg s?1 m?1]

if ma<me
    m = ma;       %% where m [kg s?1 m?1] is the actual mass flux evaporating from the conductor surface
else
```

```
    m =me;
end

Tb = inv((1/373.12)-((R*log10(Pa*9.8692e-6)/H)));  %the boiling point%

Te = min(Ts+273,Tb); % evaporation temperature%

Tw = Ts+273; %Tw [K] is the water surface temperature%
Tw_temp = Tw-273.15;
Le  =  0.0000614342*Tw_temp^3  -  0.00158927*Tw_temp^2  +  2.36418*Tw_temp  -
2500.79; %The specific latent heat of evaporation%

qe = m*(Le+cw*(Te-(Ta+273))); %The precipitation heat loss due to evaporation%

Qe_actual(i,1) = qe;

%% Imax: Dynamic current rating DTR Calculation%%
I_actual_s3(i,1) = sqrt((qr+qc+qe-qs)/RTs);

end
%% Section-4:Actual DTR calculation%%
Qe_actual = zeros(24,1);    % To store data calculated
Qs_actual = zeros(24,1);
Qc_actual = zeros(24,1);
Qr_actual = zeros(24,1);
Ie_actual = zeros(24,1);

for i=1:1:24
%% Qc: Convection Cooling Calculation%%

Vw = LVY4(i,1); % Actual Velocity given
Ta = LY4(i,1); %% Ambient temperature
phi = LAY4(i,1)*pi()/180; % Wind angle @ radian angle
Pr = LPY4(i,1)*25.4; %% Precipitation rate converted in in/hr

% Calculation Section %

T_film = (Ts+Ta)/2;

Rho_f = (1.293-1.525e-4*He + 6.379e-9*He^2)/(1+0.00367*T_film); % kg/m^3

Mu_f = (1.458e-6*(T_film+273)^1.5)/(T_film+383.4); % kg/m-s or N-s/m^2

kf  = 2.424e-2+7.477e-5*T_film-4.407e-9*T_film^2;  % Thermal  conductivity  of  air
W/m-deg C

NRe = D0*Rho_f*Vw/Mu_f; % Reynolds Number

K_angle  =  1.194-cos(phi)+0.194*cos(2*phi)+0.368*sin(2*phi);     %  Wind  direction
factor

qc1 = K_angle*(1.01+1.35*NRe^0.52)*kf*(Ts-Ta); %watts/m
qc2 = K_angle*0.754*NRe^0.6*kf*(Ts-Ta); % watts/m

qc = max(qc1,qc2);

Qc_actual(i,1) = qc;


%% Qr: Radiation Cooling Calculation%%

qr  =  17.8*D0*e*(((Ts+273)/100)^4-((Ta+273)/100)^4);  %  Watt/m  heat  loss  due  to
radiation
```

```
Qr_actual(i,1) = qr;

%% Qs: Heat gain from sun Calculation%%
% Modeled as day of the year %
Qs_actual(i,1) = DTRdata(9,1);

%% Qe: Precipitation cooling Calculation%%

%Calculation Section%

w  =  6.7e-5*Pr^0.846;  %  w  [kg  m?3] is  the  liquid  water  content  of  the
precipitation

maf  = sqrt((0.001*Pr*Rho_w)^2+(3600*Vw*w)^2);  % The liquid mass flux density maf
[kg m?2 h?1] impinging onto the conductor

ma = maf*D0/3600; % ma [kg s?1 m?1] is the mass flux rate of water striking the
conductor surface

Pc = n*pi()*d*(0.5+1/n); % Pc [m] is the conductor perimeter

ec  =  133.322*10^(8.07131-(1730.63/(Ts+273-39.724)));  %  ec  [Pa]  is  the  saturation
vapour pressure of water at the conductor temperature

ea  =  133.322*10^(8.07131-(1730.63/(Ta+273-39.724)));  %  ea  [Pa]  is  the  saturation
vapour pressure of water at air temperature

h  = max(qc1,qc2)/(pi()*D0*(Ts-Ta));  % h  [Wm?2  K?1] is  the  convective  heat  transfer
coefficient

me = Pc*h*k*(ec-R_H*ea)/(cp*Pa); % The evaporative mass flux me [kg s?1 m?1]

if ma<me
    m  = ma;       %% where m [kg s?1 m?1] is the actual mass flux evaporating
from the conductor surface
else
    m =me;
end

Tb = inv((1/373.12)-((R*log10(Pa*9.8692e-6)/H)));   %the boiling point%

Te = min(Ts+273,Tb); % evaporation temperature%

Tw = Ts+273; %Tw [K] is the water surface temperature%
Tw_temp = Tw-273.15;
Le   =   0.0000614342*Tw_temp^3   -   0.00158927*Tw_temp^2   +   2.36418*Tw_temp   -
2500.79; %The specific latent heat of evaporation%

qe = m*(Le+cw*(Te-(Ta+273))); %The precipitation heat loss due to evaporation%

Qe_actual(i,1) = qe;

%% Imax: Dynamic current rating DTR Calculation%%
I_actual_s4(i,1) = sqrt((qr+qc+qe-qs)/RTs);

end

%% Section-5:Actual DTR calculation%%
Qe_actual = zeros(24,1);    % To store data calculated
Qs_actual = zeros(24,1);
Qc_actual = zeros(24,1);
Qr_actual = zeros(24,1);
Ie_actual = zeros(24,1);
```

```
for i=1:1:24
%% Qc: Convection Cooling Calculation%%

Vw = LVY5(i,1); % Actual Velocity given
Ta = LY5(i,1); %% Ambient temperature
phi = LAY5(i,1)*pi()/180; % Wind angle @ radian angle
Pr = LPY5(i,1)*25.4; %% Precipitation rate converted in in/hr

% Calculation Section %

T_film = (Ts+Ta)/2;

Rho_f = (1.293-1.525e-4*He + 6.379e-9*He^2)/(1+0.00367*T_film); % kg/m^3

Mu_f = (1.458e-6*(T_film+273)^1.5)/(T_film+383.4); % kg/m-s or N-s/m^2

kf = 2.424e-2+7.477e-5*T_film-4.407e-9*T_film^2; % Thermal conductivity of air W/m-deg C

NRe = D0*Rho_f*Vw/Mu_f; % Reynolds Number

K_angle = 1.194-cos(phi)+0.194*cos(2*phi)+0.368*sin(2*phi); % Wind direction factor

qc1 = K_angle*(1.01+1.35*NRe^0.52)*kf*(Ts-Ta); %watts/m
qc2 = K_angle*0.754*NRe^0.6*kf*(Ts-Ta); % watts/m

qc = max(qc1,qc2);

Qc_actual(i,1) = qc;


%% Qr: Radiation Cooling Calculation%%

qr = 17.8*D0*e*(((Ts+273)/100)^4-((Ta+273)/100)^4); % Watt/m heat loss due to radiation

Qr_actual(i,1) = qr;

%% Qs: Heat gain from sun Calculation%%
% Modeled as day of the year %
Qs_actual(i,1) = DTRdata(9,1);

%% Qe: Precipitation cooling Calculation%%

%Calculation Section%

w = 6.7e-5*Pr^0.846; % w [kg m?3] is the liquid water content of the precipitation

maf = sqrt((0.001*Pr*Rho_w)^2+(3600*Vw*w)^2); % The liquid mass flux density maf [kg m?2 h?1] impinging onto the conductor

ma = maf*D0/3600; % ma [kg s?1 m?1] is the mass flux rate of water striking the conductor surface

Pc = n*pi()*d*(0.5+1/n); % Pc [m] is the conductor perimeter

ec = 133.322*10^(8.07131-(1730.63/(Ts+273-39.724))); % ec [Pa] is the saturation vapour pressure of water at the conductor temperature

ea = 133.322*10^(8.07131-(1730.63/(Ta+273-39.724))); % ea [Pa] is the saturation vapour pressure of water at air temperature
```

```
h = max(qc1,qc2)/(pi()*D0*(Ts-Ta)); % h [Wm?2 K?1] is the convective heat transfer coefficient

me = Pc*h*k*(ec-R_H*ea)/(cp*Pa); % The evaporative mass flux me [kg s?1 m?1]

if ma<me
    m = ma;      %% where m [kg s?1 m?1] is the actual mass flux evaporating from the conductor surface
else
    m =me;
end

Tb = inv((1/373.12)-((R*log10(Pa*9.8692e-6)/H)));  %the boiling point%

Te = min(Ts+273,Tb); % evaporation temperature%

Tw = Ts+273; %Tw [K] is the water surface temperature%
Tw_temp = Tw-273.15;
Le = 0.0000614342*Tw_temp^3 - 0.00158927*Tw_temp^2 + 2.36418*Tw_temp - 2500.79; %The specific latent heat of evaporation%

qe = m*(Le+cw*(Te-(Ta+273))); %The precipitation heat loss due to evaporation%

Qe_actual(i,1) = qe;

%% Imax: Dynamic current rating DTR Calculation%%
I_actual_s5(i,1) = sqrt((qr+qc+qe-qs)/RTs);

end

%% Section-6:Actual DTR calculation%%
Qe_actual = zeros(24,1);   % To store data calculated
Qs_actual = zeros(24,1);
Qc_actual = zeros(24,1);
Qr_actual = zeros(24,1);
Ie_actual = zeros(24,1);

for i=1:1:24
%% Qc: Convection Cooling Calculation%%

Vw = LVY6(i,1); % Actual Velocity given
Ta = LY6(i,1); %% Ambient temperature
phi = LAY6(i,1)*pi()/180; % Wind angle @ radian angle
Pr = LPY6(i,1)*25.4; %% Precipitation rate converted in in/hr

% Calculation Section %

T_film = (Ts+Ta)/2;

Rho_f = (1.293-1.525e-4*He + 6.379e-9*He^2)/(1+0.00367*T_film); % kg/m^3

Mu_f = (1.458e-6*(T_film+273)^1.5)/(T_film+383.4); % kg/m-s or N-s/m^2

kf = 2.424e-2+7.477e-5*T_film-4.407e-9*T_film^2; % Thermal conductivity of air W/m-deg C

NRe = D0*Rho_f*Vw/Mu_f; % Reynolds Number

K_angle = 1.194-cos(phi)+0.194*cos(2*phi)+0.368*sin(2*phi);     % Wind direction factor

qc1 = K_angle*(1.01+1.35*NRe^0.52)*kf*(Ts-Ta); %watts/m
qc2 = K_angle*0.754*NRe^0.6*kf*(Ts-Ta); % watts/m
```

```
qc = max(qc1,qc2);

Qc_actual(i,1) = qc;


%% Qr: Radiation Cooling Calculation%%

qr = 17.8*D0*e*(((Ts+273)/100)^4-((Ta+273)/100)^4); % Watt/m heat loss due to
radiation

Qr_actual(i,1) = qr;

%% Qs: Heat gain from sun Calculation%%
% Modeled as day of the year %
Qs_actual(i,1) = DTRdata(9,1);

%% Qe: Precipitation cooling Calculation%%

%Calculation Section%

w = 6.7e-5*Pr^0.846; % w [kg m?3] is the liquid water content of the
precipitation

maf = sqrt((0.001*Pr*Rho_w)^2+(3600*Vw*w)^2); % The liquid mass flux density maf
[kg m?2 h?1] impinging onto the conductor
ma = maf*D0/3600; % ma [kg s?1 m?1] is the mass flux rate of water striking the
conductor surface
Pc = n*pi()*d*(0.5+1/n); % Pc [m] is the conductor perimeter
ec = 133.322*10^(8.07131-(1730.63/(Ts+273-39.724))); % ec [Pa] is the saturation
vapour pressure of water at the conductor temperature
ea = 133.322*10^(8.07131-(1730.63/(Ta+273-39.724))); % ea [Pa] is the saturation
vapour pressure of water at air temperature
h = max(qc1,qc2)/(pi()*D0*(Ts-Ta)); % h [Wm?2 K?1] is the convective heat transfer
coefficient
me = Pc*h*k*(ec-R_H*ea)/(cp*Pa); % The evaporative mass flux me [kg s?1 m?1]

if ma<me
    m = ma;       %% where m [kg s?1 m?1] is the actual mass flux evaporating
from the conductor surface
else
    m =me;
end
Tb = inv((1/373.12)-((R*log10(Pa*9.8692e-6)/H))); %the boiling point%
Te = min(Ts+273,Tb); % evaporation temperature%
Tw = Ts+273; %Tw [K] is the water surface temperature%
Tw_temp = Tw-273.15;
Le = 0.0000614342*Tw_temp^3 - 0.00158927*Tw_temp^2 + 2.36418*Tw_temp - 2500.79; %%
The specific latent heat of evaporation
qe = m*(Le+cw*(Te-(Ta+273))); %% The precipitation heat loss due to evaporation
Qe_actual(i,1) = qe;
%% Imax: Dynamic current rating DTR Calculation %%
I_actual_s6(i,1) = sqrt((qr+qc+qe-qs)/RTs);

end
%% Actual DTR calculation of whole transmission line %%
DTR_Actual_1 = zeros(24,1);
STR = zeros(24,1);
for i=1:1:24
    DTR_Actual_1(i,1)    =    min(    min(min(I_actual_s1(i,1),I_actual_s2(i,1)),
min(I_actual_s3(i,1),I_actual_s4(i,1))), min(I_actual_s5(i,1),I_actual_s6(i,1)));
    STR_1(i,1) = I_STR;
end
```

```
%%    Graph Print Section        %%
t=transpose([0:1:23]);
c1=STR_1;
c2=DTR_Actual_1;
c1_up = [t,c1];
c2_low = [t,c2];
figure(1)
curve = [c1_up;flipud(c2_low)];
fill(curve(:,1),curve(:,2),'g')
legend('Extra TL Capacity Released for RE Generators')
grid, xlabel('Time Hr'), ylabel('Thermal Rating A'), title('DTR Dana-Kushma-New
Butwal 220 kV TL')

figure(2)
plot(t,DTR_Actual_1,'red'); grid, xlabel('Time Hr'), ylabel('Thermal Rating A'),
title('DTR Dana-Kushma-New Butwal 220 kV TL')
hold on
plot(t,STR_1,'+blue');
hold off
legend('Actual DTR','STR
```

ANNEX C: WEATHER DATA AT DIFFERENT WEATHER LOCATION

C1: Temperature Data for Different Weather Locations on 25/11/2020

Temperature (Deg. C) Data for Date: 25/11/2020							
ToD	**W1**	**W2**	**W3**	**W4**	**W5**	**W6**	**W7**
0	15.6	11.3	12.4	12.3	12.4	10.7	12.2
1	15.4	11.1	12.3	12.3	12.5	10.8	12.4
2	15.2	10.9	12.1	12.1	12.3	10.7	12.3
3	15.1	10.9	12.1	12.1	12.4	10.8	12.4
4	15.2	11	12.1	12.2	12.4	10.8	12.3
5	15.2	10.9	12.1	12.1	12.3	10.6	12.1
6	16.6	12.3	13.4	13.3	13.5	11.8	13.2
7	19.6	15.2	16.2	16.1	16.2	14.4	15.8
8	22.1	17.6	18.6	18.4	18.4	16.5	17.9
9	23.8	19.3	20.3	20	20	18.1	19.6
10	24.9	20.4	21.4	21.1	21.1	19.2	20.6
11	25.7	21.1	22.1	21.8	21.8	19.8	21.2
12	26.1	21.5	22.4	22.1	22	20.1	21.4
13	26	21.4	22.3	22	21.9	19.9	21.2
14	25.8	21.1	22	21.7	21.5	19.5	20.7
15	24.9	20.3	21.1	20.8	20.6	18.6	19.8
16	22.8	18.1	19	18.7	18.6	16.6	17.8
17	20	15.4	16.2	15.9	15.8	13.8	15
18	19.5	14.9	15.8	15.6	15.5	13.6	14.8
19	19	14.4	15.4	15.1	15.1	13.2	14.5
20	18	13.6	14.6	14.4	14.5	12.6	14
21	17.1	12.7	13.8	13.7	13.8	12	13.5
22	16.5	12.2	13.3	13.3	13.5	11.8	13.3
23	16.4	12.1	13.3	13.3	13.6	11.9	13.4

C2: Wind Velocity Data for Different Weather Locations on 25/11/2020

Wind Velocity (m/s) Data for Date: 25/11/2020							
ToD	**W1**	**W2**	**W3**	**W4**	**W5**	**W6**	**W7**
0	0.9	0.9	0.9	0.9	0.9	1	1
1	0.8	0.8	0.8	0.9	0.9	0.9	0.9
2	0.9	0.9	0.9	0.9	0.9	0.9	0.9
3	0.9	0.9	0.9	0.9	0.9	0.9	0.9
4	0.9	0.9	0.9	0.9	0.9	0.9	0.9
5	0.9	0.9	0.9	0.9	0.9	0.9	0.8
6	0.9	0.9	0.8	0.8	0.8	0.8	0.8
7	1.3	1.1	1	0.8	0.7	0.7	0.6
8	1.5	1.4	1.2	1.1	0.9	0.8	0.8
9	1.4	1.4	1.3	1.2	1.2	1.1	1.1
10	1.5	1.5	1.5	1.6	1.6	1.6	1.6
11	1.8	1.8	1.9	1.9	2	2	2
12	2	2.1	2.1	2.2	2.2	2.2	2.2
13	2.2	2.2	2.3	2.3	2.3	2.3	2.3
14	2	2.1	2.1	2.1	2.1	2.1	2.1
15	1.2	1.3	1.3	1.4	1.4	1.4	1.4
16	0.9	0.9	0.9	0.8	0.8	0.8	0.8
17	0.9	0.8	0.8	0.7	0.6	0.6	0.6
18	0.7	0.7	0.7	0.7	0.7	0.7	0.7
19	0.8	0.8	0.8	0.9	0.9	1	1
20	1	1	1	1	1.1	1.1	1.1
21	1.1	1.1	1.1	1.1	1.1	1.1	1.1
22	1.1	1.1	1.1	1.1	1.2	1.2	1.2
23	1.1	1.1	1.1	1.2	1.2	1.2	1.2

C3: Wind Incidence Angle Data for Different Weather Locations on 25/11/2020

Wind Incidence (Deg.) Data for Date: 25/11/2020							
ToD	W1	W2	W3	W4	W5	W6	W7
0	69	69	26	26	26	26	26
1	69	69	30	30	30	30	30
2	63	63	32	32	32	32	32
3	64	64	34	34	34	34	34
4	72	72	38	38	38	38	38
5	84	84	43	43	43	43	43
6	90	90	46	46	46	46	46
7	87	87	52	52	52	52	52
8	84	84	74	74	74	74	74
9	79	79	35	35	35	35	35
10	38	38	12	12	12	12	12
11	3	3	4	4	4	4	4
12	19	19	16	16	16	16	16
13	30	30	23	23	23	23	23
14	37	37	28	28	28	28	28
15	40	40	31	31	31	31	31
16	42	42	41	41	41	41	41
17	51	51	86	86	86	86	86
18	72	72	31	31	31	31	31
19	54	54	7	7	7	7	7
20	19	19	0	0	0	0	0
21	9	9	1	1	1	1	1
22	3	3	2	2	2	2	2
23	6	6	3	3	3	3	3

C4: Precipitation Data for Different Weather Locations on 25/11/2020

Precipitation (mm/hr) Data for Date: 25/11/2020							
ToD	**W1**	**W2**	**W3**	**W4**	**W5**	**W6**	**W7**
0	0	0	0	0	0	0	0
1	0	0	0	0	0	0	0
2	0	0	0	0	0	0	0
3	0	0	0	0	0	0	0
4	0	0	0	0	0	0	0
5	0	0	0	0	0	0	0
6	0	0	0	0	0	0	0
7	0	0	0	0	0	0	0
8	0	0	0	0	0	0	0
9	0	0	0	0	0	0	0
10	0	0	0	0	0	0	0
11	0	0	0	0	0	0	0
12	0	0	0	0	0	0	0
13	0	0	0	0	0	0	0
14	0	0	0	0	0	0	0
15	0	0	0	0	0	0	0
16	0	0	0	0	0	0	0
17	0	0	0	0	0	0	0
18	0	0	0	0	0	0	0
19	0	0	0	0	0	0	0
20	0	0	0	0	0	0	0
21	0	0	0	0	0	0	0
22	0	0	0	0	0	0	0
23	0	0	0	0	0	0	0

C5: Temperature Data for Different Weather Locations on 15/10/2020

Temperature (Deg. C) Data for Date: 15/10/2020							
ToD	**W1**	**W2**	**W3**	**W4**	**W5**	**W6**	**W7**
0	25.4	21	22	21.9	22	20.2	21.7
1	25.1	20.6	21.7	21.5	21.6	19.8	21.2
2	25	20.5	21.6	21.4	21.5	19.6	21.1
3	24.9	20.5	21.5	21.3	21.3	19.5	21
4	24.6	20.2	21.2	21	21.1	19.3	20.8
5	24.1	19.7	20.7	20.6	20.7	19	20.6
6	25	20.6	21.7	21.7	21.8	20.1	21.7
7	27.6	23.2	24.3	24.3	24.4	22.7	24.3
8	29.7	25.2	26.1	26	26	24.2	25.6
9	30.9	26.3	27.2	27	27	25.1	26.5
10	31.7	27.1	28.1	27.8	27.8	25.9	27.3
11	32.4	27.8	28.7	28.4	28.4	26.5	27.8
12	32.7	28.1	29	28.7	28.6	26.7	28
13	32.8	28.2	29	28.7	28.6	26.6	27.9
14	32.8	28.1	28.9	28.6	28.4	26.4	27.6
15	32.1	27.4	28.2	27.9	27.7	25.6	26.8
16	30	25.4	26.2	25.9	25.8	23.8	25
17	27.9	23.3	24.2	23.9	23.7	21.7	23
18	27.4	22.8	23.8	23.5	23.4	21.5	22.8
19	27	22.5	23.5	23.2	23.2	21.3	22.6
20	26.8	22.3	23.3	23.1	23.1	21.2	22.6
21	26.3	21.9	22.9	22.8	22.8	21	22.5
22	25.9	21.5	22.6	22.4	22.6	20.8	22.3
23	25.3	20.9	22	21.8	22	20.2	21.8

C6: Wind Velocity Data for Different Weather Locations on 15/10/2020

Wind Velocity (m/s) Data for Date: 15/10/2020							
ToD	**W1**	**W2**	**W3**	**W4**	**W5**	**W6**	**W7**
0	0.5	0.5	0.5	0.4	0.4	0.4	0.4
1	0.6	0.6	0.5	0.5	0.5	0.4	0.4
2	0.6	0.6	0.5	0.5	0.5	0.5	0.5
3	0.6	0.6	0.6	0.6	0.6	0.6	0.6
4	0.6	0.6	0.6	0.7	0.7	0.7	0.7
5	0.7	0.7	0.7	0.7	0.7	0.7	0.7
6	0.8	0.7	0.7	0.6	0.6	0.6	0.6
7	0.4	0.5	0.6	0.6	0.7	0.7	0.7
8	1	1.2	1.4	1.5	1.7	1.8	1.8
9	1.5	1.7	1.8	2	2.2	2.2	2.3
10	1.8	2	2.1	2.3	2.4	2.5	2.5
11	1.9	2.1	2.2	2.4	2.5	2.6	2.6
12	2	2.2	2.3	2.4	2.6	2.6	2.7
13	2	2.1	2.2	2.4	2.5	2.6	2.6
14	1.9	2	2.1	2.3	2.4	2.5	2.5
15	1.7	1.8	1.8	1.9	2	2.1	2.1
16	1.1	1.1	1.2	1.2	1.3	1.3	1.3
17	0.9	0.9	0.8	0.8	0.8	0.8	0.8
18	0.8	0.8	0.8	0.7	0.7	0.7	0.7
19	0.8	0.7	0.6	0.6	0.5	0.5	0.5
20	0.7	0.6	0.6	0.5	0.4	0.4	0.4
21	0.5	0.5	0.4	0.3	0.2	0.1	0.1
22	0.5	0.4	0.4	0.3	0.3	0.3	0.3
23	0.5	0.5	0.5	0.5	0.5	0.5	0.5

C7: Wind Incidence Angle Data for Different Weather Locations on 15/10/2020

Wind Incidence (Deg.) Data for Date: 15/10/2020							
ToD	W1	W2	W3	W4	W5	W6	W7
0	5	5	73	73	73	73	73
1	24	24	63	63	63	63	63
2	47	47	62	62	62	62	62
3	59	59	55	55	55	55	55
4	60	60	49	49	49	49	49
5	55	55	48	48	48	48	48
6	53	53	56	56	56	56	56
7	49	49	1	1	1	1	1
8	78	78	22	22	22	22	22
9	76	76	25	25	25	25	25
10	75	75	27	27	27	27	27
11	75	75	28	28	28	28	28
12	75	75	30	30	30	30	30
13	75	75	32	32	32	32	32
14	73	73	33	33	33	33	33
15	74	74	32	32	32	32	32
16	64	64	29	29	29	29	29
17	39	39	27	27	27	27	27
18	29	29	34	34	34	34	34
19	27	27	35	35	35	35	35
20	35	35	36	36	36	36	36
21	51	51	41	41	41	41	41
22	86	86	36	36	36	36	36
23	12	12	34	34	34	34	34

C8: Precipitation Data for Different Weather Locations on 15/10/2020

Precipitation (mm/hr) Data for Date: 15/10/2020							
ToD	**W1**	**W2**	**W3**	**W4**	**W5**	**W6**	**W7**
0	0	0	0	0	0	0	0
1	0	0	0	0	0	0	0
2	0	0	0	0	0	0	0
3	0	0	0	0	0	0	0
4	0	0	0	0	0	0	0
5	0	0	0	0	0	0	0
6	0	0	0	0	0	0	0
7	0	0	0	0	0	0	0
8	0	0	0	0	0	0	0
9	0	0	0	0	0	0	0
10	0	0	0	0	0	0	0
11	0	0	0	0	0	0	0
12	0	0	0	0	0	0	0
13	0	0	0	0	0	0	0
14	0	0	0	0	0	0	0
15	0	0	0	0	0	0	0
16	0	0	0	0	0	0	0
17	0	0	0	0	0	0	0
18	0	0	0	0	0	0	0
19	0	0	0	0	0	0	0
20	0	0	0	0	0	0	0
21	0	0	0	0	0	0	0
22	0	0	0	0	0	0	0
23	0	0	0	0	0	0	0

C9: Temperature Data for Different Weather Locations on 12/06/2020

Temperature (Deg. C) Data for Date: 12/06/2020							
ToD	**W1**	**W2**	**W3**	**W4**	**W5**	**W6**	**W7**
0	28.8	24.2	25.1	24.8	24.6	22.6	23.9
1	28.3	23.8	24.6	24.4	24.3	22.3	23.6
2	27.9	23.4	24.3	24.1	24	22.1	23.4
3	27.6	23.1	24	23.8	23.8	21.9	23.3
4	27.4	22.9	23.9	23.7	23.7	21.8	23.2
5	28	23.5	24.5	24.3	24.3	22.5	23.9
6	29.1	24.6	25.6	25.4	25.4	23.6	25.1
7	30.3	25.7	26.7	26.4	26.3	24.4	25.8
8	31.7	27	27.9	27.6	27.5	25.5	26.8
9	33.5	28.9	29.8	29.4	29.3	27.3	28.7
10	35.6	30.9	31.8	31.5	31.4	29.4	30.7
11	37.1	32.4	33.3	32.9	32.8	30.7	31.9
12	37.9	33.2	34	33.6	33.4	31.3	32.3
13	38	33.3	34.1	33.7	33.4	31.3	32.3
14	37.5	32.8	33.6	33.2	32.9	30.8	31.9
15	36.3	31.6	32.4	32.1	31.9	29.8	30.9
16	34.9	30.2	31.1	30.7	30.5	28.5	29.6
17	33.3	28.7	29.5	29.2	29	26.9	28.1
18	31.7	27.1	27.9	27.6	27.4	25.3	26.5
19	30.9	26.3	27.1	26.8	26.6	24.6	25.8
20	30.3	25.6	26.5	26.2	26	24	25.2
21	29.7	25	25.9	25.6	25.4	23.4	24.7
22	29.1	24.5	25.4	25.1	24.9	22.9	24.2
23	28.6	24	24.9	24.6	24.5	22.6	23.9

C10: Wind Velocity Data for Different Weather Locations on 12/06/2020

Wind Velocity (m/s) Data for Date: 12/06/2020							
ToD	**W1**	**W2**	**W3**	**W4**	**W5**	**W6**	**W7**
0	3.2	2.9	2.5	2.1	1.8	1.6	1.5
1	3.1	2.7	2.3	1.9	1.6	1.4	1.3
2	2.9	2.4	2	1.6	1.3	1.1	1
3	2.6	2.1	1.7	1.3	1	0.8	0.7
4	2.3	1.9	1.6	1.2	0.8	0.7	0.6
5	2.8	2.4	2.1	1.8	1.5	1.3	1.3
6	3.5	3.1	2.8	2.5	2.3	2.1	2.1
7	3.7	3.4	3.1	2.8	2.6	2.4	2.4
8	3.5	3.2	2.9	2.7	2.4	2.2	2.2
9	3.3	3.1	2.8	2.6	2.4	2.3	2.2
10	3.3	3.1	3	2.8	2.7	2.6	2.6
11	3.6	3.5	3.4	3.3	3.2	3.2	3.1
12	4	3.8	3.7	3.6	3.5	3.4	3.4
13	4.2	4.1	3.9	3.8	3.6	3.6	3.5
14	4.2	4.1	4	3.8	3.7	3.6	3.6
15	4	3.9	3.8	3.6	3.5	3.5	3.5
16	3.5	3.4	3.3	3.2	3.2	3.1	3.1
17	2.8	2.7	2.6	2.5	2.4	2.4	2.3
18	1.5	1.5	1.4	1.3	1.3	1.3	1.2
19	1	1	0.9	0.9	0.9	0.8	0.8
20	0.9	0.8	0.8	0.7	0.7	0.7	0.7
21	0.9	0.8	0.7	0.7	0.6	0.6	0.6
22	0.8	0.8	0.7	0.7	0.6	0.6	0.6
23	0.8	0.7	0.6	0.6	0.5	0.5	0.5

C11: Wind Incidence Angle Data for Different Weather Locations on 12/06/2020

Wind Incidence (Deg.) Data for Date: 12/06/2020							
ToD	W1	W2	W3	W4	W5	W6	W7
0	62	62	26	26	26	26	26
1	63	63	29	29	29	29	29
2	62	62	37	37	37	37	37
3	60	60	53	53	53	53	53
4	59	59	72	72	72	72	72
5	62	62	77	77	77	77	77
6	66	66	64	64	64	64	64
7	71	71	52	52	52	52	52
8	78	78	39	39	39	39	39
9	79	79	21	21	21	21	21
10	70	70	14	14	14	14	14
11	60	60	17	17	17	17	17
12	54	54	19	19	19	19	19
13	50	50	18	18	18	18	18
14	46	46	15	15	15	15	15
15	43	43	11	11	11	11	11
16	43	43	8	8	8	8	8
17	45	45	6	6	6	6	6
18	47	47	4	4	4	4	4
19	51	51	1	1	1	1	1
20	55	55	3	3	3	3	3
21	55	55	7	7	7	7	7
22	56	56	8	8	8	8	8
23	61	61	11	11	11	11	11

C12: Precipitation Data for Different Weather Locations on 12/06/2020

Precipitation (mm/hr) Data for Date: 12/06/2020							
ToD	**W1**	**W2**	**W3**	**W4**	**W5**	**W6**	**W7**
0	0.01	0.01	0.01	0.01	0.01	0.01	0.01
1	0.58	0.58	0.58	0.58	0.58	0.58	0.58
2	0.58	0.58	0.58	0.58	0.58	0.58	0.58
3	0.58	0.58	0.58	0.58	0.58	0.58	0.58
4	0	0	0	0	0	0	0
5	0	0	0	0	0	0	0
6	0	0	0	0	0	0	0
7	0	0	0	0	0	0	0
8	0	0	0	0	0	0	0
9	0.01	0.01	0.01	0.01	0.01	0.01	0.01
10	0.04	0.04	0.04	0.04	0.04	0.04	0.04
11	0.14	0.14	0.14	0.14	0.14	0.14	0.14
12	0.3	0.3	0.3	0.3	0.3	0.3	0.3
13	0.44	0.44	0.44	0.44	0.44	0.44	0.44
14	0.47	0.47	0.47	0.47	0.47	0.47	0.47
15	0.37	0.37	0.37	0.37	0.37	0.37	0.37
16	0.29	0.29	0.29	0.29	0.29	0.29	0.29
17	0.25	0.25	0.25	0.25	0.25	0.25	0.25
18	0.45	0.45	0.45	0.45	0.45	0.45	0.45
19	0.44	0.44	0.44	0.44	0.44	0.44	0.44
20	0.33	0.33	0.33	0.33	0.33	0.33	0.33
21	0.3	0.3	0.3	0.3	0.3	0.3	0.3
22	0.31	0.31	0.31	0.31	0.31	0.31	0.31
23	0.3	0.3	0.3	0.3	0.3	0.3	0.3

C13: Temperature Data for Different Weather Locations on 22/03/2020

Temperature (Deg. C) Data for Date: 22/03/2020							
ToD	**W1**	**W2**	**W3**	**W4**	**W5**	**W6**	**W7**
0	19.1	14.5	15.4	15.2	15.1	13.2	14.4
1	18.8	14.2	15.2	14.9	14.9	13	14.3
2	18.5	14	15	14.8	14.8	12.9	14.3
3	18.2	13.7	14.8	14.6	14.7	12.9	14.3
4	17.8	13.4	14.5	14.4	14.5	12.8	14.2
5	17.6	13.2	14.3	14.2	14.4	12.7	14.1
6	20.1	15.6	16.7	16.6	16.7	14.9	16.3
7	22.6	18.2	19.2	19	19	17.2	18.5
8	25.3	20.6	21.4	21.1	20.9	18.9	20.1
9	26.9	22.2	23	22.6	22.4	20.3	21.4
10	28	23.2	24	23.6	23.3	21.2	22.3
11	28.7	23.9	24.7	24.2	24	21.8	22.9
12	29	24.2	25	24.5	24.2	22	23.1
13	29.1	24.3	25.1	24.7	24.4	22.2	23.2
14	28.9	24.1	24.9	24.4	24.1	21.9	23
15	28.2	23.5	24.2	23.8	23.5	21.4	22.4
16	26.7	21.9	22.7	22.3	22.1	20	21
17	23.4	18.7	19.5	19.1	18.8	16.7	17.8
18	22.4	17.6	18.4	18	17.8	15.6	16.7
19	21.8	17.1	18	17.6	17.4	15.3	16.4
20	21.1	16.5	17.4	17.1	16.9	14.9	16
21	20.7	16.1	17.1	16.8	16.7	14.8	16
22	20.5	16	17	16.8	16.8	15	16.2
23	20.1	15.7	16.7	16.6	16.6	14.8	16.1

C14: Wind Velocity Data for Different Weather Locations on 22/03/2020

Wind Velocity (m/s) Data for Date: 22/03/2020							
ToD	**W1**	**W2**	**W3**	**W4**	**W5**	**W6**	**W7**
0	1.2	1.1	1.1	1.1	1.1	1.1	1.1
1	1.2	1.1	1.1	1.1	1.1	1.1	1.1
2	1.2	1.1	1.1	1.1	1.1	1.1	1.1
3	1.1	1.1	1.1	1	1	1	1
4	1.1	1.1	1.1	1	1	1	1
5	1.2	1.2	1.1	1	1	0.9	0.9
6	2	1.7	1.5	1.2	0.9	0.7	0.7
7	2.2	2.1	1.9	1.8	1.7	1.6	1.6
8	1.7	1.9	2.1	2.3	2.5	2.6	2.6
9	1.7	2	2.4	2.8	3.1	3.3	3.3
10	1.9	2.3	2.6	3	3.4	3.6	3.6
11	2.1	2.4	2.7	3.1	3.4	3.6	3.7
12	2.2	2.5	2.8	3.1	3.4	3.5	3.6
13	2.3	2.6	2.8	3.1	3.4	3.5	3.6
14	2.5	2.7	2.9	3.1	3.3	3.5	3.5
15	2.5	2.6	2.8	3	3.1	3.2	3.3
16	1.7	1.9	2	2.1	2.3	2.3	2.4
17	1	1	1	1.1	1.1	1.1	1.2
18	1	1	1	1	1	1	1
19	1	1	1	1	1	1	1
20	1	1	1	1	1	1	0.9
21	1	1	0.9	0.9	0.9	0.9	0.8
22	1	0.9	0.8	0.7	0.6	0.6	0.6
23	0.9	0.8	0.7	0.6	0.5	0.4	0.4

C15: Wind Incidence Angle Data for Different Weather Locations on 22/03/2020

Wind Incidence (Deg.) Data for Date: 22/03/2020							
ToD	W1	W2	W3	W4	W5	W6	W7
0	9	9	16	16	16	16	16
1	15	15	16	16	16	16	16
2	28	28	24	24	24	24	24
3	48	48	41	41	41	41	41
4	66	66	53	53	53	53	53
5	76	76	60	60	60	60	60
6	79	79	73	73	73	73	73
7	86	86	22	22	22	22	22
8	50	50	1	1	1	1	1
9	4	4	11	11	11	11	11
10	23	23	16	16	16	16	16
11	42	42	22	22	22	22	22
12	54	54	27	27	27	27	27
13	62	62	30	30	30	30	30
14	70	70	33	33	33	33	33
15	77	77	36	36	36	36	36
16	80	80	35	35	35	35	35
17	82	82	29	29	29	29	29
18	83	83	33	33	33	33	33
19	88	88	40	40	40	40	40
20	75	75	52	52	52	52	52
21	65	65	68	68	68	68	68
22	56	56	85	85	85	85	85
23	49	49	82	82	82	82	82

C16: Precipitation Data for Different Weather Locations on 22/03/2020

Precipitation (mm/hr) Data for Date: 22/03/2020							
ToD	**W1**	**W2**	**W3**	**W4**	**W5**	**W6**	**W7**
0	0	0	0	0	0	0	0
1	0	0	0	0	0	0	0
2	0	0	0	0	0	0	0
3	0	0	0	0	0	0	0
4	0	0	0	0	0	0	0
5	0	0	0	0	0	0	0
6	0	0	0	0	0	0	0
7	0	0	0	0	0	0	0
8	0	0	0	0	0	0	0
9	0	0	0	0	0	0	0
10	0	0	0	0	0	0	0
11	0	0	0	0	0	0	0
12	0	0	0	0	0	0	0
13	0	0	0	0	0	0	0
14	0	0	0	0	0	0	0
15	0	0	0	0	0	0	0
16	0	0	0	0	0	0	0
17	0	0	0	0	0	0	0
18	0	0	0	0	0	0	0
19	0	0	0	0	0	0	0
20	0	0	0	0	0	0	0
21	0	0	0	0	0	0	0
22	0	0	0	0	0	0	0
23	0	0	0	0	0	0	0

C17: Temperature Data for Different Weather Locations on 28/02/2020

Temperature (Deg. C) Data for Date: 28/02/2020							
ToD	**W1**	**W2**	**W3**	**W4**	**W5**	**W6**	**W7**
0	15.6	11.3	12.4	12.3	12.4	10.7	12.2
1	15.4	11.1	12.3	12.3	12.5	10.8	12.4
2	15.2	10.9	12.1	12.1	12.3	10.7	12.3
3	15.1	10.9	12.1	12.1	12.4	10.8	12.4
4	15.2	11	12.1	12.2	12.4	10.8	12.3
5	15.2	10.9	12.1	12.1	12.3	10.6	12.1
6	16.6	12.3	13.4	13.3	13.5	11.8	13.2
7	19.6	15.2	16.2	16.1	16.2	14.4	15.8
8	22.1	17.6	18.6	18.4	18.4	16.5	17.9
9	23.8	19.3	20.3	20	20	18.1	19.6
10	24.9	20.4	21.4	21.1	21.1	19.2	20.6
11	25.7	21.1	22.1	21.8	21.8	19.8	21.2
12	26.1	21.5	22.4	22.1	22	20.1	21.4
13	26	21.4	22.3	22	21.9	19.9	21.2
14	25.8	21.1	22	21.7	21.5	19.5	20.7
15	24.9	20.3	21.1	20.8	20.6	18.6	19.8
16	22.8	18.1	19	18.7	18.6	16.6	17.8
17	20	15.4	16.2	15.9	15.8	13.8	15
18	19.5	14.9	15.8	15.6	15.5	13.6	14.8
19	19	14.4	15.4	15.1	15.1	13.2	14.5
20	18	13.6	14.6	14.4	14.5	12.6	14
21	17.1	12.7	13.8	13.7	13.8	12	13.5
22	16.5	12.2	13.3	13.3	13.5	11.8	13.3
23	16.4	12.1	13.3	13.3	13.6	11.9	13.4

C18: Wind Velocity Data for Different Weather Locations on 28/02/2020

Wind Velocity (m/s) Data for Date: 28/02/2020							
ToD	**W1**	**W2**	**W3**	**W4**	**W5**	**W6**	**W7**
0	1	0.9	0.8	0.7	0.7	0.6	0.6
1	1	0.9	0.8	0.8	0.7	0.6	0.6
2	1	0.9	0.8	0.7	0.6	0.6	0.6
3	0.9	0.8	0.7	0.6	0.5	0.5	0.4
4	0.8	0.7	0.6	0.5	0.3	0.3	0.2
5	0.8	0.6	0.5	0.3	0.2	0.1	0.1
6	0.6	0.5	0.4	0.2	0.1	0.1	0
7	0.9	0.8	0.8	0.7	0.7	0.7	0.7
8	0.7	0.9	1.1	1.3	1.4	1.5	1.6
9	1.7	1.9	2.1	2.3	2.4	2.5	2.5
10	2.3	2.5	2.7	2.9	3.1	3.2	3.2
11	2.5	2.7	3	3.2	3.4	3.5	3.6
12	2.6	2.8	3.1	3.3	3.5	3.7	3.7
13	2.5	2.7	2.9	3.2	3.4	3.5	3.6
14	2	2.2	2.4	2.7	2.9	3	3.1
15	1.7	1.9	2	2.2	2.4	2.4	2.5
16	1	1.2	1.3	1.4	1.5	1.5	1.5
17	1	1	0.9	0.9	0.9	0.9	0.9
18	0.9	0.9	0.8	0.8	0.8	0.7	0.7
19	0.9	0.8	0.7	0.6	0.6	0.5	0.5
20	0.9	0.9	0.8	0.7	0.6	0.6	0.5
21	1	0.9	0.9	0.8	0.7	0.7	0.7
22	1	1	0.9	0.8	0.8	0.7	0.7
23	1.1	1	0.9	0.9	0.8	0.8	0.8

C19: Wind Incidence Angle Data for Different Weather Locations on 28/02/2020

Wind Incidence (Deg.) Data for Date: 28/02/2020							
ToD	W1	W2	W3	W4	W5	W6	W7
0	40	40	61	61	61	61	61
1	30	30	55	55	55	55	55
2	22	22	51	51	51	51	51
3	11	11	41	41	41	41	41
4	6	6	47	47	47	47	47
5	26	26	78	78	78	78	78
6	41	41	80	80	80	80	80
7	53	53	17	17	17	17	17
8	9	9	7	7	7	7	7
9	7	7	2	2	2	2	2
10	2	2	5	5	5	5	5
11	15	15	11	11	11	11	11
12	31	31	18	18	18	18	18
13	41	41	23	23	23	23	23
14	47	47	24	24	24	24	24
15	56	56	26	26	26	26	26
16	59	59	29	29	29	29	29
17	65	65	36	36	36	36	36
18	78	78	59	59	59	59	59
19	78	78	82	82	82	82	82
20	55	55	45	45	45	45	45
21	41	41	30	30	30	30	30
22	29	29	19	19	19	19	19
23	19	19	12	12	12	12	12

C20: Precipitation Data for Different Weather Locations on 28/02/2020

Precipitation (mm/hr) Data for Date: 28/02/2020							
ToD	**W1**	**W2**	**W3**	**W4**	**W5**	**W6**	**W7**
12	0	0	0	0	0	0	0
1	0	0	0	0	0	0	0
2	0	0	0	0	0	0	0
3	0	0	0	0	0	0	0
4	0	0	0	0	0	0	0
5	0	0	0	0	0	0	0
6	0	0	0	0	0	0	0
7	0	0	0	0	0	0	0
8	0	0	0	0	0	0	0
9	0	0	0	0	0	0	0
10	0	0	0	0	0	0	0
11	0	0	0	0	0	0	0
12	0.01	0.01	0.01	0.01	0.01	0.01	0.01
13	0.03	0.03	0.03	0.03	0.03	0.03	0.03
14	0.04	0.04	0.04	0.04	0.04	0.04	0.04
15	0.05	0.05	0.05	0.05	0.05	0.05	0.05
16	0.05	0.05	0.05	0.05	0.05	0.05	0.05
17	0.04	0.04	0.04	0.04	0.04	0.04	0.04
18	0.31	0.31	0.31	0.31	0.31	0.31	0.31
19	0.21	0.21	0.21	0.21	0.21	0.21	0.21
20	0.13	0.13	0.13	0.13	0.13	0.13	0.13
21	0.09	0.09	0.09	0.09	0.09	0.09	0.09
22	0.06	0.06	0.06	0.06	0.06	0.06	0.06
23	0.04	0.04	0.04	0.04	0.04	0.04	0.04

Gmail Search mail

9 of 317

[IOEGC16] Editor Decision

Inbox ×

Kobid Mon, Mar 24, 10:40 AM
to me

Khil Nath Aryal.

We are pleased to inform you that your manuscript titled "Application of Dynamic Thermal Rating for Congestion Management in Regions with High Renewable En Case Study in Dana-Kushma-New Butwal 220 kV Transmission Line" submitted to 16th IOE Graduate Conference is **Accepted** for presentation in the Conference in the Peer-Reviewed Proceedings. Please note that inclusion in hard copy proceedings is contingent upon your timely response to further edits, if any, during the p

With Warm Regards,
IOEGC-16 Editorial Team

Khil nath Aryal <aryal2allu7@gmail.com> Thu, Mar 27, 1:18 PM
to Sanjaya, Shahabuddin

Khil Nath Aryal

Dynamic Thermal Rating for Congestion Management in Regions with Renewable Energy Generation: A Case

Tribhuvan University

Document Details

Submission ID
trn:oid:::3117:447279339

Submission Date
Apr 9, 2025, 3:39 PM GMT+5:45

Download Date
Apr 9, 2025, 3:43 PM GMT+5:45

File Name
Final Thesis Report Plagiarism.pdf

File Size
12 MB

60 Pages

13,506 Words

74,819 Characters

Match Groups

- 108 Not Cited or Quoted 9%
  Matches with neither in-text citation nor quotation marks
- 0 Missing Quotations 0%
  Matches that are still very similar to source material
- 0 Missing Citation 0%
  Matches that have quotation marks, but no in-text citation
- 0 Cited and Quoted 0%
  Matches with in-text citation present, but no quotation marks

Top Sources

7% Internet sources
4% Publications
0% Submitted works (Student Papers)

Top Sources

The sources with the highest number of matches within the submission. Overlapping sources will not be displayed

1	Internet	
nea.org.np		1%
2	Internet	
www.spotlightnepal.com		<1%
3	Internet	
prism.ucalgary.ca		<1%
4	Internet	
www.nea.org.np		<1%
5	Internet	
opencommons.uconn.edu		<1%
6	Internet	
fastercapital.com		<1%
7	Publication	
Amjad Anvari-Moghaddam, Sina Ghaemi, Shi You, Frede Blaabjerg. "Power-to-X in...		<1%
8	Internet	
www.coursehero.com		<1%
9	Publication	
Xiaorong Sun, Chenhao Jin. "Spatio-temporal weather model-based probabilistic f...		<1%
10	Internet	
1library.net		<1%

11	Publication Jim McMenamin. "Financial Management - An Introduction", Routledge, 2019	<1%
12	Internet elibrary.tucl.edu.np	<1%
13	Internet ltu.diva-portal.org	<1%
14	Internet arxiv.org	<1%
15	Internet www.giiresearch.com	<1%
16	Internet www.bizmanualz.com	<1%
17	Publication Prerna Tundwal. "chapter 8 Empowering Sustainability", IGI Global, 2023	<1%
18	Publication Yi Yang, Ronald G. Harley, Deepak Divan, Thomas G. Habetler. "MLPN based Para...	<1%
19	Internet eparlib.nic.in	<1%
20	Publication Peter Schell. "Dynamic prediction of energy delivery capacity of power networks: ...	<1%
21	Internet utilitymagazine.com.au	<1%
22	Publication Edward Linacre. "Climate Data and Resources - A reference and guide", Routledg...	<1%
23	Publication Kongsen Wang, Gehao Sheng, Xiuchen Jiang. "Risk assessment of transmission d...	<1%
24	Internet sicd.se	<1%